Rockefeller University
Digital Commons @ RU

Student Theses and Dissertations

2018

The Role of Neuronal Pentraxin 1 in Promoting Pancreatic Cancer Progression

Yuehyi Gloria Wu

Follow this and additional works at: https://digitalcommons.rockefeller.edu/student_theses_and_dissertations

 Part of the Life Sciences Commons

THE ROLE OF NEURONAL PENTRAXIN 1 IN PROMOTING PANCREATIC CANCER PROGRESSION

A Thesis Presented to the Faculty of

The Rockefeller University

in Partial Fulfillment of the Requirements for

the degree of Doctor of Philosophy

by

Yuehyi Gloria Wu

June 2018

© Copyright by Yuehyi Gloria Wu 2018

THE ROLE OF NEURONAL PENTRAXIN 1 IN PROMOTING PANCREATIC CANCER PROGRESSION

Yuehyi Gloria Wu, Ph.D.
The Rockefeller Unviersity 2018

Pancreatic cancer is a deadly malignancy because it is usually diagnosed at an advanced stage and does not respond to the majority of treatments. More than 80% of patients present with advanced stage disease at the time of diagnosis and metastatic pancreatic cancer has a median survival of eight to eleven months under current standard of care. In the United States, pancreatic cancer is the fourth leading cause of cancer death. Efforts in using targeted agents to treat pancreatic cancer have mostly been fruitless. The dismal survival outcome of this disease and lack of success in clinical trials indicate the necessity for new models and improved approaches toward therapies. Understanding the cellular and physiological basis of metastatic pancreatic cancer is therefore of great interest to the medical and scientific community with regard to developing new targeted therapies and diagnostic biomarkers.

The first part of this thesis describes the establishment of two complementary pancreatic cancer metastasis mouse models using *in vivo* selection of liver-metastatic pancreatic cancer cells from their poorly metastatic parental population. The first mouse model utilized a xenograft system, and the second

model used a syngeneic system. Transcriptomic profiling was used to identify genes that were differentially expressed between the *in vivo* selected, highly metastatic cells and their poorly metastatic parental population in both mouse models. This approach identified Neuronal Pentraxin 1 (NPTX1) as a potential metastasis promoter because it was highly expressed in the *in vivo* selected, highly metastatic cancer cells compared to the poorly metastatic parental cells.

Through *in vivo* functional assays, NPTX1 was found to promote pancreatic cancer progression. NPTX1 was necessary to promote progression of established liver macro-metastases, a rate limiting step in the metastasis cascade. The second part of this thesis presents mechanistic studies that describe NPTX1's role in promoting cancer cell proliferating under a hypoxic tumor microenvironment. This proliferation advantage allows cancer cells to survive both in the primary tumor and promotes distal organ metastatic colonization.

The final part of this study reveals NPTX1 to be clinically relevant in patient samples. NPTX1 was found to be expressed in pancreatic tumor samples, but not in healthy pancreatic tissues. In addition, NPTX1 could be detected in the plasma of the xenograft mouse model, demonstrating the diagnostic and therapeutic potential of this secreted protein in pancreatic cancer.

To Benoit, my Parents and Carol

for their love and unconditional supports

ACKNOWLEDGMENTS

I would like to first thank my thesis advisor, Dr. Sohail Tavazoie, for his time, support and mentorship for the past 4 years. I am extremely privileged to have this opportunity to learn from him and be a student in his laboratory. His generous support, energy, and scientific curiosity will be a lasting inspiration for me for the rest of my career.

I would also like extend my utmost thanks to members of the Tavazoie laboratory for their support and scientific inputs. I would like to thank Dr. Claudio Alarcon, a wonderful friend, colleague and mentor, for his invaluable contributions to the work presented in this thesis, the stimulating scientific discussions, and encouragements. I also want to thank Dr. Zhiji Ren, a wonderful colleague for his constant encouragements and scientific inputs. I thank Helen Tien who have helped me significantly in the mouse studies and Logan Mendez who also contributed to the work presented in this thesis. I also want to extend my thank to all of the current and former members of the Tavazoie lab especially Jiamin Loo, Lisa Fish, Bernardo Tavora, Hani Goodarzi, Caitlin Sengelaub, Massoud Tavazoie, Raissa Tanqueco, Xuhang Liu, Nils Halberg, Rohit Mital, Ethan Weinberg, Jessica Posada, Mark Derbyshire, Benjamin Ostendorf, Lisa Noble, Ethan Ravetch, Norihiro Yamaguchi, Hyeseung Lee, and Alexander Nguyen. I am also grateful to the Tavazoie Lab administrator Eiko Nishiuchi and former lab administrator Emily Mandel for keeping the lab running smoothly.

I would also like to thank the members of my thesis committee: Dr. Daniel Mucida, Dr. Ping Chi, Dr. Kivanc Birsoy, and former member, Dr. Charlie Rice, for advice and suggestions throughout the progression of my project. Their critical insights have been invaluable for the completion of this thesis.

I would like to thank Dr. Christine Iacobuzio-Donahue for providing invaluable clinical samples and also for taking time off her busy schedule to be my external examiner.

I would like to thank all my former scientific mentors including Dr. Lacramioara Bintu from Stanford University, Dr. Carlos Bustamante from UC Berkeley, Dr. Courtney Hodges from Baylor, and Dr. Mikhail Kashlev from the NCI for being constant inspirations in my career.

I would like to thank the Tri-Institutional MD-PhD program for the funding and constant support. I would like to especially thank Dr. Olaf Andersen for his time and Ruth Gotian for running the program smoothly. I would also like to thank the Dena's Office at Rockefeller University for their help over the past 4 years.

Finally I would like to thank my husband, Benoit, my parents, my sister Carol, and my friends whose unconditional supports made this thesis project possible.

TABLE OF CONTENTS

LIST OF FIGURES

Chapter III:

30. 5-Azacytidine treated PANC1 cells increases NPTX1 expression.
31. Transcription factor binding sites in NPTX1 promoter.
32. Depletion of EGR1 with siRNA leads to decreased NPTX1 expression in PANC1 LM3 cells.

Chapter IV:

1. PANC1 LM3 cells with NPTX1 knockdown proliferate at the same rate as control cells under standard cell culture condition *in vitro*.
2. Knockdown of NPTX1 in PANC1 LM3 cells suppresses tumor cell proliferation *in vivo*.
3. *In vivo* apoptosis measured using a DEVD-luciferin system shows no significant different between PANC1 LM3 cells with and without knockdown of NPTX1.
4. PANC1 LM3 liver metastatic nodules are extensively hypoxic compared to the parental PANC1 cells *in vivo*.
5. PANC1 LM3 cells proliferate faster under hypoxic and anoxic conditions compared to PANC1 cells.
6. NPTX1 promotes proliferation of PANC1 LM3 cells in hypoxia.
7. PANC1 LM3 cells with suppressed NPTX1 expression proliferate at the same rate under normoxia.
8. PANC1 LM3 cells with suppressed NPTX1 expression proliferate at the same rate under low serum (2% FBS) growth
9. PANC1 LM3 cells with suppressed NPTX1 expression proliferate at the same rate under low glucose (1mg/mL) growth condition
10. Knockdown of NPTX1 cancer cells decrease infiltrating myofibroblasts in the liver metastatic nodules.
11. Hepatic stellate cells does not rescue suppressed metastatic growth due to NPTX1 knockdown in PANC1 LM3 cells.

12. Recombinant human NPTX1 suppresses hepatic stellate cells activation *in vitro*.
13. Conditioned medium from PANC1 LM3 cells with or without NPTX1 knockdown do not activate hepatic stellate cells *in vitro*.
14. Knockdown of NPTX1 in PANC1 LM3 cells does not alter number of endothelial cells in the liver metastatic nodules in vivo.
15. Knockdown of NPTX1 in PANC1 LM3 cells does not alter number of macrophages in the liver metastatic nodules *in vivo*.
16. The immune cell infiltrates of KPC tumors with Nptx1 knockdown do not differ significantly from control.
17. Proliferation of the highly metastatic PANC1 LM3 cells in hypoxia is not affected by suppression of HIF1a level.

Chapter V

1. Pancreatic tumor samples express NPTX1 at significantly higher level compared to normal pancreatic tissues.
2. Pancreatic cancer tumors express NPTX1 at the mRNA level.
3. Patient derived pancreatic tumor cell lines express high level of NPTX1.
4. Pancreatic cancer cell lines secrete NPTX1 protein into the extracellular space.
5. NPTX1 is detected in the plasma of the pancreatic cancer mouse xenograft model but not in healthy controls mice.

LIST OF TABLES

Chapter II

Chapter III

Chapter I Introduction

Pancreatic adenocarcinoma is a deadly malignancy with a dismal median survival of less than one year. Metastasis is the primary cause of death in pancreatic cancer and most patients present with or will eventually develop metastatic disease. My project presents an effort to identify regulators of pancreatic cancer metastasis that can be therapeutically targeted. Both xenograft and syngeneic mouse models were used to *in vivo* select for pancreatic cancer cells that are highly metastatic compared to their parental cell line. Transcriptomic profiling was performed comparing the gene expression of the highly metastatic sub-lines to the parental cells with the aims of: 1) identifying novel genes that regulate metastatic colonization of pancreatic cancer, 2) characterizing the cellular and molecular mechanisms utilized by these genes in metastatic colonization, and 3) determining the clinical relevance, therapeutic potential, and diagnostic value of these metastasis regulating genes.

Epidemiology, causes, and prognosis

Pancreatic ductal adenocarcinoma is a deadly disease because it is usually diagnosed at an advanced stage and does not respond to current treatments. Worldwide, the incidence of all types of pancreatic cancer (85% of all the pancreatic tumors are adenocarcinomas) ranges from 1 to 10 cases per 100,000 people (Torre et al., 2015). Pancreatic ductal adenocarcinoma is the most common

malignancy of the pancreas and this tumor (commonly and here referred to as pancreatic cancer) presents a substantial health problem. In the United States, each year about 43,000 patients die from pancreatic cancer and it is the fourth leading cause of cancer death. If the outcomes are not improved, the disease is predicted to be the second leading cause of cancer-related mortality within the next decade (Rahib et al., 2014).

More than 80% of patients present with advanced stage disease at the time of diagnosis (Stathis and Moore, 2010) and metastatic pancreatic adenocarcinoma has a median survival of eight to eleven months under current standard of care (Ryan et al., 2014). Efforts in using other agents to treat pancreatic cancer have mostly been fruitless and more than twenty Phase III clinical trials have failed (Ryan et al., 2014). The dismal survival outcome of this disease and lack of success in clinical trials indicates the necessity for new models and improved approaches toward therapies.

There are several risk factors and established genetic syndromes associated with pancreatic adenocarcinoma. Age is the major determinant of pancreatic cancer with most patients diagnosed at >50 years of age with peak incidence in the seventh and eighth decade of life. Risk factors associated with pancreatic adenocarcinoma include: smoking (Bosetti et al., 2012), long-standing diabetes

mellitus (Ben et al., 2011), obesity (Aune et al., 2012), and chronic pancreatitis (Duell et al., 2012). Genetic syndromes and associated genes include: hereditary pancreatitis (PRSS1, SPINK1) (Rebours et al., 2008), familial atypical multiple mole and melanoma syndrome (p16) (Vasen et al., 2000), and hereditary breast and ovarian cancer syndromes (BRCA1, BRCA2, PALB2) (Iqbal et al., 2012) (Jones et al., 2009). Although it is estimated that 5 to 10% of pancreatic cancers have an inherited component, the genetic basis for familial aggregation has not been identified in most cases (Klein et al., 2004; Roberts et al., 2016). Presently, in most cases of pancreatic adenocarcinoma, the causes of the disease are unknown.

Pancreatic cancer carries an extremely poor prognosis for several reasons. First, it is usually diagnosed at an advanced stage due to the lack of specific symptoms and lack of early detection methodologies inherent to other cancer types. Such early detection approaches include mammograms for breast cancer and colonoscopy for colon cancer. Second, pancreatic cancer is aggressive with early metastatic spread. Third, most pancreatic cancer is largely resistant to all current therapies including chemotherapy, radiotherapy, and molecularly targeted therapy. Finally, pancreatic cancer harbors multiple genetic and epigenetic alterations and has a complex and dense microenvironment. These factors contribute to the dismal overall 5-year survival rate of <7%. Almost all patients

who survive past 5 years are the 10-20% of patients who are qualified and have undergone surgical resection. The 5-year survival rate in this subgroup of patients is 15-25% (He et al., 2014).

Biological features and pathophysiology

The defining features of pancreatic adenocarcinoma include a very high rate of activating mutations in KRAS (>90%), progression from distinct types of precursor lesions, local invasion and distant metastasis, extensive stroma (desmoplasia) leading to hypovascularity and a hypoxic microenvironment, reprogramming of the cellular metabolism, and immune suppression.

Molecular carcinogenesis

Pancreatic cancer most frequently arises from pancreatic intraepithelial neoplasia (PanIN) but can also arise from other precursor lesions such as intraductal papillary mucinous neoplasms and mucinous cystic neoplasms (Tanaka, 2014; Ying et al., 2016). PanIN are microscopic premalignant pancreatic lesions associated with the pancreatic ducts harboring the signature mutations of pancreatic cancer. Like the stepwise model from polyp-to-adenocarcinoma established in colon cancer, pancreatic intraepithelial neoplasia progresses from low grade to high grade in types 1, 2, and 3. They are associated with accumulating genetic alterations.

Pancreatic cancer exhibit altered autocrine and paracrine signaling cascades that promotes cell proliferation and metastasis. Many signaling molecules such as transforming growth factor-a (TGF-a), insulin-like growth factor 1 (IGF 1), fibroblast growth factors (FGFs) and hepatocyte growth factors (HGH) and their respective receptors such as epidermal growth factor (EGFR), receptor tyrosine-protein kinase erbB-2 (HER2), HER3, IGF1 receptor (IGF1R), FGF receptors (FGFRs), and HGF receptors (HGFR) activate multiple pathways to enhance carcinogenesis and metastasis (Preis and Korc, 2011). In addition, pancreatic cancer cells also activate pro-survival and anti-apoptotic pathways such as signal transducer and activator of transcription 3 (STAT3), nuclear factor-kB (NF-kB) and AKT. Many genes such as WNT and NOTCH that are typically activated during development are also activated in pancreatic cancer.

Mutational landscape

More than 90% of all pancreatic cancer cases have activating KRAS mutations, and these mutations are already present at the earliest stage of PanIN (Kanda et al., 2012). Inactivating mutations of TP53, CDKN2A, and SMAD4 occur in 50-80% of pancreatic cancers and are detected with increasing frequency in type 2 and 3 lesions of PanIN. This suggests that KRAS mutations contribute to the initiation of tumor and the subsequent mutations in TP53, CDKN2A, and

SMAD4 occur as the tumor progresses (Hustinx et al., 2005). While point mutations of individual genes reveal many aspects of the disease pathophysiology, other types of genomic events also contribute to carcinogenesis. These genomic events include epigenetic modifications, deletions, and copy number alterations. For example, CDKN2A is commonly inactivated by DNA methylation, and CDKN2A and SMAD4 are commonly inactivated through homozygous deletion. Unfortunately, no therapy targeting KRAS, TP53, CDKN2A, and SMAD4 has been approved for the treatment of pancreatic cancer.

Microenvironment

One defining hallmark of pancreatic cancer is its dense collagenous stroma (desmoplasia) (DuFort et al., 2016; Seymour et al., 1994). The pancreatic cancer stroma is composed of both extracellular matrix (ECM) protein components and cellular elements. Other factors in the stroma that may interact with cancer cells include growth factors that can directly contribute to the survival of tumor cells (Neesse et al., 2013). The cellular elements of the stroma include proliferating myofibroblasts (also referred to as cancer-associated fibroblasts) that produce the collagenous matrix. The precursors of these myofibroblasts in the pancreas are the pancreatic stellate cells and in the case of liver metastasis, the precursors of the myofibroblasts are the hepatic stellate cells. An active bi-directional

interaction between the stromal stellate cells and cancer cells has been demonstrated (Apte et al., 2013; Ohlund et al., 2017). In addition, the stromal stellate cells can also contribute to immune evasion in pancreatic cancer by sequestering tumor-suppressive CD8+ T cells (Ene-Obong et al., 2013) and promoting action of myeloid-derived suppressor cells—an immunosuppressive innate immune cell population (Mace et al., 2013).

Although multiple studies have indicated a facilitating role for stromal stellate cells in progression and metastasis of pancreatic cancer, several studies using genetic techniques (Lee et al., 2014; Ozdemir et al., 2014) or signaling pathway inhibition (Rhim et al., 2014) have shown the opposite effect. It is likely that the stroma has context and timing dependent roles in pancreatic cancer.

Other cell types infiltrating the pancreatic tumor stroma include immune cells, endothelial cells, and neuronal cells. The immune cells include T cells, myeloid-derived suppressor cells and macrophages. The immune cell infiltrates in pancreatic cancer closely resemble an immunosuppressive phenotype which restricts immune surveillance and at the same time creates an inflammatory program that supports tumorigenesis. This immunosuppressive phenotype is observed both in early and late stage of the cancer (Amedei et al., 2014; Inman et al., 2014). From earliest stage of tumor formation, immunosuppressive regulatory

T cells and Gr1+CD11b+ myeloid cells (myeloid-derived suppressor cells) are recruited to the stroma leading to a blockage of T-cell mediated anti-tumor immunity. In addition, macrophages with tumorigenic potentials are recruited to early and advanced lesions (Lesina et al., 2011).

The microenvironment has many indirect effects on disease progression. Pancreatic tumors possess low microvascular density, leaky vasculature, limited profusion, and intramural hypoxia. The dense and fibrous stroma can potentially contribute to the reduced blood flow and the high interstitial pressure that has been hypothesized to impair drug delivery (Provenzano et al., 2012). This dense extracellular matrix results in an extremely hypoxic environment for cancer cells. In one study, physicians measured the oxygen tension in clinically resected pancreatic cancer and found the tumors to be extremely hypoxic (Koong et al., 2000) with oxygen tensions ranging from non detectable to 5.3 mm Hg. In comparison, the normal pancreatic tissue had oxygen tensions ranging from 24.3 mmHg to 92.7 mmHg in the same study.

Metabolic alterations

Pancreatic cancer is characterized by a severely hypoxic and nutrient-deprived microenvironment. Consequently the cancer cells must contend with this severe metabolic stress and a number of acquired alterations in nutrient acquisition and

use are required for the growth and survival of pancreatic cancer cells (Erkan et al., 2009). Many of these adaptive mechanisms by pancreatic cancer cells are driven by oncogenic KRAS and hypoxia-inducible transcription 1α (HIF1α). For example, oncogenic KRAS directly and indirectly promotes acquisition of extracellular nutrients such as increased glucose uptake, and directs the scavenging of serum lipids and proteins by an endocytic mechanism, macropinocytosis (Commisso et al., 2013). Oncogenic KRAS can also constitutively drive high level of autophagy to provide intermediate metabolites for biosynthesis and energy production (Yang et al., 2011).

Current therapeutic interventions

The majority of patients present with locally advanced and unresectable disease because of metastasis most commonly to the liver and peritoneum or vascular involvement. Fewer than 20% of patients have resectable disease, and 80% of patients who have undergo surgery and adjuvant treatment will relapse and ultimately die of the disease. While surgery is the only potential cure to the disease, the outcomes of patients treated with surgery are poor. Gemcitabine was first approved in 1997 by the FDA based on a randomized trial comparing gemcitabine with 5-fluorouracil. The clinical benefit achieved was symptom improvement and a modest survival benefit (Burris et al., 1997). In 2011, a

combination of folinic acid (leucovorin), 5-fluorouracil, irinotecan and oxaliplatinum (FOLFIRINOX) demonstrated improved overall and progression free survival benefits compared to gemcitabine monotherapy (Conroy et al., 2011). In 2012, gemcitabine and albumin bound paclitaxel showed improved efficacy compared to gemcitabine monotherapy and was approved by the FDA (Von Hoff et al., 2013). Currently, FOLFIRINOX and gemcitabine–nab-paclitaxel are considered standard treatment for patients who have good performance status and are more likely to tolerate the side effects of either treatments. To date, there has not been a widely adopted targeted treatment against pancreatic cancer.

Biomarkers for diagnosis and screening

The most widely used biomarker in pancreatic cancer is serum cancer antigen 19-9 (CA 19-9). CA19-9 lacks sensitivity or specificity to be useful for early detection of pancreatic cancer, but it is currently used to monitor disease progression (Ballehaninna and Chamberlain, 2012). A more sensitive and specific biomarker is needed to help in early detection of the disease and increase the number of patients who qualify for curative surgery.

Pancreatic cancer metastasis

Many factors contribute to the difficulty in treating pancreatic cancer. Most importantly, unlike cancers such as breast or colorectal cancer where many

patients are diagnosed at an early stage and can be treated by locally resecting the primary tumor, most pancreatic cancer patients present with advanced metastatic disease (Oberstein and Olive, 2013). Thus, in additional to developing effective screening methods, targeting metastasis is essential in treating pancreatic cancer.

Metastasis is the multi-step process of cancer cells breaking away from the primary tumor to enter the blood stream (intravasation), surviving in the blood circulation, arriving at a distal organ (extravasation) where the cancer cells must adopt specific phenotypes and mechanisms to survive in a foreign environment as micro-metastases, and proliferating into macro-metastases (colonization) (Gupta and Massague, 2006). The last step in cancer metastasis: colonization of the distal organ is hypothesized to be the rate-limiting step in metastasis, since large numbers of micro-metastases can form but will not develop into clinically significant macro-metastases (Hanahan and Weinberg, 2011). This hypothesis is supported by the case of colorectal cancer where resection of liver macro-metastasis can lead to long term survival (Fong et al., 1999), even though many tumor cells are likely to reach the liver and form dormant micro-metastasis (Taylor, 1996). Therefore, an ideal therapy against metastasis should target the rate-limiting colonization step to prevent or halt metastasis progression.

Metastasis has been hypothesized to occur early in pancreatic cancer. Clinical observations that patients with small or undetectable primary tumor still have high chance of metastasis and the common occurrence of metastasis after complete resection of the primary tumor supports this view (Tuveson and Neoptolemos, 2012). A recent study using a mouse genetic model to lineage trace pancreatic cancer cells also supports this hypothesis. In this mouse genetic model, micro-metastases in the liver are observed before the occurrence of invasive pancreatic cancer (Rhim et al., 2012). Circulating tumor cells were also observed in mice with pre-invasive pancreatic cancer (Rhim et al., 2012). Another study utilizing clinical imaging, autopsy data, and mathematical modeling approaches also predicted that most patients will have micro-metastases at the time of diagnosis even when the orthotopic tumor is relatively small (Haeno et al., 2012).

If most pancreatic cancer patients present with, or eventually will develop metastatic disease, therapies that target the primary tumor would only be palliative and the disease will progress rapidly. There is a lack of targeted therapy in pancreatic cancer that is able to effectively control metastatic progression, such as Herceptin for breast cancer (Slamon et al., 2001). Thus, there

is a great need to understand the molecular mechanism of PDAC metastasis and to design screening methods and novel therapies that are effective in suppressing metastatic progression, specifically at the rate-limiting, colonization step.

Experimental models

There are several widely used pancreatic cancer model systems *in vivo*. These experimental models have yielded important insight into pancreatic cancer pathophysiology. Experimental models used in this thesis include: traditional cancer cell lines, xenograft models (Caldas et al., 1994) and genetically engineered mutant mice (GEMM) syngeneic models (Aguirre et al., 2003; Guerra et al., 2007; Hingorani et al., 2003; Hingorani et al., 2005).

Syngeneic mouse model of pancreatic cancer tumorigenesis and metastasis

Mouse models of pancreatic cancer introduce the most frequently found human pancreatic cancer mutant alleles into the mouse pancreas. These GEMM models have confirmed the causative roles for many mutant gens previously identified in human pancreatic cancer genomes. For example, GEMM models have revealed the causative role of oncogenic KRAS to be sufficient to initiate PanIN and these mice spontaneously progress to locally invasive and metastatic pancreatic cancer closely resembling the human disease. Additional mutations in the canonical tumor suppressor genes that are also frequently found in clinical pancreatic

cancer genomes, such as CDKN2A, TP53, or SMAD4 have been shown to accelerate tumor progression with distinct histologies. The most widely used GEMM to study pancreatic cancer is with oncogenic Kras and mutant Tp53, and is referred to as the Kras LSL.G12D/+; p53 R172H/+; Pdx Cre tg/+ (KPC) mouse for the rest of the thesis.

One limitation of the GEMM is the cost and timeframe to develop and maintain the required mouse colony. Syngeneic mouse model using GEMM derived cancer cell line (Torres et al., 2013) allografted into a syngeneic mouse is one potential solution. This KPC syngeneic mouse model allows the study of the metastatic cascade under an immuno-competent background.

Xenograft model of pancreatic cancer metastasis

In order to study pancreatic cancer metastasis *in vivo* with human pancreatic cancer cells, xenograft mouse models in which cells are implanted or injected into immunodeficient mice are developed. Depending on the stage(s) of the metastatic cascade that are under investigation, investigators have transplanted or inoculated cells into mice at various sites (Loo et al., 2015).

Besides inoculation of pancreatic cancer at orthotopic sites (Kim et al., 2009), direct introduction of pancreatic cancer cells into the circulation can be

performed through portal vein injection or intrasplenic injection, both of which result in dissemination of pancreatic cancer cells into the portal circulation and into the liver parenchyma. Compared to intra-pancreatic injection, these procedures bypass the earlier stages of the metastatic cascade such as invasion of the primary tumor and intravasation into the circulation. Instead, survival of pancreatic cancer cells in the circulation and later stages are examined.

Regardless of which stage of the metastatic cascade is under investigation, xenograft models of cancer metastasis have proven of great utility in delineating the mechanisms involved in metastasis as *in vivo* modeling of cancer progression can provide insights that are not readily apparent in *in vitro* systems. A criticism of xenograft models of human cancer cell metastasis is that immunodeficient mice are used, which could not provide any information on interactions between the immune system and cancer cells. Thus, complimenting the xenograft model with the syngeneic mouse model will allow investigation into mechanisms that are crucial in the human disease yet account for the immune components.

***In vivo* selection**

In vivo selection of cancer cells is a technique pioneered by Fidler and colleagues in 1973 (Fidler, 1973). It can be utilized to enrich for specific cell populations with desired phenotypes from more heterogeneous populations. Within the context of cancer biology, *in vivo* selection had been utilized to select for breast cancer cells

with enhanced capacity for lung, bone and brain metastasis. Transcriptomic profiling and mechanistic studies comparing the parental heterogeneous breast cancer population and the *in vivo* selected organ-metastatic sub-lines had resulted in the identification of genes that regulate metastasis to the respective organs by breast cancer cells (Kang et al., 2003; Minn et al., 2005; Png et al., 2011; Tavazoie et al., 2008). More recently, *in vivo* selection was performed with melanoma cells and mediators of melanoma metastasis to the lungs were identified (Pencheva et al., 2012) as well as with colon cancer cells and promoters of colon cancer metastasis were also identified (Loo et al., 2015). Similar cellular phenotypes were identified in breast and melanoma cancer cells that were *in vivo* selected for lung colonization capacity, although different genes and pathways were utilized in breast cancer and melanoma respectively. This highlights the possibility that with regard to organ colonization, there might be common phenotypes that are selected for irrespective of cancer type. With regard to pancreatic cancer, an *in vivo* selection model for liver colonization, the final step of metastasis has not been yet been demonstrated. Given the utility of *in vivo* selection for identifying molecular mediators of breast, melanoma, and colon cancer metastasis, novel mediators of pancreatic cancer metastasis can be identified with an appropriate model of liver colonization and *in vivo* selection.

Innovation

To date, all approved chemotherapies for PDAC target proliferation of cancer cells and no targeted therapies are available. Attempts in adopting other targeted therapies such as Cetuximab (anti-EGFR) or Bevacizumab (anti-VEGF) have failed in stage III clinical trials (Ryan et al., 2014). Many studies of PDAC have focused on genes that are frequently mutated such as KRAS, p53, CDKN2A, and SMAD4. These highly mutated genes play essential roles in tumorgenesis and cancer progression; however, most of the known highly mutated genes in pancreatic cancer are tumor suppressors that cannot yet be therapeutically targeted. Most of the established targeted cancer therapies inhibit tumor promoters, such as vemurafenib (BRAF inhibition) in melanoma and trastuzumab (Her2 antibody) in breast cancer. The only widely mutated tumor promoter in pancreatic cancer, KRAS, has proven to be extremely difficult to inhibit therapeutically. In addition, while metastasis is the major cause of mortality in cancer, there has yet to be an approved therapeutic that specifically targets this step in cancer progression.

This project, which employs a combination of *in vivo* selection in mouse xenograft and syngeneic models coupled with transcriptomic profiling, presents an innovative approach in search for metastatic regulators that can be

therapeutically targeted. The highly liver-metastatic pancreatic cancer sub-lines isolated using *in vivo* selection allow the potential discovery of novel metastasis pathways that may not be pursued otherwise. Discovery of previously unexplored genes in the metastasis colonization pathway could also be the first step in developing targeted therapies in PDAC that can effectively treat metastatic disease.

Specific aims

Aim 1. Identify novel genes that regulate metastatic colonization of the liver by pancreatic cancer

Liver is the most common metastasis site in pancreatic cancer (Yachida and Iacobuzio-Donahue, 2009) and most gastrointestinal cancers. In order to study metastatic colonization of the liver by pancreatic adenocarcinoma cells, an *in vivo* selection approach was utilized to isolate highly liver-metastatic sub-lines from the poorly metastatic parental pancreatic cancer cell lines. The highly liver-metastatic sub-lines were then compared to the poorly liver-metastatic parental line by transcriptomic profiling using RNA sequencing. Genes that were differentially expressed between the highly metastatic sub-lines and the poorly metastatic parental line were hypothesized to play a significant role in metastatic colonization. The ability of these candidate genes to modulate metastasis was then assessed by gain-of-function and loss-of-function experiments in multiple pancreatic cancer cell lines using the *in vivo* liver metastatic colonization assay.

Aim 2. Characterize the cellular and molecular mechanisms utilized by these genes during metastasis colonization

To understand the molecular and cellular mechanisms employed by the candidate gene to modulate metastasis in the liver microenvironment, the cellular phenotypes that were likely to be involved were investigated.

Aim 3. Determine the clinical relevance, therapeutic potential, and diagnostic value of these metastasis-regulating genes in pancreatic cancer.

To determine whether the candidate gene is expressed by human pancreatic tumors, the expression of the candidate gene was assessed by qRT-PCR in both clinical PDAC samples and healthy pancreatic tissues. Potential diagnostic and therapeutic value of the candidate gene was evaluated.

Chapter II Materials and Methods

Animal studies

All animal work was conducted in accordance with a protocol approved by the Institutional Animal Care and Use Committee (IACUC) at The Rockefeller University. 5-6 weeks old age-matched male NOD-SCID-GAMMA mice were used for intrahepatic colonization assays, liver metastatic colonization assays, pancreatic orthotropic metastasis assays and orthotopic tumor growth assays involving PANC1, BxPC, MiaPaCa2, KPC, PANC1-LM3 and KPC-LM2 cell-lines. 5-6 weeks old age-matched male B6129SF1/J mice were used for experiments involving KPC cell line. For all experiments involving anesthesia and surgery, mice were monitored after surgery to ensure recovery from anesthesia before returning to clean cages. Breeding pairs of all mice strains were originally obtained from Jackson Laboratories and bred in house to establish colonies for experiments, with supplemental purchase from Jackson Laboratories when necessary.

***In vivo* selection**

5×10^5 PANC1 and KPC cells expressing a luciferase reporter were suspended in a 20 ul volume of 1:1 PBS/Matrigel mixture and injected directly into the livers of mice (intrahepatic injection, described in detail below). Pancreatic cancer liver nodules were allowed to develop over a period of 3-6 weeks and monitored by bioluminescence imaging. Nodules formed were excised and dissociated by collagenase and hyaluronidase digestion (described in detail below) into single cell suspensions. The cells were allowed to expand *in vitro* before re-injection into mice. After two to three iterations of *in vivo* selection, multiple highly metastatic PANC1-LM3 and KPCLM2 sub-lines were established from nodules obtained from independent mice. The *in vivo* selected cells were passaged 5 times *in vitro* and were visually checked to contain no murine primary stromal cells before all downstream analyses.

Intrahepatic injection for *in vivo* selection and liver colonization

Each mouse was first anesthetized with injection of ketamine/xylazine solution into the peritoneal cavity. When the mouse was deeply anesthetized (confirmed by lack of reflex response after pinching of hind legs), the fur above the abdomen

wall was shaved and the shaved abdomen wall was scrubbed with iodine and 70% alcohol. A 20 mm incision was made through the skin and peritoneum just below the sternum of the mouse to expose the liver. The left lobe of the liver was gently pulled out with a forcep and Q-tip, and cells in a 20μL volume of 1:1 PBS/ Matrigel (Corning) mixture were injected slowly using a 28-gauge needle attached to a 1/2 cc insulin syringe (Becton Dickinson). Blanching and bulging of the liver at the site of injection without reflux of injected cells indicated a successful injection. The needle was retracted slowly and a Q-tip placed over the site of injection with gentle pressure for about 20 seconds to prevent bleeding and spillage of injected cells. The left lobe was then returned to its original location using a Q-tip and the peritoneum of the mouse closed with surgical 6-0 sutures (Roboz) and the skin closed with 9mm wound clips (Roboz).

Intrasplenic injection for liver metastatic colonization assays

Each mouse was first anesthetized as described above. The left flank of the anesthetized mouse was shaved and scrubbed with butadiene and 70% alcohol. A 10 mm incision was then made in the skin and peritoneum just below the ribcage of the mouse to expose the spleen. The spleen was gently exteriorized with a pair of forceps and stabilized using a Q-tip. 3-5 x 10^5 Cells in 50μL volume of PBS were injected slowly using a 28-gauge needle attached to a 1/2 cc insulin

syringe. A blanching of the spleen without reflux of injected cells indicated a successful injection. The needle was retracted slowly and a Q-tip placed over the site of injection with gentle pressure to prevent bleeding and leakage of the injected cells. After 30 seconds, the spleen was removed using a cautery and the peritoneum of the mouse closed with surgical 6-0 sutures (Roboz) and the skin closed with 9mm wound clips (Roboz).

Pancreatic injection for orthotropic growth and metastasis assays

Each mouse was first anesthetized as described above. The left flank of the anesthetized mouse was shaved and scrubbed with iodine and 70% alcohol. A 10 mm incision was then made in the skin and peritoneum just below the ribcage of the mouse to expose the spleen with the pancreas attached. The spleen and pancreas were gently exteriorized with a pair of forceps and stabilized using a Q-tip. 5×10^5 Cells in a 20 µL volume of 1:1 PBS/Matrigel mixture were injected slowly using a 28-gauge needle attached to a 1/2 cc insulin syringe while the pancreas was stretched by holding the end of the spleen. A bulging of the pancreas without reflux of injected cells indicated a successful injection. The needle was retracted slowly and a Q-tip placed over the site of injection with gentle pressure to prevent bleeding and leakage of the injected cells. The

pancreas and spleen were returned into the original cavity location and the peritoneum of the mouse was closed with surgical 6-0 sutures (Roboz) and the skin was closed with 9mm wound clips (Roboz).

Retro-orbital injection of luciferin and DEVD-luciferin for bioluminescent imaging

Each mouse was anesthetized using an isoflurane anesthesia chamber. After anesthesia, the mouse was placed on its left flank and restrained using the thumb and index finger of the non-dominant hand. At the same time, the index finger and thumb were used to draw back the skin below the right eye of the mouse. 100μL luciferin substrate (Perkin Elmer) was then injected using a 28-gauge insulin needle on a 1cc syringe into the retrobulber sinus of the mouse. For *in vivo* caspase activity bioluminescent imaging, 100μL of amino-DEVD-luciferin substrate (15mg/mL) (Promega) was injected for bioluminescent imaging. 5 hours after imaging with DEVD-luciferin, regular luciferin substrate (15mg/mL) was injected and imaging performed to obtain a normalization signal. The needle was then retracted slowly and the anesthetized mouse can be placed into the IVIS imaging system for bioluminescent imaging. Mice were imaged with their abdomens facing up, at 30s after injection of luciferin and at 5 minute after injection of DEVD-luciferin. Images were taken with exposure times ranging

from 5s to 5min dependent on metastatic burden to avoid saturation of the CCD camera sensor, leading to inaccurate measurements.

Tail vein injection for lung and other distal organ metastasis assay

Intravenous tail vein injection was used to assess the lung and other distal organ metastatic capability of pancreatic cancer cells. Mice inoculated with pancreatic cancer cells were randomized for treatment. Each mouse was restrained using a restrainer (Braintree Scientific) designed for tail vein injection. The tail of the moue were then gently warmed in 37 degree Celsius water, and wiped with 70% alcohol. $2x\ 10^{6}$ pancreatic cancer cells in 100 μL of PBS were injected into the lateral tail vein of the mouse using a 27 1/2 -gauge needle attached to a 1cc syringe. A paling of the vein and noticeable delivery of PBS up the tail indicated a successful injection. The needle was retracted slowly and a kim-wipe was used to exert gentle pressure on the site of injection to stop the bleeding. The mouse was released after 30 seconds.

Subcutaneous injections for *in vivo* tumor growth assays

Each mouse was first anesthetized as described above. 1×10^6 cells were suspended in 100 µl of 1:1 PBS:Matrigel mixture and injected into the subcutaneous flanks of the anesthetized mouse using a 27-gauge needle on a 1-cc syringe. Tumor growth was measured using digital calipers starting 7 days after injection or whenever the tumor was palpable. Each mouse was anesthetized using an isoflurane anesthesia chamber. Palpable tumors were then grasped and measured. Volumes of tumors were calculated using the formula, Volume = $(\text{width})^2 \times (\text{length})/2$.

Liver extraction and tumor nodule extraction

Each mouse was first deeply anesthetized with a lethal dose of ketamine/xylazine solution. After confirmation of anesthesia from lethal dose of ketamine/xylazine or death, the abdomen was scrubbed with betadine and 70% ethanol. A 30mm incision was then made and the liver or other tumor nodules exteriorized using a small tweezer with the help of a Q-tip. The liver of the mouse or other tumor nodules were then cut free of the abdominal cavity and washed gently with PBS for three times. It could then be used for downstream experiments.

Tumor nodule dissociation into cells for culture

Each excised liver metastatic tumor nodule was first washed three times in PBS. After washing, the tumor nodule was minced up as finely as possible with a pair number 10 surgical scalpels and re-suspended in 15mL of antibiotics-supplemented PBS. The minced tumor nodule was then collected by centrifugation at 800g for 10 min using 50mL Falcon tubes. The PBS was removed and the nodule re-suspended in ACK buffer (Lonza) for lysis of residual red blood cells. After 10 min incubation at room temperature, the minced nodule was collected by centrifugation at 800g for 10 minutes, and re-suspended in enzymatic digestion media (300u/mL Collagenase, 0.25mg/mL Hyaluronidase, 24u/mL DNAseI; Worthington Biochemicals) and incubated with gentle agitation for 2hrs at 37 degree Celsius. After enzymatic digestion, cells were collected by centrifugation at 800g for 10 minutes. The pellet was re-suspended and incubated in 5mL trypsin-EDTA for 10min at 37 degree Celsius. After trypsin digestion, 10mL of D10F was added to stop the digestion and cells were collected again by centrifugation at 800g for 10 minutes. After the trypsin digestion, the supernatant was carefully aspirated until at least 5mL of cell culture media was left in the 50mL Falcon tube. The pellets and remaining media were then resuspended in 10mL of cell culture media, and filtered successively through 70μm and 40μm cell strainers to remove undigested debris and plated onto

treated cell culture plates. Freshly plated cells were monitored daily with exchange of fresh cell culture media for contamination and tested for mycoplasma contamination before transitioning into routine culture or other processing such as transcriptomic profiling.

***Ex vivo* tumor cell sorting from liver metastases in the xenograft model**

Immediately following tumor nodule extraction and single cell suspension as described above, xenografted human tumor cells could be sorted out from the other contaminating primary mouse cell using flow cytometry. Tumor cell suspension was centrifuged at 800g for 10 minutes at 4 degree Celsius and resuspended in 10mL of 22% OptiPrep (Sigma-Aldrich) diluted in regular cell culture media. Tumor cell suspension in 22% OptiPrep was layered on top of a 10 mL 40% Optiprep, and lastly a 10mL cell culture media was layered on top of the 22% OptiPrep. This density gradient was then centrifuged at 800g for 10 min at 4 degree Celsius. Cells at the 22% OptiPrep and cell culture media interface were collected. The cells were then washed once with regular cell media and centrifuged at 800g for 10 minutes at 4 degree Celsius. When the cell pellets approximately resembled 2-4 $x10^6$ PANC1 or PANC1 LM3 cells, they were resuspended in 400uL of FACS buffer (5 mg/mL BSA, 10 mM HEPES, 2.5 uM EDTA in PBS). 80uL of Mouse Cell Depletion Kit magnetic beads (Miltenyi

Biotec, 130-104-694) was added to the tumor cell suspension. The tumor cell and magnetic beads mixture was incubated at 4 degree Celsius for 15 minutes. In the mean time, 3mL of cold FACS buffer was used to wash the LS Columns (Miltenyi Biotec, 130-042-401). After the incubation of the magnetic beads with tumor cells, 5mL of cold FACS buffer was added to the magnetic beads and tumor cell suspension. This mixture was then added to the LS Columns and the flow-through was collected on ice. Lastly, 1mL of cold FACS buffer was added to the LS Column to wash out remaining cells. The flow-through was then centrifuged at 800g for 10 minutes at 4 degree Celsius and the cell number was counted. The tumor cells were resuspended in 40uL FACS buffer and a mixture of anti-human HLA conjugated with FITC (eBioscience, 11-9983-42) and anti-mouse IgG2a κ Isotype conjugated with APC (Biolegend, 116619) antibodies were added with the ratio of 1uL of each antibody per million cells. The samples were then sent to the flow-cytometry facility at The Rockefeller University and cells that were FITC + and APC- were collected. The collected cells were pure human pancreatic cancer cells and can be subsequently cultured or analyzed.

Plasma collection from mice

Each mouse was first deeply anesthetized with a lethal dose of ketamine/ xylazine solution. After anesthesia, the chest of the mouse was scrubbed with betadine and 70% ethanol. The chest cavity of the mouse was then quickly cut open and the heart exposed. Whole blood was collected from the mouse via cardiac puncture using a 27-gauge needle attached to a 1cc syringe. Up to 500µL of blood can be collected. The blood is collected in the lavender top, EDTA coated tube (BD). Cells were removed from plasma by centrifugation for 10 minutes at 1,000 x g using a refrigerated centrifuge. Collected serum was then aliquoted and stored at -80 degree Celsius.

***In vivo* inducible shRNA knock down of NPTX1**

PANC1 LM3 cells labeled with the luciferase reporter were transduced with lentivirus carrying the tet-on pLKO-shNPTX1 constructed. $3x10^5$ of the PANC1 LM3 cells transduced with the doxycycline inducible shRNA construct were injected through the spleen into the liver of 6-week old Nod-Scid-Gamma mice. The tumor cells were allowed to grow for 7 or 14 days, and the mice were randomly assigned to two groups. One group receive doxycycline chow and doxycycline water with glucose, while the other group receive amoxicillin chow

and water with glucose. Both groups receive fresh chow and water every 2 days. Bioluminescence signal from the liver was measured every 7 days.

Isolation of murine primary hepatic stellate cells

Murine primary hepatic stellate cells were isolated following published protocol (Mederacke et al., 2015). 10 week old B6 male mice were used for all murine primary hepatic stellate cell isolation.

Isolation of tumor infiltrating immune cells

Upon excision, tumors were finely minced and incubated in HBSS (Gibco) supplemented with 2% FCS (HBSS-2), Collagenase 8 at 0.05mg/mL (Sigma), 1mM sodium pyruvate (Gibco), 25mM HEPES (Thermo Fisher), and DNaseI at 10mg/mL (Roche) at 37C on a shaker at 80RPM for 30 minutes. The mixture was then thoroughly titrated and passed through a 70um filter and neutralized with HBSS-2 to dilute the collagenase. Tumor-infiltrating lymphocytes were subsequently purified via density gradient centrifugation using Percoll (GE Healthcare). Briefly, the cells were resuspended in 35% Percoll and then 70% Percoll was added to the bottom of the suspension by a glass Pasteur pipette. The suspension was spun at 2100 RPM for 20 minutes at room temperature with the brake off. After the spin, the pellet of red blood cells was removed, as well as excess percoll/buffer, leaving a purified population of tumor-infiltrating lymphocytes at the interface. The isolated lymphocytes were washed twice with HBSS-2 prior to staining.

Tumor Flow Cytometry

Cell staining for flow cytometry was performed on ice and protected from light. Cells isolated from tissue were incubated with Fc block (TruStain fcX, anti-mouse CD16/32 Ab, Biolegend) to prevent nonspecific binding. The relevant surface antibodies were diluted in Fc block and allowed to incubate for 20 minutes. Cells were subsequently washed and fixed (Fixation Buffer or Fix/Perm, for intracellular staining, BD Biosciences). For intracellular staining, relevant antibodies, diluted in Perm/Wash Buffer (BD Biosciences), were applied to cells and allowed to incubate for 30 minutes. After staining steps, cells were washed once with FACS buffer (25mM HEPES, 2% FBS, 10mM EDTA, 0.1% sodium azide in PBS) and filtered through 70um mesh prior to flow cytometry analysis. The stained cells were run on a LSRII Flow Cytometer using BD FACSDiva software (BD Biosciences). Data were processed on FlowJo software (Treestar). Forward and side scatter were used to exclude dead cells and doublets.

Cell culture

The PANC1, BxPC, MiaPaca2 cell-lines were purchased from ATCC. 293T, MiaPaca2, KPC (B6/S129), Lx-2 and PANC1 cells were cultured in DMEM media (Life Technologies) supplemented with 10% FBS (Sigma-Aldrich), sodium

pyruvate (Life Technologies), L-glutamine (Life Technologies), amphotericin B (Lonza) and penicillin-streptomycin (Life Technologies). BxPC cells were cultured in RPMI media (Life Technologies) supplemented with 10% FBS (Sigma-Aldrich), sodium pyruvate (Life Technologies), L-glutamine (Life Technologies), amphotericin B (Lonza) and penicillin-streptomycin (Life Technologies). For hypoxic cell cultures, cells were cultured in 0.5 % oxygen within a cell culture chamber with adjustable oxygen setting (Baker Ruskinn Invivo2 400 workstation).

Transcriptomic profiling

Total RNA was extracted from PANC1, PANC1-LM3, KPC, KPC-LM2 cells using a Total RNA Purification Kit (Norgen Biotek) with on-column RNAse free DNAse (Norgen Biotek) treatment. The total RNA extracted was then processed using the Ribo-Zero Gold rRNA Removal Kit (Illumina) following the manufacturer's protocol. The resulting RNA was prepared into a sequencing library using ScriptSeq™ v2 RNA-Seq Library Preparation Kit (Illumina) following the manufacturer's protocol. The resulting library was analyzed using Tapestation to check for the RNA quality before the library was sequenced using Illumina HiSeq 2500 by The Rockefeller University genomics core facility. Reads were first trimmed to remove linker sequences and low-quality bases using Cutadapt. TopHat2 was then used to map the reads to the human (RefSeq

transcriptome index hg19) or mouse transcriptome (RefSeq transcriptome index mm10). Cufflinks was then used to estimate RPKM (reads per kilobase per million mapped reads) values and compare parental and highly metastatic sub-lines samples.

Generation of lentivirus, retrovirus, knock-down, inducible knock-down, and over-expressing cells.

For generation of lentivirus delivering shRNAs or over-expression vectors, 293T cells were seeded onto 10cm plates such that cell confluency would be approximately 70% the next day. 3μg each of pRSV-Rev, pCMV-VSVG-G and pCgpV packaging vectors (Cell Biolabs) were co-transfected with 9μg the appropriate pLKO-shRNA, tet-on pLKO-shRNA, or pLenti-overexpression plasmids using 37.5 μl of Lipofectamine 2000 in antibiotic-free DMEM media. After 16hrs, the media was replaced with fresh antibiotic-free media. After 24hrs, virus-containing supernatant was collected and filtered through a 0.45μm filter. For transduction of cells, 2mL of the appropriate virus was used to transduce 1 x 10^5 cells in the presence of 8μg/mL polybrene. Media was replaced 24hrs later.

48 hrs after transduction, antibiotic selection was performed with either blasticidin (10- 15μg/mL) or puromycin (2-4μg/mL) for 2-7 days alongside a population of untransduced control cells. Selection is deemed completed after

un-transduced control cells were killed by antibiotic selection. After selection, cells were allowed to recover in selective antibiotic free media for 72hrs and tested for over- expression or knockdown of gene of interest by qRT-PCR and Western- blot where applicable. A list of the shRNA sequence is shown in Table 2.1. GeneBlock sequence of the C-terminus flag tagged NPTX1 is shown below, and cloning primers are shown in Table 2.2.

PCR for cloning or genomic DNA amplification

PCR for cloning or genomic DNA amplification was performed using Phusion enzyme (NEB) according to manufacturer's protocol. Generally 200 to 400ng of starting template were used. PCR products were visualized using gel electrophoresis, excised and purified using Qiagen gel-extraction kit. Restriction digest was performed NEB restriction enzymes, at 37 degree Celsius for 6hrs and ligation into appropriate vector performed using NEB T4 ligase, at 16 degree Celsius overnight.

Table 2.1 shRNA sequences

Gene	shRNA	Sequence
NPTX1	1	CCGGCGACGCGCTTCATCTGCACTTCTCGAGAAGTGCAGATGAAGCGCGTCGTTTTTG
NPTX1	3	CCGGCCCATGGAGATCCTCATCAATCTCGAGATTGATGAGGATCTCCATGGGTTTTTG
Nptx1	C	CCGGGAGACAAGTTTCAGCTGACATCTCGAGATGTCAGCTGAAACTTGTCTCTTTTTG
Nptx1	D	CCGGTGCGGACCAACTACATGTATGCTCGAGCATACATGTAGTTGGTCCGCATTTTTG
	Control	CCGGCAACAAGATGAAGAGCACCAACTCGAGTTGGTGCTCTTCATCTTGTTGTTTTTG

Sequence of gBlock NPTX1 with C-terminus flag tag

CGCATAGGATCCATGCCCGCTGGCAGAGCTGCGAGGACATGTGCGCTGCTCGCG
CTCTGCCTCCTCGGTGCGGGCGCCCAAGATTTTGGACCCACCAGATTCATCTGCA
CATCCGTGCCGGTTGACGCAGACATGTGCGCTGCCTCAGTGGCTGCAGGCGGCG
CTGAGGAGCTTAGATCTAGCGTACTTCAGCTCAGGGAGACAGTTCTGCAGCAGA
AAGAGACGATATTGTCACAAAAGGAGACCATTCGCGAGCTCACCGCTAAATTGG
GCCGGTGCGAATCTCAAAGCACCCTTGACCCCGGCGCTGGAGAGGCACGCGCA
GGGGGAGGCCGGAAACAGCCTGGCAGTGGCAAGAACACCATGGGGGACCTGTC
TCGGACGCCAGCTGCTGAAACCCTCAGTCAGCTGGGACAAACGCTGCAGAGTCT
TAAAACGAGGCTGGAAAATCTCGAACAATACTCCCGGCTTAACTCCTCCAGTCA
AACAAACTCCCTTAAGGATCTCCTGCAAAGCAAGATCGATGAACTGGAGAGACA
GGTGCTTAGTAGGGTCAATACACTCGAGGAGGGTAAAGGCGGCCCTAGAAACGA
TACAGAAGAAAGGGTGAAAATCGAAACTGCTCTGACAAGCCTTCACCAGAGGA
TATCAGAGCTGGAAAAGGGCCAGAAGGACAACAGGCCGGGAGACAAGTTCCAG
TTGACTTTCCCACTGAGGACCAACTACATGTACGCGAAAGTGAAGAAGTCCCTG
CCTGAAATGTACGCGTTTACTGTGTGTATGTGGCTCAAAAGCAGCGCTACTCCTG
GAGTGGGAACACCATTTTCTTACGCTGTTCCTGGCCAGGCAAATGAGTTGGTTCT
GATTGAATGGGGCAATAACCCCATGGAGATCCTGATAAACGATAAGGTGGCCAA
GTTGCCATTCGTGATCAATGACGGTAAGTGGCACCACATATGTGTCACATGGACC
ACAAGGGATGGCGTGTGGGAGGCCTACCAGGACGGGACCCAAGGGGGCTCCGG
GGAGAATTTGGCCCCTTACCACCCTATCAAACCCCAAGGTGTGCTCGTGCTGGGA
CAGGAGCAGGACACCTTGGGTGGAGGTTTTGACGCAACTCAAGCCTTCGTGGGG
GAACTGGCTCACTTCAACATCTGGGACCGCAAGCTGACCCCTGGAGAAGTCTAT
AATCTGGCCACGTGTTCTACAAAGGCTCTCAGTGGCAATGTTATTGCCTGGGCTG
AGTCACACATCGAGATCTATGGCGGCGCTACTAAGTGGACCTTCGAGGCC TGT
CGA CAA ATC AAC GAC TAC AAA GAC GAT GAC GAC AAG TGA

Table 2.2 Cloning primers

Cloning primer	Sequence
NPTX1 O/E Cflag F	CGCATAGGATCC ATG CCC GCT GGC AGA GCT GCG AGG ACA TGT GCG CTG CT
NPTX1 O/E Cflag R	CGC ATA GTC GAC TCA CTT GTC GTC ATC GTC TTT GTA GTC GTT GAT TTG TCG ACA

DsiRNA mediated gene knockdown

DsiRNA (IDT) was transfected into cells using lipofectamine 2000™ for 6 hours.

Cells were used for hypoxia proliferation assay 72 hours post transfection.

DsiRNA design ID that were used are shown in Table 2.3.

Table 2.3 DsiRNA ID

Gene	DsiRNA ID
NPTX1	hs.Ri.NPTX1.13.1
NPTX1	hs.Ri.NPTX1.13.2
NPTX1	hs.Ri.NPTX1.13.3
EGR1	hs.Ri.EGR1.13.1
EGR1	hs.Ri.EGR1.13.2
HIF1a	hs.Ri.HIF1A.13.1
HIF1a	hs.Ri.HIF1A.13.2

Analysis of mRNA expression

Total RNA was extracted from the various cell lines using Total RNA Extraction Kit (Norgen Biotek). For quantification of mRNA, 1μg of total RNA was reverse transcribed using the cDNA First-Strand Synthesis Kit (18080-051, Invitrogen). Approximately 50ng of the resulting cDNA was then mixed with SYBR green PCR Master MIX (4309155, Applied Biosystems) and appropriate primers (Table

2.4 and 2.5). Quantitative mRNA expression data was obtained using an ABI Prism 7900HT Real-Time PCR System (Applied Biosystems). GAPDH was used as an endogenous control for normalization.

Table 2.4 Human qRT-PCR primers

Gene	Forward primer	Reverse primer
GAPDH	AGCCACATCGCTCAGACAC	GCCCAATACGACCAAATCC
NPTX1	CCT GGA GAA CCT CGA GCA	GAT CCT TGA GGC TGT TGG TC
ACTA2	CGT GGC TAT TCC TTC GTT ACT AC	CAG GCA ACT CGT AAC TCT TCT C
EGR1	CTT CAA CCC TCA GGC GGA CA	GGA AAA GCG GCC AGT ATA GGT
HIF1a	GAA AGC GCA AGT CTT CAA AG	TGG GTA GGA GAT GGA GAT GC

Table 2.5 Mouse qRT-PCR primers

Gene	Forward primer	Reverse primer
Gapdh	AGGTCGGTGTGAACGGATTTG	GGGGTCGTTGATGGCAACA
Nptx1	CCA AGC TGC CGT TTG TAA TC	GAT AGG GTG CCA AGT TCT CTC
Acta2	CCG ATA GAA CAC GGC ATC AT	CTC CAG AGT CCA GCA CAA TAT

Cell proliferation assays in hypoxia, anoxia, and normoxia

For *in vitro* cell proliferation assays in normoxia, 8×10^4 PANC1 LM3 or PANC1 cells were seeded onto 6-well plates (Falcon) in triplicates. Cells were kept in culture for 6 days before collection through trypsin digestion and counted using the Scepter™ 2.0 Handheld Automated Cell Counter (Millipore) or stained with trypsin blue and counted using a hemocytometer. Experiments were repeated for at least three times. For *in vitro* hypoxia proliferation assays, 8×10^4 PANC1 LM3 or PANC1 cells were seeded in 6-wells plate in triplicates and were cultured in 0.5% oxygen (Baker Ruskinn Invivo2 400 workstation) in regular cell culture media for 6 days before counting. Experiments were repeated at least two times. Cell counts were normalized to that of control conditions. For *in vitro* anoxia proliferation assays, 8×10^4 PANC1 LM3 or PANC1 cells were seeded in 6-wells plate in triplicates and were cultured in anoxic condition using Bio-Bag™ (BD). Cells were cultured for 3 days and were washed once with PBS before being trypsinized for cell counting. Live and dead cells were counted after Trypan Blue staining using a hemocytometer. Only cells cultured in the same Bio-Bag™ are compared.

Collection of cell culture supernatant for western blot

6×10^6 cells were seeded onto 15cm cell culture dishes. After allowing cells to attach overnight, cells were washed gently three times with 15 mL PBS and routine culture media was replaced with 15mL serum free media and cultured for an additional 16 hrs. Supernatant was collected and filtered using 0.22 uL filter. The filtered supernatant was then centrifuged for 800g for 10min to remove debris. Subsequently, the supernatant was concentrated using a spin column with 10kD cut-off filter to approximately 250uL prior to downstream applications. To perform extracellular NPTX1 western blot, 750uL (or 3x volume of the filtered supernatant concentrate) of ice-cold acetone was added to 250uL of the concentrated supernatant and incubated in -20 degree celsius overnight. The supernatant-acetone mixture was then centrifuged at maximum speed in a table top centrifuge for 10 seconds under 4 degree celsius twice. The supernatant was then aspirated carefully and the pellets were left to dry in a fume hood on ice. After the remaining acetone evaporated, the pellets were resuspended in loading buffer . The samples were then boiled at 95 degrees celsius for 5 minutes, and

were span down at maximum speed for 5 minutes again at room temperature to ensure there was not precipitate and the whole pellet was completely dissolved.

Western-Blot

Cell lysates or concentrated extracellular supernatant were prepared by either lysing cells grown on 10cm plates in 1mL of RIPA buffer containing protease inhibitors or the supernatant collection method described above. Lysate or the supernatant concentrate were quantitated using Bio-Rad BCA kit. 40μg protein from cell lysates were separated on a 4-12% SDS-PAGE and transferred to a PVDF membrane. Membrane was blocked for 1hr in 5% milk in TBST (except for FLAG antibody, blocking was performed in 5% BSA in TBST for 1hr). Antibodies were incubated overnight in 5% BSA in TBST at 4 degrees with gentle rocking. The NPTX1 antibody was purchased from Abcam (Cat. ab191201, 1:500 dilution). (GAPDH antibody was purchased from Genetex (Cat. GTX627408, 1:5000 dilution). The FLAG antibody was purchased from Sigma (Cat. F3165, 1:1000 dilution). Horseradish peroxidase-conjugated secondary antibodies were purchased from GE Health Sciences and used at a dilution of 1:2000, in 2.5% milk in TBST for 1hr. In between antibody incubation, membranes were washed 3X in

TBST, 5mins per wash. Chemiluminescent detection of proteins was performed using Pierce ECL plus kit.

Histology

Livers were prepared by 48 hour fixation with 4% paraformaldehyde in 4C while shaking. After fixation, the livers were embedded in paraffin. 5μm thick paraffin sections were stained with primary antibodies shown in Table 2.6. Primary antibodies were detected using various Alexa Flour dye-conjugated secondary antibodies. Fluorescence was obtained using a Zeiss laser scanning confocal microscope (LSM 510).

Subcutaneous tumours were excised and submerged into 4% paraformaldehyde for 24 hours. The fixed tissue was embedded in paraffin and sectioned in 5 μm thick slices. Sections were stained with primary antibodies shown in Table 2.6. Primary antibodies were detected using various Alexa Flour dye-conjugated secondary antibodies. Fluorescence was obtained using a Zeiss laser scanning confocal microscope (LSM 510).

An intraperitoneal injection of 60mg/kg pimonidazole HCl/Hypoxyprobe (NPI Inc) was infused into each mice. 90 min after, the mice were anaesthetized and the livers were extracted following protocols described above. The livers were submerged in 4% paraformaldehyde for 24 hours at 4 degree Celsius shaking.

The livers were then embedded in OCT and frozen on dry ice. 10 μm section was cut and stained with pimonidazole antibody conjugated to Dylight™549. The sections were then imaged using a Zeiss laser scanning confocal microscope (LSM 510).

Table 2.6 Antibodies used in histology

Gene	Company	Clone	Host	Dilution
Vimentin	Vector Lab	VP-V684	Mouse	1:50
Ki-67	Abcam	ab 15580	Rabbit	1:200
Endomucin	Santa Cruz	V. 7C7	Rat	1:200
F4/80	Biorad	MCA497	Rat	1:100
aSMA	Millipore	ASM-1	Mouse	1:1000
aSMA	Abcam	E184	Rabbit	1:500

Mouse plasma NPTX1 ELISA

NPTX1 levels in mouse plasma of the xenograft pancreatic cancer model were quantified using the human NPTX1 ELISA kit (Biomatik, EKU06234) following the manufacture's protocol.

Analysis of Genomic Copy Number

Total genomic DNA was extracted and purified from cell populations using the DNeasy kit (Qiagen). For DNA content normalization, GAPDH was used as endogenous control. Primers used in the qRT-PCR for genomic copy number is shown in Table 2.7 .

Table 2.7 Genomic copy number qRT-PCT primers

Gene	Forward primer	Reverse primer
NPTX1	AAGACAACCGCCCTGGA	CACTCAATGAGGACCAGCTC
GAPDH	AGCCACA TCGCTCAGACAC	GCCCAATACGACCAAATCC

Patient derived pancreatic cancer cell lines, tumor sample RNA and normal pancreatic RNA

All patient derived pancreatic cancer cell lines and tumor sample RNA were generously shared by Dr. Christine Iacobuzio-Donahue from Memorial-Sloan Kettering Cancer Center. Normal pancreatic RNA was purchased from OriGene and Thermo Fisher Scientific.

Chapter III: The Systematic Discovery of Metastatic Regulators in Pancreatic Cancer

Establishment of xenograft and syngeneic mouse models to study liver metastatic colonization of pancreatic cancer cells

As a first step to discover novel metastatic regulators in pancreatic cancer, I performed *in vivo* selection to develop both syngeneic and xenograft mouse models comprised of poorly and highly metastatic pancreatic cancer cells. *In vivo* selection has already been successfully applied to study metastasis in multiple cancer models and identified important genetic programs that regulate various steps of the metastatic cascade (Loo et al., 2015; Pencheva et al., 2012; Tavazoie et al., 2008). This approach takes advantage of the heterogeneity of cancer cell populations, where small subpopulation of cells express enhanced metastatic capability. This subpopulation of cells possess survival advantages compared to the parental cells *in vivo*, and by injecting those parental cells into mice and isolating metastatic nodules and repeating the same process multiple times, this subpopulation of highly metastatic cells can be selected or isolated from the more heterogeneous parental population. Once the highly metastatic cells are selected, they can be compared at the transcriptomic level to the parental population to uncover the molecular signatures these highly metastatic cells utilize to metastasize. The highly metastatic subpopulation differentially express genetic programs that are crucial to cellular functions important to specific steps in the metastatic cascade. Based on this hypothesis, many prior studies have identified

molecular programs that functionally regulate metastasis by comparing the transcriptomic profiles of the *in vivo* selected, highly metastatic derivatives to the parental populations.

Most of the prior studies have performed *in vivo* selection using an immunocompromised mouse model in order to allow metastatic growth of human derived cancer cells. With the advancements in the murine pancreatic cancer models, it could also be possible to *in vivo* select a murine cancer models derived cell line under a syngeneic and immunocompetent background. This syngeneic model would take account into the immune regulation of metastasis when comparing the gene expression of highly metastatic cells and the lowly metastatic parental populations.

In order to identify genetic regulators of metastasis in pancreatic cancer, I chose to use the PANC1 human pancreatic cancer cell line because it is a widely used cell line available through ATCC and it contains the most prevalent mutations in KRAS and TP53. I used PANC1 line to perform *in vivo* selection using the immunocompromised Nod Scid Gamma mice. Nod Scid Gamma mice lack an adaptive immune system and nature killer cells, and have defective macrophages and dendritic cells to allow xenograft of human derived cell lines. To complement this approach I took advantage of a murine cancer cell line derived

from the mouse pancreatic cancer model: K-rasLSL.G12D/+; p53R172H/+; PdxCre (KPC mouse) (Torres et al., 2013) and performed *in vivo* selection under a syngeneic and immunocompetent context.

Since the majority of pancreatic cancer patients present to the clinic with seeded macro-metastases in distal organs, I was interested in identifying genetic programs that regulate the later steps of metastatic progression, especially distal organ metastatic colonization. The most common site of distal metastasis in pancreatic cancer is the liver. I performed *in vivo* selection to isolate a subpopulation of cancer cells that could better survive and colonize the liver. To perform this *in vivo* selection, I directly injected PANC1 and KPC cells intrahepatically to specifically select for a subpopulation of cancer cells with enhanced liver metastatic colonization capabilities and followed the injection by surgical resection of liver colonies, dissociation of cells, and subsequently re-injected the isolated cancer cells back into the liver (Figure 3.1).

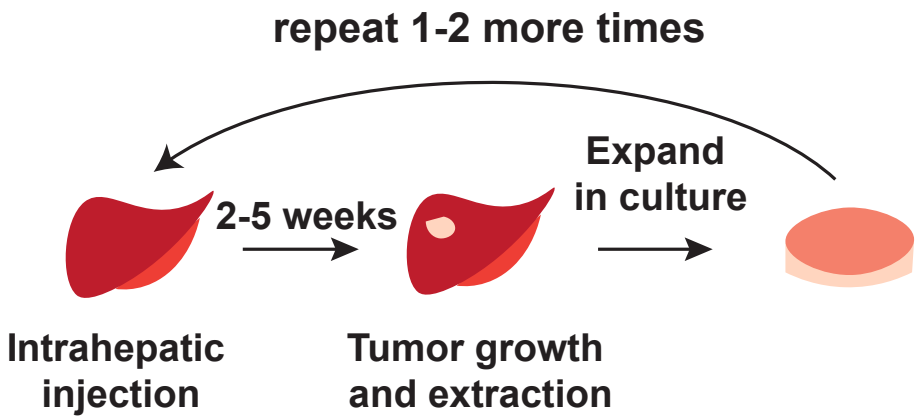

Figure 3.1 Schematics of the strategy to derive highly-metastatic pancreatic cancer cells using *in vivo* selection.

5×10^5 luciferase labeled PANC1 were intrahepatically injected into the immunodeficient Nod Scid Gamma mice with matrigel, and 5×10^5 luciferase labeled KPC cells were intrahepatically injected into the syngeneic and immunocompetent B6129SF1/J mice with matrigel. Tumor cells were monitored using bioluminescence imaging and allowed to grow for 2-5 weeks before tumor nodules were extracted and expanded *in vitro*.

After repeating this selection procedure two to three times, I isolated several second or third generation liver colonizing cells, KPC LM2 and PANC1 LM3 sublines. The independently derived KPC LM2 and PANC1 LM3 (Figure 3.2) sublines were passaged *in vitro* and their liver metastatic capabilities were compared by splenic injection of equal number of cells into the portal circulation. In both the xenograft and murine syngeneic systems, the *in vivo* selected PANC1 LM3 and KPC LM2 cells displayed significantly enhanced metastatic capabilities (>30 fold by third week in PANC1 LM3, and >100 folds by second week in KPC LM2, Figure 3.3 and 3.4)—arguing for successful achievement of *in vivo* selection for enhanced metastatic fitness in the liver.

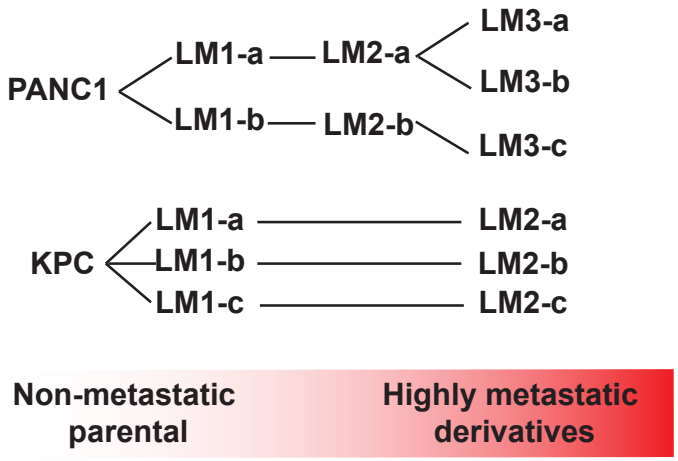

Figure 3.2 Lineages of the independently *in vivo* selected PANC1 and KPC cells. Multiple independently derived KPC LM2 or PANC1 LM3 cells were established using *in vivo* selection.

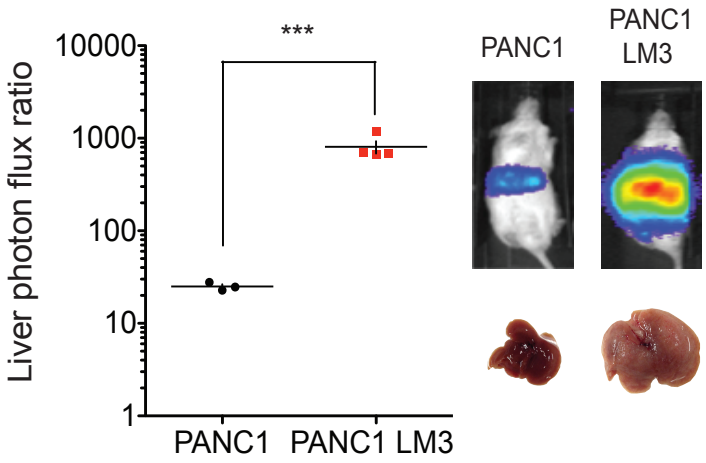

Figure 3.3 ***In vivo*** **selected PANC1 LM3 cells colonize the liver more efficiently compared to the parental PANC1 cells.** Highly metastatic PANC1 LM3 cells could colonize the liver 30 folds more efficiently compared to the PANC1 parental cells by day 19 after splenic injection of 5 x 10^5 cells into the NSG mice. ***P<0.001 by 2-tail student's t-test.

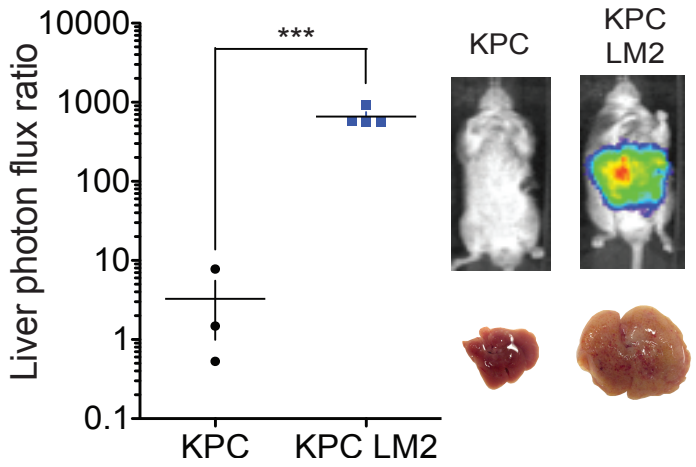

Figure 3.4 ***In vivo*** **selected KPC LM2 cells colonize the liver more efficiently compared to the parental KPC cells.** Highly metastatic KPC LM2 cells could colonize the liver 500 folds more efficiently compared to the KPC parental cells by day 12 after splenic injection of 3 x 10^5 cells into the B6129SF1/J mice. ***P<0.001 by 2-tail student's t-test.

While the parental PANC1 cells stalled and stopped further metastatic colonization of the liver after two weeks of initial growth, the highly metastatic PANC1 LM3 cells continued to grow rapidly until the liver was completely colonized and increased several fold larger in size (Figure 3.5). The enhanced liver metastatic colonization capability of the PANC1 LM3 cells were retained after more than 25 passages *in vitro* (Figure 3.6), demonstrating that the selected subpopulation of highly metastatic cells expressed metastasis promoting molecular programs that were inheritable.

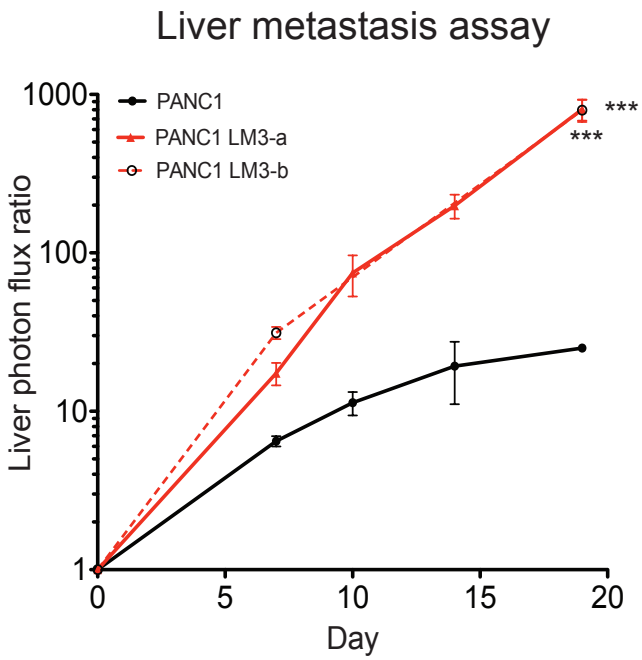

Figure 3.5 Liver metastatic colonization growth curves comparing parental PANC1 to the highly metastatic PANC1 LM3 sub-lines. The highly metastatic PNAC1 LM3 cells continued to colonize the liver while the parental PANC1 cells stalled in growth after the second week. Metastatic growth was monitored using bioluminescence imaging. ***P<0.001 by 2-tail student's t-test.

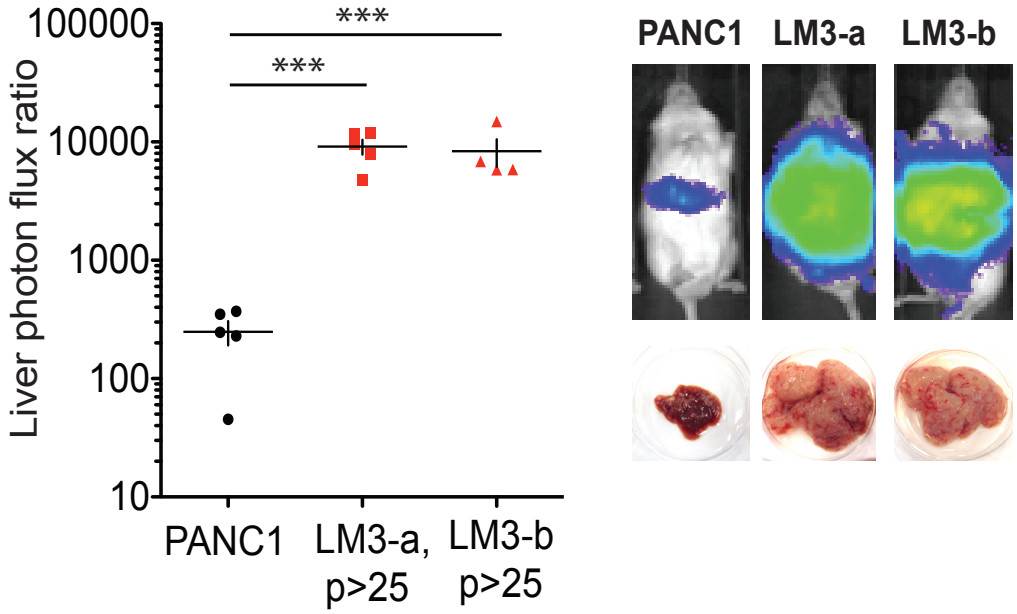

Figure 3.6 The highly metastatic PANC1 LM3 sub-lines retain the increased liver metastatic colonization capabilities after 25 passages *in vitro*. Two independently derived PANC1 LM3 cell lines were passaged *in vitro* for more than 25 passages and their liver metastatic colonization capabilities were compared to the parental PANC1 cells. Passaged PANC1 LM3 cells retained their highly metastatic capabilities. ***P<0.001 by 2-tail student's t-test.

Metastatic colonization, the formation of micro-metastases and subsequently macro-metastases, is a significant rate-limiting step during metastatic growth. The highly metastatic PANC1 LM3 cells were selected by their abilities to survive and grow in the liver microenvironment and when implanted into the pancreas of the Nod Scid Gamma mice, PANC1 LM3 cells were able to metastasize to distal organs such as the liver while the parental cells were unable to metastasize and mostly stayed locally in the pancreas (Figure 3.7). The highly metastatic KPC LM2 cells displayed similar traits (Figure 3.8).

To investigate if the *in vivo* selected PANC1 LM3 cells displayed organ specific tropism and could metastasize to the lung, I injected the PANC1 and PANC1 LM3 cells into the venous circulation. After the PANC1 LM3 cells were injected into the venous circulation via tail vein, five out of five mice developed widely-spread metastases in distal organs including the liver, lung, peritoneum and the adrenal glands while only two out of the five mice injected with parental cells exhibited limited metastatic growth (Figure 3.9). When implanted subcutaneously, the highly metastatic KPC LM2 cells also grew significantly faster compared to the parental cells (Figure 3.10). These findings reveal that the

in vivo selected PANC1 LM3 and KPC LM2 cells were highly metastatic to multiple distal organs as well as having enhanced tumor growth capabilities.

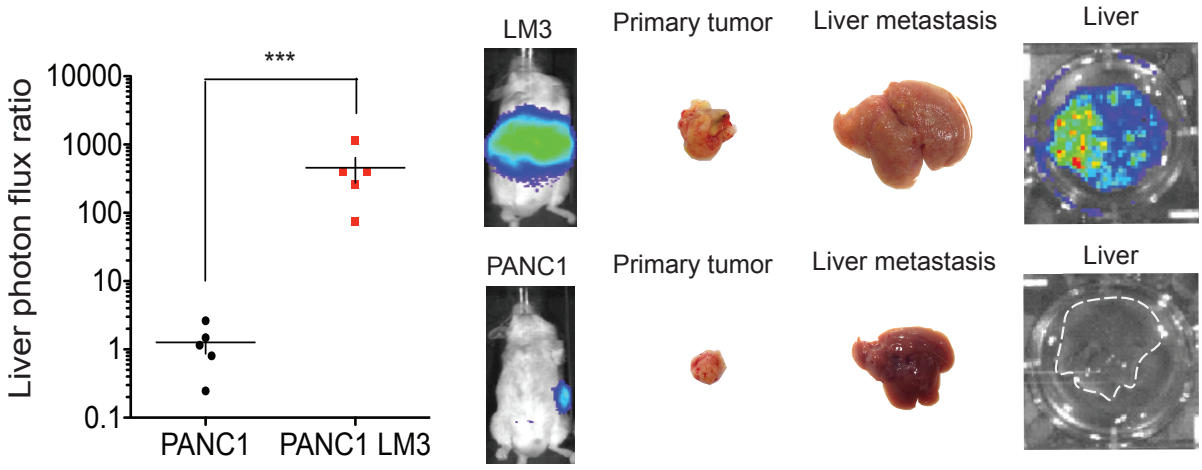

Figure 3.7 The highly metastatic PANC1 LM3 cells colonize the liver more efficiently from the pancreas compared to PANC1 cells. 5x 10^5 of PANC1 or PANC1 LM3 cells were injected into the pancreas of NSG mice with materiel. Mice were imaged and sacrificed 6 weeks post injection. *** $p<0.001$ using 2 sided student's t-test.

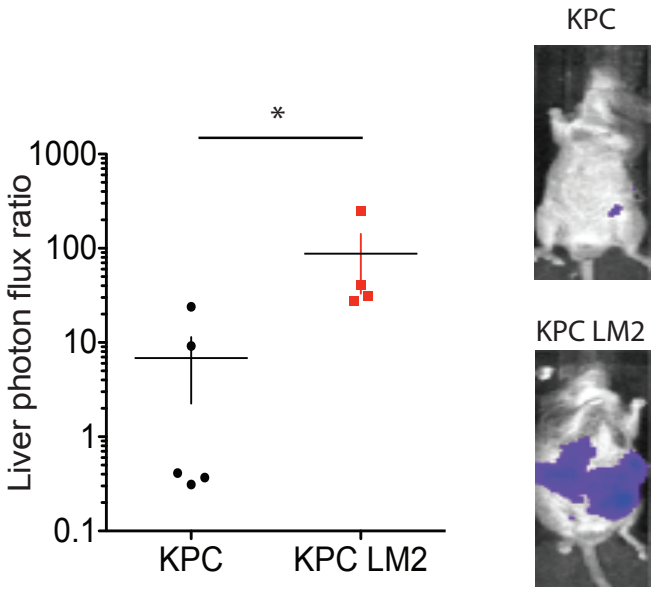

Figure 3.8 The highly metastatic KPC LM2 cells colonize the liver more efficiently from the pancreas compared to KPC cells. 3x 10^5 of KPC or KPC LM2 cells were injected into the pancreas of B6129SF1/J mice with materiel, and the mice were imaged and sacrificed 4 weeks post injection. *p<0.05 using 2 sided student's t-test.

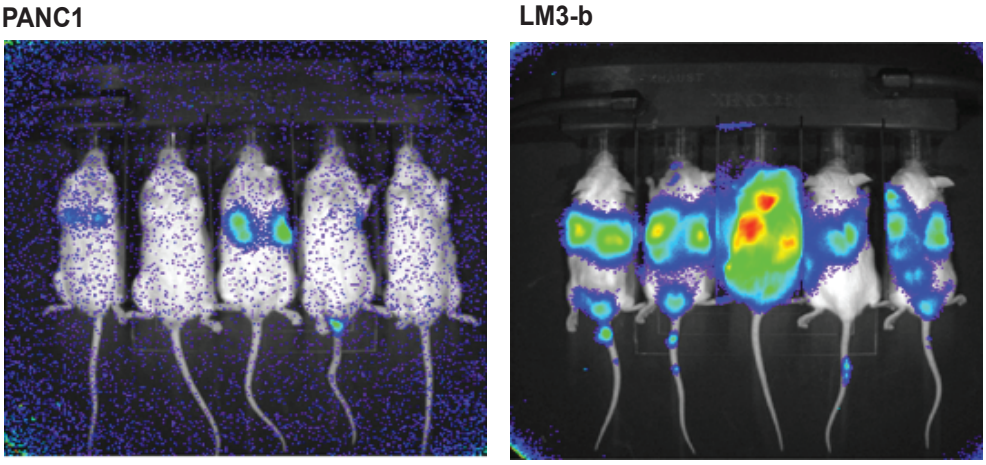

Figure 3.9 PANC1 LM3 cells have enhanced systemic metastatic capabilities compared to the parental PANC1 cells. 2x 10^4 PANC1 or PANC1 LM3 cells were injected via tail vein of the NSG mice. Mice were imaged at day 53.

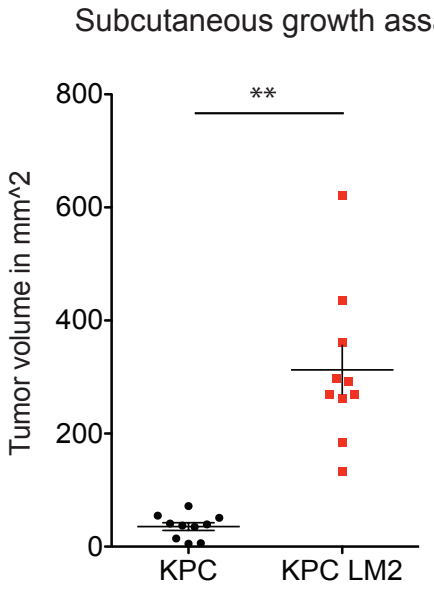

Figure 3.10 KPC LM2 cells have enhanced tumor growth capabilities compared to the parental KPC cells. 1x 10^6 KPC and KPC LM2 cells were injected subcutaneously and the tumor size was measured at day 28. ** $p<0.01$ using 2 sided student's t-test.

Highly metastatic pancreatic cancer cells express higher levels of NPTX1 than their respective parental populations.

We next sought to identify the molecular programs that led to the enhanced metastatic and tumor growth capabilities of the PANC1 LM3 and KPC LM2 cells. *In vitro*, both the PANC1 LM3 and KPC LM2 cells grew slower compared to their respective parental cell lines (Figure 3.11). Thus, *in vivo* selection did not select for faster growing cells and the enhanced metastatic and orthotopic tumor growth capabilities *in vivo* were not due to intrinsically faster growing cells. The *in vivo* selected PANC1 LM3 and KPC LM2 cells were specific subpopulations that could survive and proliferate at higher efficiency in the tumor microenvironment *in vivo*. Since the KPC LM2 cells were *in vivo* selected under an immunocompetent background, we sought to characterize the immune modulating capabilities of the highly metastatic KPC LM2 cells by profiling the infiltrating immune cells in the liver metastases. The KPC LM2 liver metastases exhibited multiple characteristics of tumor immunosuppression including decreased CD8+ T cells, increased myeloid derived suppressor cells, and decreased B-cells (Figure 3.12).

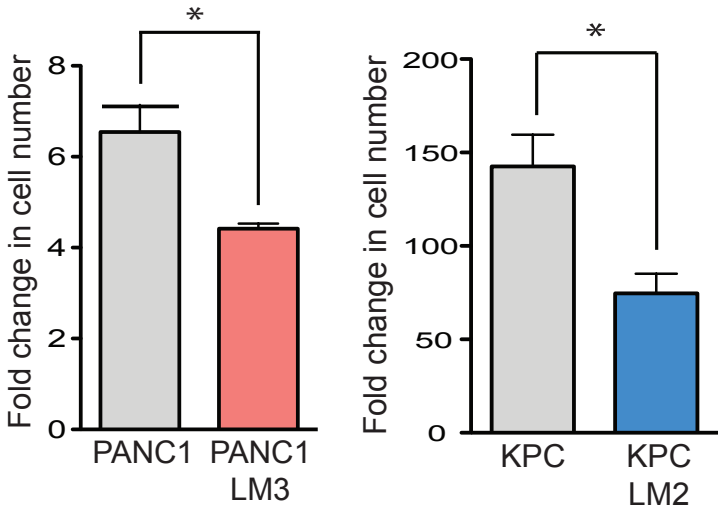

Figure 3.11 The highly metastatic PANC1 LM3 and KPC LM2 cells proliferate at a slower rate *in vitro* compared to the parental PANC1 and KPC cells. PANC1 LM3 cells proliferated at a slower rate compared to the parental PANC1 cells *in vitro* under standard cell culture condition. *In vivo* selected KPC LM2 cells also proliferated at a slower rate *in vitro* compared to the parental KPC cells population. * $p<0.05$ using 2 sided student's t-test.

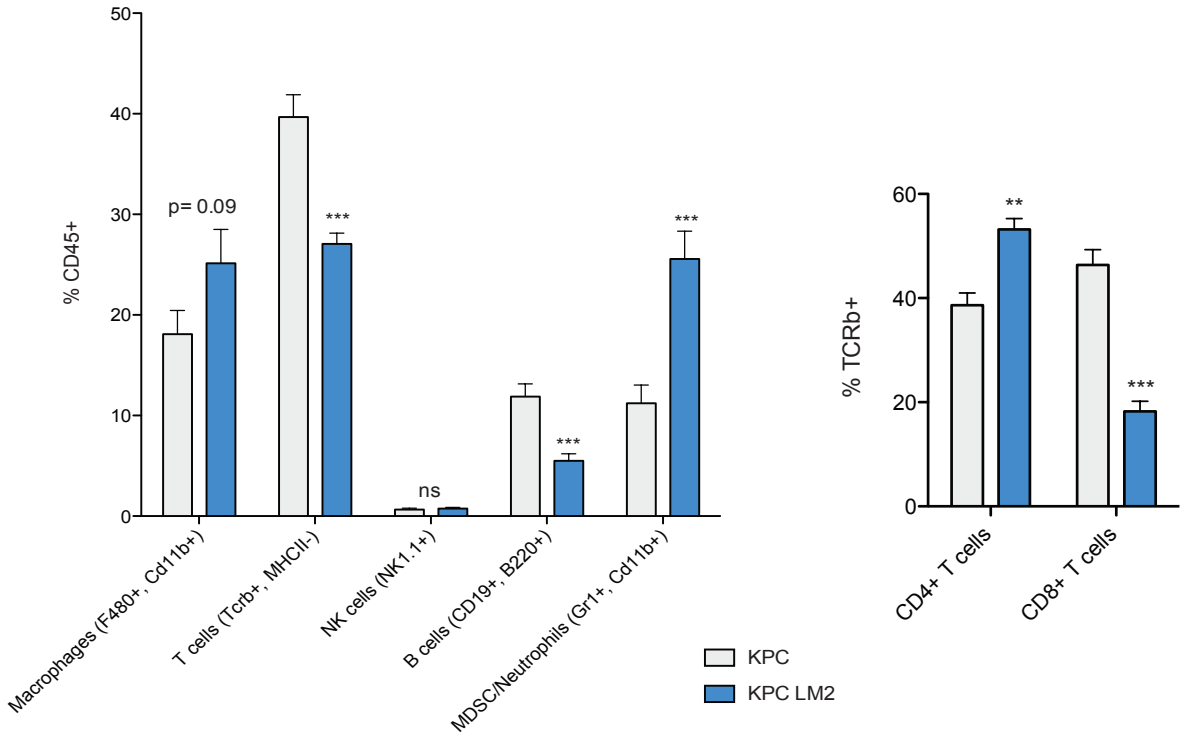

Figure 3.12 The highly metastatic KPC LM2 cells are associated with a immunosuppressive microenvironment in liver metastatic nodules. 5x 10^5 KPC or KPC LM2 cells were injected into the portal circulation. At Day 10, the murine livers with metastatic growth were harvested and the immune cell infiltrates of the liver metastases were profiled using flow cytometry. ** $p<0.01$ using 2 sided student's t-test. *** $p<0.001$ using 2 sided student's t-test.

To better understand the gene expression changes in the highly metastatic PANC1 LM3 and KPC LM2 cells, I performed transcriptomic profiling comparing the lowly metastatic parental cells, PANC1 and KPC, with three independently derived, highly metastatic PANC1 LM3 or KPC LM2 sub-lines to identify metastasis-regulating molecular programs. Compared to the parental PANC1 cells, the highly metastatic PANC1 LM3 cells expressed 154 significantly up-regulated genes (adjusted p-value <0.05) and 121 down-regulated genes. The highly metastatic KPC LM2 cells expressed 205 significantly up-regulated genes and 67 down-regulated genes (Figure 3.13) compared to their respective lowly-metastatic parental KPC cells.

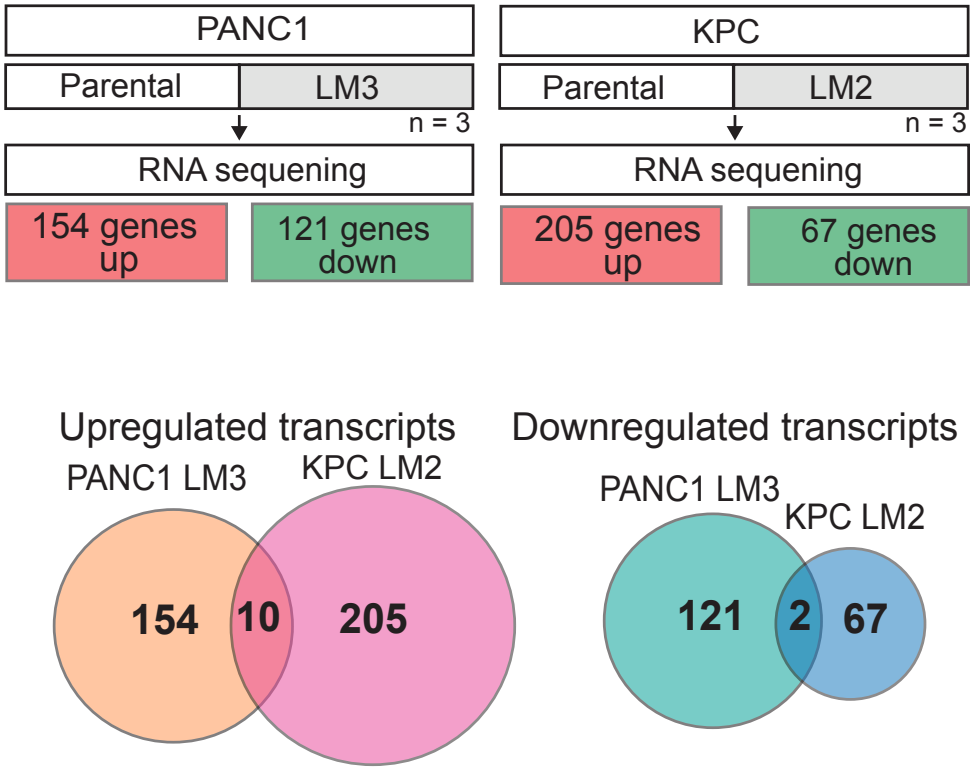

Figure 3.13 Transcriptomic profiling revealed 12 commonly de-regulated genes in both PANC1 LM3 and KPC LM2 cells compared to their respective parental PANC1 and KPC cells. Transcriptomic profiling was performed on three independently *in vivo* selected sub-lines in each system. 10 genes were commonly up-regulated in both PANC1 LM3 and KPC LM2 compared to the parental cells, and 2 genes were commonly down-regulated in both systems.

I then overlapped the significantly up-regulated and down-regulated genes to identify commonly de-regulated genes in both the xenograft and syngeneic systems. I found 10 commonly up-regulated genes and 2 commonly down-regulated genes. When these 12 commonly de-regulated genes were ranked by their average p-values among the xenograft and syngeneic models, the most significantly de-regulated gene identified was Neuronal Pentraxin 1 (NPTX1, Table 3.1). NPTX1 was expressed 7.45 folds higher on average in multiple independently selected PANC1 LM3 derivatives compared to the parental cells, and 7.57 fold higher on average in the multiple independently selected KPC LM2 derivatives (Table 3.1 and Figure 3.14).

NPTX1 is a secreted glycoprotein that is involved in synaptic plasticity and apoptosis upon oxygen and glucose deprivation in the nervous system (Schlimgen et al., 1995; Sia et al., 2007; Thatipamula and Hossain, 2014). It was previously described as exclusively expressed in the nervous system, and under healthy condition, NPTX1 was not expressed in the pancreas (Atlas, 2017). The function of NPTX1 outside of the nervous system has been poorly characterized, and the functional role of NPTX1 in cancer otherwise remains unknown.

Table 3.1 Commonly de-regulated genes ranked by average P-value. 12 genes were commonly de-regulated between PANC1 LM3 and KPC LM2 compared to parental cells. Genes were ranked by average P-value.

Gene ID		PANC1 LM3 (Log2 fold change)	KPC LM2 (Log2 fold change)	Average p-value
NPTX1	neuronal pentraxin I	2.91439	2.92003	3.18E-14
COL6A1	collagen 6A1	5.4328	2.13477	5.01E-11
DSC2	desmocollin 2	1.80064	3.41506	3.59E-08
RHOBTB3	rho-related BTB domain containing 3	-1.14907	-1.54822	1.14E-07
COL5A1	collagen 5A1	1.37378	2.04274	4.25E-07
COL6A2	collagen 6A2	5.96115	1.61443	9.48E-07
NES	nestin	1.42819	1.32981	3.44E-06
CLDN4	claudin 4	-1.92114	-2.05676	1.41E-05
DSG2	desmoglein 2	1.25029	1.43351	1.55E-05
NAV3	neuron navigator 3	2.89781	1.53956	9.34E-05
GLDC	glycine dehydrogenase	1.30227	1.89255	2.42E-04
CACNA2D1	calcium channel, voltage-dependent, alpha 2/delta subunit 1	1.28834	1.20153	2.69E-04

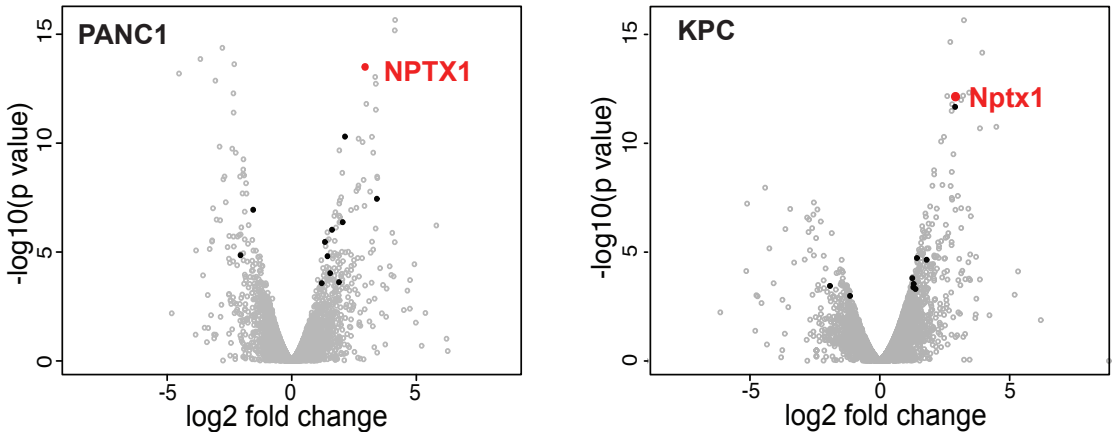

Figure 3.14 Volcano plot of transcriptomic profiling comparing the highly metastatic PANC1 LM3 and KPC LM2 cells to their parental PANC1 and KPC cells. The 12 commonly de-regulated genes are highlighted in black, while NPTX1 and Nptx1 are highlighted in red.

NPTX1 promotes human and murine pancreatic cancer metastatic and tumor progression.

To confirm the transcriptomic profiling findings, I validated the expression levels of human NPTX1 and murine Nptx1 in the highly metastatic sub-lines compared to the respective poorly metastatic parental cells. By qRT-PCR, I confirmed a consistent up-regulation of NPTX1 in the PANC1 LM3 and KPC LM2 sub-lines compared to their respective parental cells (Figure 3.15). To further investigate the functional role of NPTX1 in pancreatic cancer, I stably knocked down NPTX1 in PANC1 LM3 cells with two independent shRNA's delivered through a lentiviral mediated system and performed liver metastatic colonization assays (Figure 3.16). Suppression of NPTX1 in PANC1 LM3 cells led to robust reduction in liver metastatic colonization (>40 folds reduction by fourth week of liver metastasis assay) and knockdown of Nptx1 using two independent shRNA's in KPC cells also led to significantly reduced liver metastatic colonization (Figure 3.17 and 3.18). Knockdown of NPTX1 with two independent shRNAs in a second human pancreatic cancer cell line, MiaPaCa2 (P53 and KRAS mutants), also caused significantly reduced liver metastatic colonization (Figure 3.19).

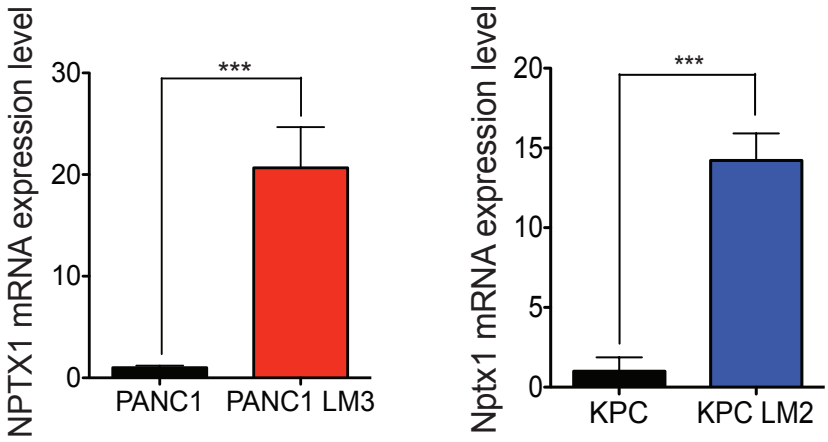

Figure 3.15 Highly metastatic PANC1 LM3 cells express NPTX1 at a higher level compared to the lowly-metastatic parental PANC1 cells. Highly metastatic KPC LM2 cells expressed Nptx1 at a higher level compared to the lowly metastatic parental KPC cells. *** p<0.001 using 2 sided student's t-test.

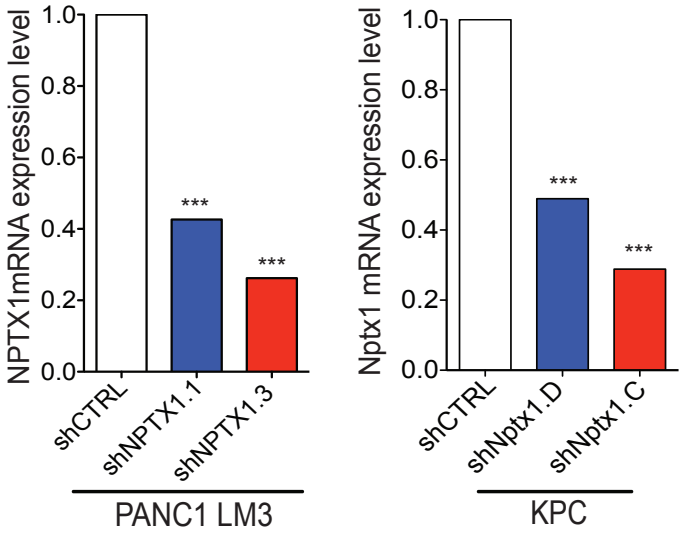

Figure 3.16 Depletion of NPTX1 in the PANC1 LM3 cells using a lentiviral mediated shRNA system yielded >50% knockdown with two independent shRNA hairpins. Depletion of Nptx1 in the KPC cells using a lentiviral mediated shRNA system also yielded >50% knockdown at the mRNA level. ***p<0.001 using 2 sided student's t-test.

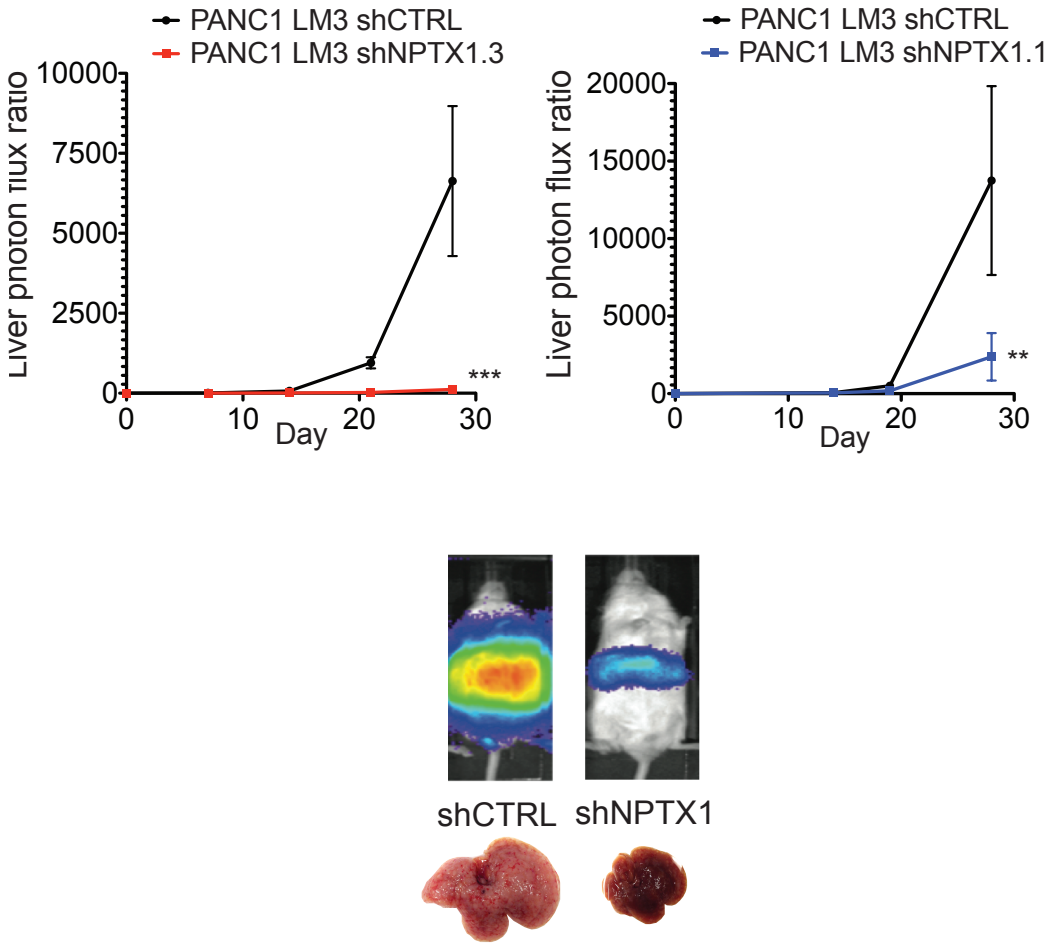

Figure 3.17 Endogenous NPTX1 promotes liver metastatic colonization by PANC1 LM3 cells. Depletion of NPTX1 using a lentiviral mediated shRNA system with two independent shRNA's in the highly metastatic PANC1 LM3 cells led to significant reduction in liver metastatic colonization *in vivo* using the NSG xenograft mouse model. ***p<0.001 using 1-sided student's t-test. **p<0.01 using 1-sided student's t-test.

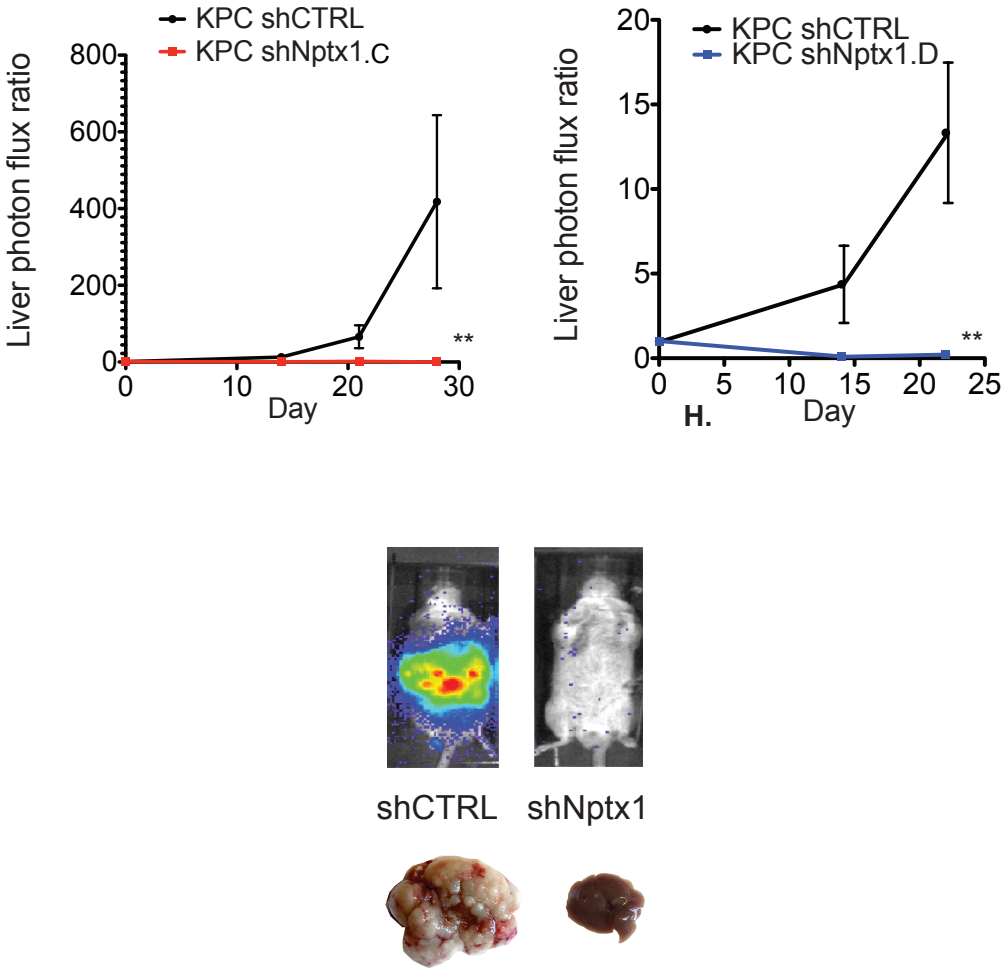

Figure 3.18 Endogenous Nptx1 promotes liver metastatic colonization by KPC cells. Depletion of Nptx1 using a lentiviral mediated shRNA system in the KPC cells led to significant reduction in liver metastasis i*n vivo* using a immunocompetent, syngeneic mouse model. **p<0.01 using 1-sided student's t-test.

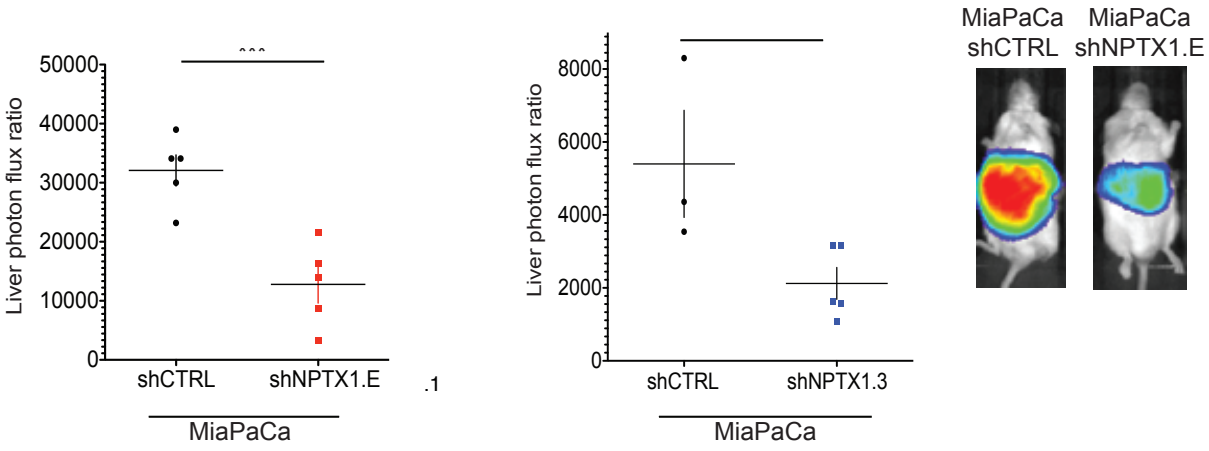

Figure 3.19 Endogenous NPTX1 promotes liver metastatic colonization by MiaPaCa cells. Depletion of NPTX1 using a lentiviral mediated shRNA system with two independent shRNA in the MiaPaCa cell line led to significant reduction in liver metastatic colonization *in vivo* using the NSG xenograft mouse model. ***p<0.001 using 1-sided student's t-test. *p<0.05 using 1-sided student's t-test.

The highly metastatic PANC1 LM3 derivatives not only had enhanced abilities to metastasize to distal organs, but also enhanced orthotopic tumor growth capabilities. NPTX1 knockdown in PANC1 LM3 cells also led to a reduction in orthotopic tumor growth (Figure 3.20), indicating that NPTX1 promoted growth in orthotopic tumors as well as metastatic sites. Additionally, orthotopic implantation of NPTX1 depleted PANC1 LM3 cells significantly decreased liver metastatic colonization (Figure 3.21), suggesting that suppression of NPTX1 expression was sufficient to inhibit distal organ metastasis.

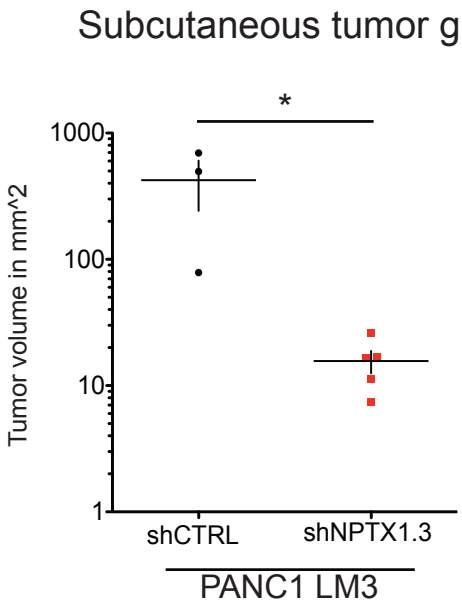

Figure 3.20 Endogenous NPTX1 promotes orthotopic tumor growth by PANC1 LM3 cells. Depletion of NPTX1 using a lentiviral mediated shRNA system in the highly metastatic PANC1 LM3 cells led to significant reduction in orthotopic tumor growth *in vivo* using the NSG xenograft mouse model. *$p<0.05$ using 2-sided student's t-test.

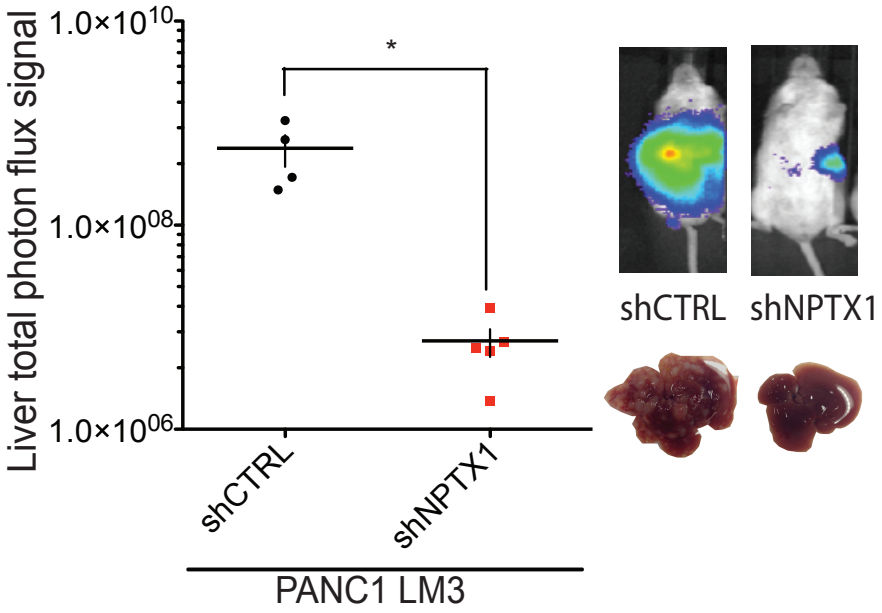

Figure 3.21 Endogenous NPTX1 promotes distal organ metastasis from the pancreas in PANC1 LM3 cells. Depletion of NPTX1 in PANC1 LM3 cells inhibited metastasis from the pancreas. 5x 10^5 PANC1 LM3 control or NPTX1 knockdown cells were injected into the pancreas with matrigel. Mice were imaged and sacrificed at week 5 after the injection. *$p<0.05$ using 2-sided student's t-test.

The highly metastatic PANC1 LM3 sub-lines differed from their PANC1 parental cells most significantly after the initial metastatic seeding, especially during the third week of growth in the liver as analyzed by bioluminescence imaging during metastatic colonization assays (Figure 3.5). Based on this observation, I investigated if NPTX1 promoted the growth of existing metastases by temporally suppressing NPTX1 expression after cancer cells were allowed to initially colonize the liver for several days. I generated a PANC1 LM3 cell line stably transduced with lentriviral particles carrying a doxycycline (DOX)-inducible shRNA targeting NPTX1. In the presence of DOX, NPTX1 expression was decreased, thus allowing us to observe the effect of down-reagulating NPTX1 *in vivo* post-colonization. We performed a metastatic colonization assay using NSG mice and assessed liver metastatic growth by bioluminescence imaging. Regular diet or diet containing DOX was given to the mice injected with PANC1 LM3 DOX-inducible NPTX1 knockdown cells 7 or 14 days after the injection (Figure 3.22 and 3.23 respectively). In both cases, suppressed metastatic progression was observed indicating that even after the initial establishment of macro-metastases, NPTX1 promotes distal organ metastatic outgrowth.

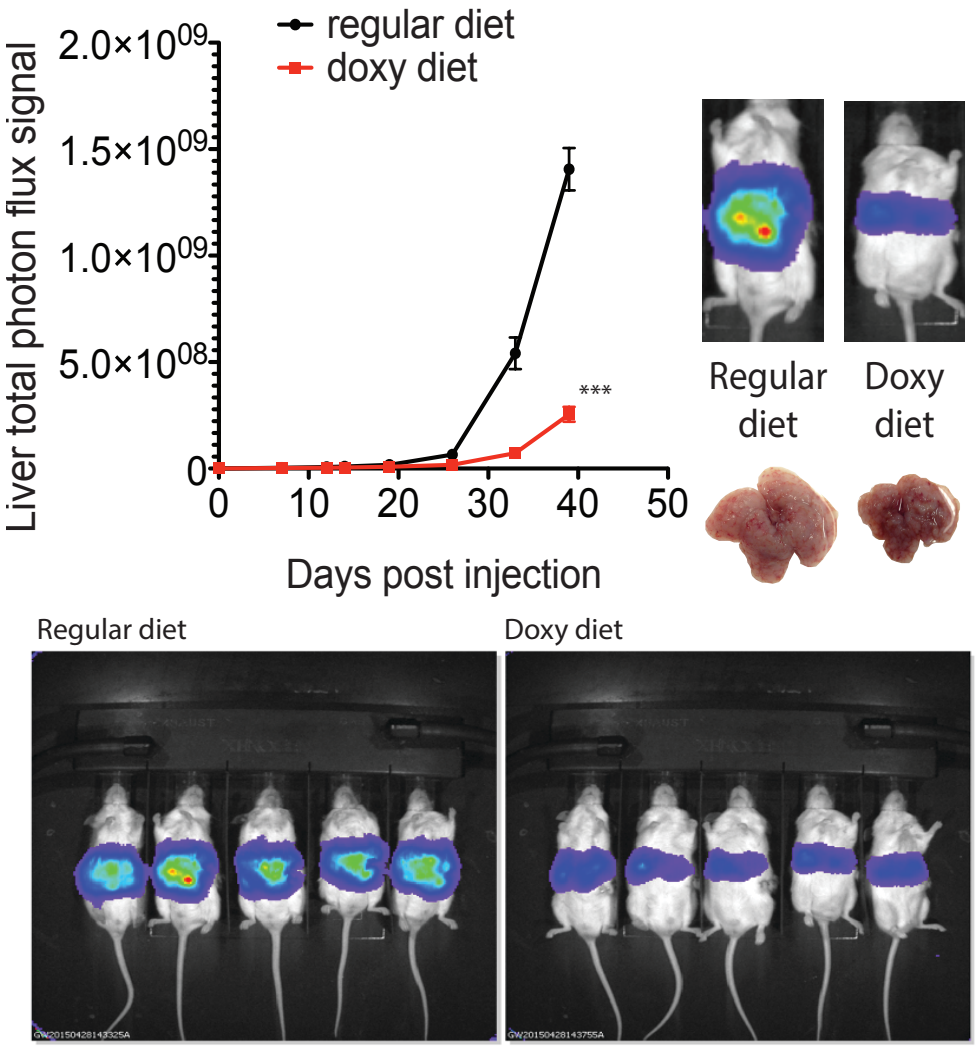

Figure 3.22 Temporal suppression of NPTX1 7 days post metastatic seeding decreases liver metastatic colonization. PANC1 LM3 cells were stably transduced with a doxycycline inducible shRNA against NPTX1. On day 0, 5x 10^5 PANC1 LM3 cells with the dox-inducible shNPTX1 construct were injected into the portal circulation of 10 NSG mice. On day 7, each mice was randomly assigned into either the regular diet or doxycycline diet group. Liver metastatic colonization was monitored using bioluminescent imaging and mice were sacrificed at day 39. ***$p<0.001$ using 2-sided student's t-test.

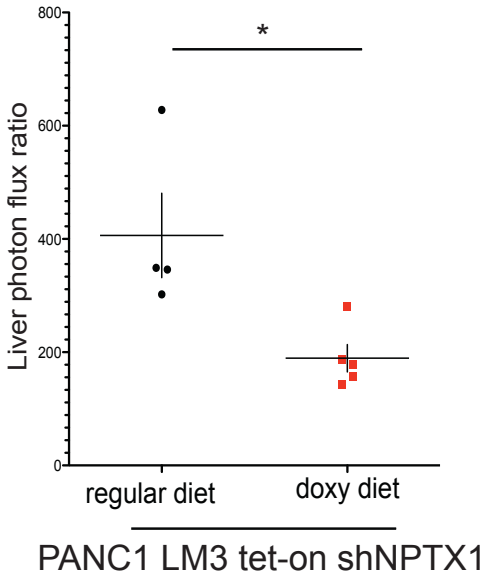

Figure 3.23 Temporal suppression of NPTX1 14 days post metastatic seeding decreases liver metastatic colonization. PANC1 LM3 cells were stably transduced with a doxycycline inducible shRNA against NPTX1. On day 0, 5x 10^5 PANC1 LM3 cells with the doxycycline inducible shNPTX1 construct were injected into the portal circulation of 10 NSG mice. On day 14, each mice was randomly assigned into either the regular diet or doxycycline diet group. Liver metastatic growth was monitored using bioluminescent imaging and mice were sacrificed at week 5. *$p<0.05$ using 2-sided student's t-test.

I concluded that NPTX1 was functionally necessary to promote both orthotopic tumor growth and progression of distal liver metastatic colonization. We next asked if NPTX1 over-expression was sufficient to enhance metastatic and orthotopic tumor growth by poorly metastatic cells. I generated parental PANC1 cells stably over-expressing NPTX1 protein or GFP control using a lentiviral mediated delivery system. PANC1 cells over-expressing NPTX1 colonized the liver at the same rate as PANC1 cells over-expressing GFP (Figure 3.24) *in vivo*. The pentraxin family proteins are known to form pentamers and higher order oligomers (Xu et al., 2003). The CMV promoter used to drive the expression of NPTX1 in PANC1 cells resulted in more than 100-fold increase in NPTX1 expression by mRNA and protein, and this high level of protein expression may inhibit the correct formation of NPTX1 oligomers. Consistent with this hypothesis, in the highly metastatic PANC1 LM3 cells with suppressed NPTX1 expression, over-expression of NPTX1 protein led to further decrease in liver metastasis compared to over-expression of GFP protein (Figure 3.25).

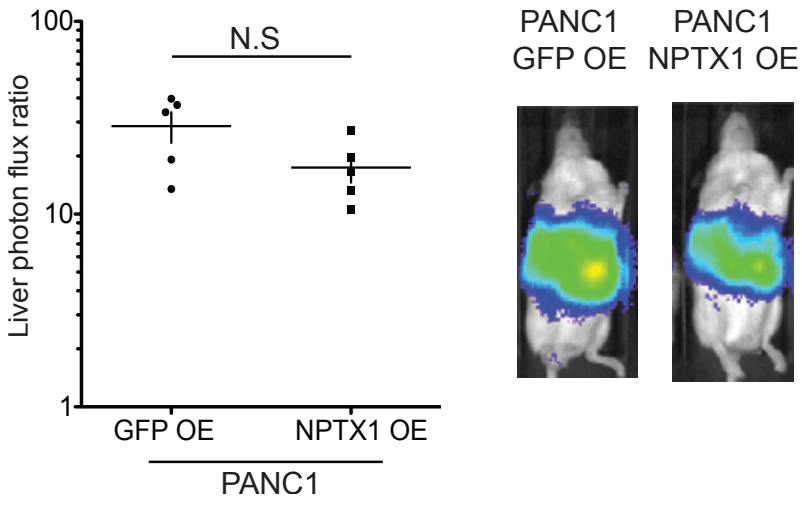

Figure 3.24 Over-expression of NPTX1 in PANC1 cells does not alter liver metastatic capability of cancer cells. 5x 10^5 PANC1 cells transduced with a CMV driven NPTX1 or GFP expression construct were injected into the portal circulation of NSG mice via the spleen. Mice were imaged and sacrificed at week 5.

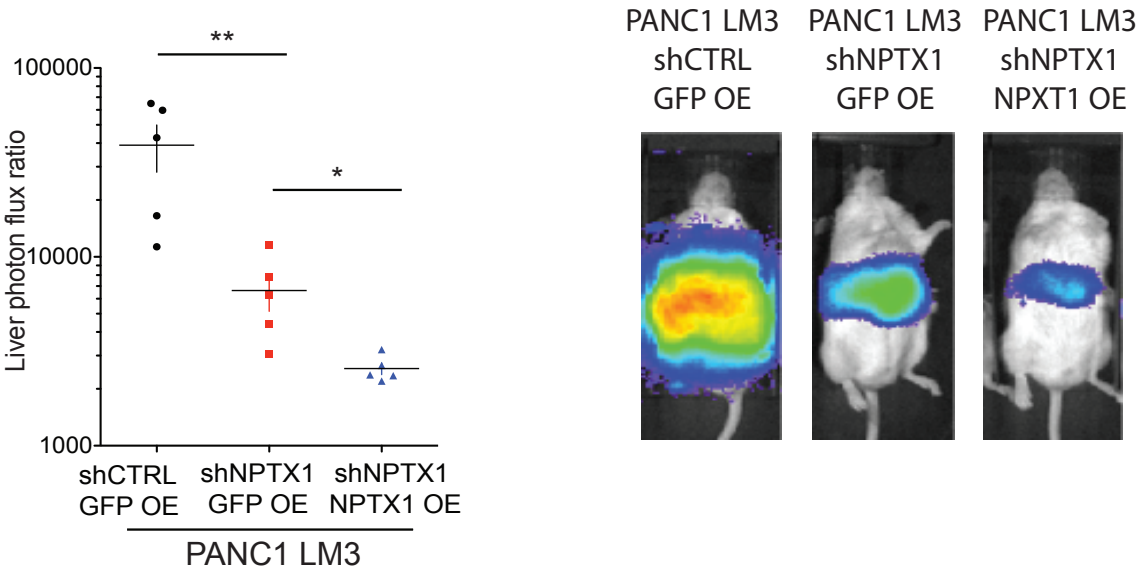

Figure 3.25 Over-expression of NPTX1 in PANC1 LM3 cells with NPTX1 knockdown lead to further suppression of liver metastatic colonization. 5x 10^5 cancer cells were injected into the portal circulations via the spleen. Mice were imaged and sacrificed at week 6. **p<0.01 using 2-sides student's t test. *p<0.05 using 2-sided student's t-test.

NPTX1 is secreted by pancreatic cancer cells and is regulated in part by epigenetic mechanism(s) and the EGR1 transcription factor

NPTX1 contains a signal peptide and is known to be secreted by neurons (Sia et al., 2007). Because NPTX1 expression by pancreatic cancer cells was not previously described, I examined if the pancreatic cancer cells also secreted NPTX1 into the extracellular space. Consistent with the enhanced expression observed at the mRNA level, I was able to detect higher levels of NPTX1 proteins by western blot in the extracellular media of highly metastatic PANC1 LM3 cells compared to the poorly metastatic PANC1 cells (Figure 3.26). In neurons, NPTX1 forms high molecular weight oligomers (Xu et al., 2003). I over-expressed NPTX1 in the PANC1 LM3 cells using a CMV promoter and found that NPTX1 was capable of forming oligomers of various molecular weights (Figure 3.27). Endogenously, the highly metastatic PANC1 LM3 cells secreted high MW oligomers of NPTX1 at a higher levels compared to the parental PANC1 cells (Figure 3.28).

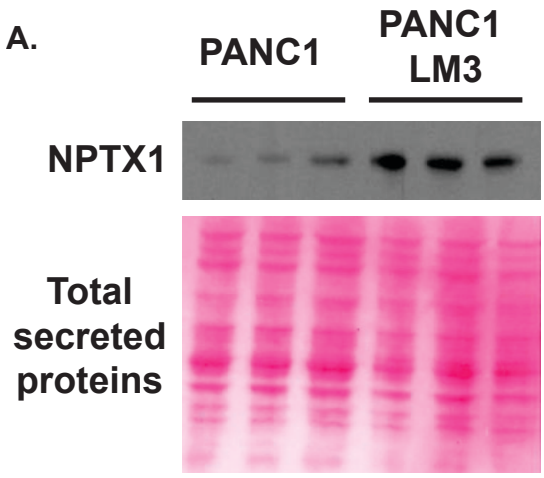

Figure 3.26 The highly metastatic PANC1 LM3 cells secret NPTX1 into the extracellular space at higher quantity compared to the lowly metastatic PANC1 cells. Top panel: NPTX1 western blot of PANC1 and PANC1 LM3 extracellular medium. Bottom panel: total secreted protein in the extracellular medium stained by Ponceau Red.

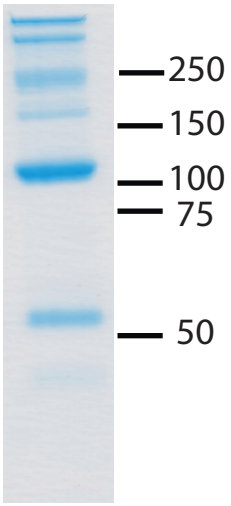

Figure 3.27 Recombinant NPTX1 protein forms multiple oligomers *in vitro*. A C-terminus flag tag was added to the NPTX1 protein for purification.

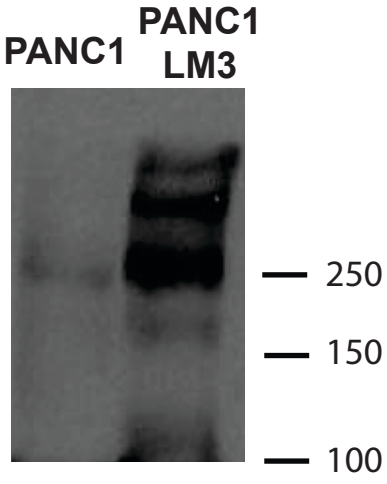

Figure 3.28 Endogenous NPTX1 protein in the extracellular space form high molecular weight oligomers in both PANC1 and PANC1 LM3 cells

We next investigated the mechanism of NPTX1's expression in highly metastatic pancreatic cancer cells. A technician in the laboratory, Logan Mandez characterized the genomic copy number of NPTX1 in PANC1 compared to PANC1 LM3 cells by qRT-PCR. Using this technique, we found that the NPTX1 genomic copy number was unchanged, indicating that gene amplification was unlikely to be the cause of the higher expression levels in the highly metastatic PANC1 LM3 sub-lines (Figure 3.29). We then sought to test the potential role of promoter methylation silencing of NTPX1 in pancreatic cells that could be lost during metastatic progression. To test this hypothesis, I treated the parental PANC1 cells *in vivo* with the DNA-methylase inhibitor 5-Azacytidine for 5 days. This 5-Aza treatment resulted in a 2.2-fold increase in NPTX1 expression in PANC1 cells as measured by qRT-PCR (Figure 3.30), suggesting that de-repression of promoter methylation of the NPTX1 gene could be one mechanism to enhance expression levels in the highly metastatic cancer cells. These results are consistent with the literature where it has been proposed that epigenetic modifications affects pancreatic cancer progression (McDonald et al., 2017) as well as many other type of cancers (Esteller, 2008).

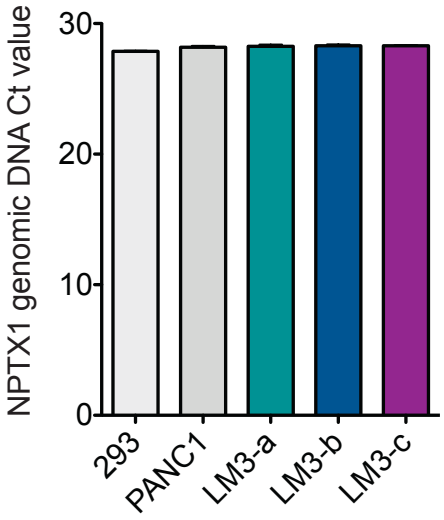

Figure 3.29 Genomic copy number of NPTX1 in 293, PANC1 and multiple sub-lines of the PANC1 LM3 cells measured by qRT-PCR. Genomic copy number was unchanged among PANC1 and the highly metastatic sub-lines.

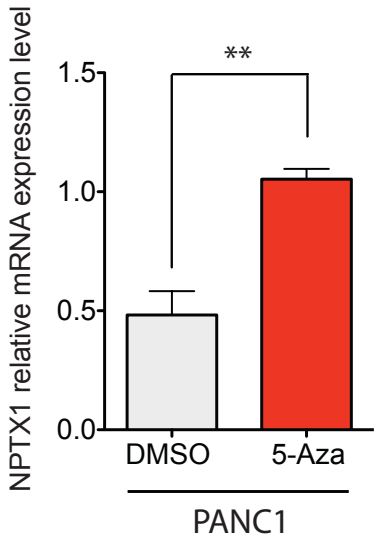

Figure 3.30 5-Azacytidine, a DNA methylase inhibitor, treated PANC1 cells up-regulate NPTX1 expression. PANC1 cells were treated with DMSO or 5-Aza for 5 days. NPTX1 expression level was measured using qRT-PCR. **p<0.01 using 2-sides student's t test.

I next searched for potential transcription factors with binding sites in the promoter region of NPTX1. If my hypothesis was correct and demethylation of the NPTX1 promoter was enough to enhance the expression of this gene then the transcription factor(s) responsible for the transcription of NPTX1 must be present already in the parental cell population. I searched for potential transcription factors with binding site in the promoter region of NPTX1. Using the UCSCS genome browser (https://genome.ucsc.edu) that contained information from Encyclopedia of DNA Elements (ENCODE) with experimental chromatin immunoprecipitation sequencing data obtained from multiple transcription factors, I identified a number of candidates that could potentially activate the transcription of NPTX1 (Figure 3.31).

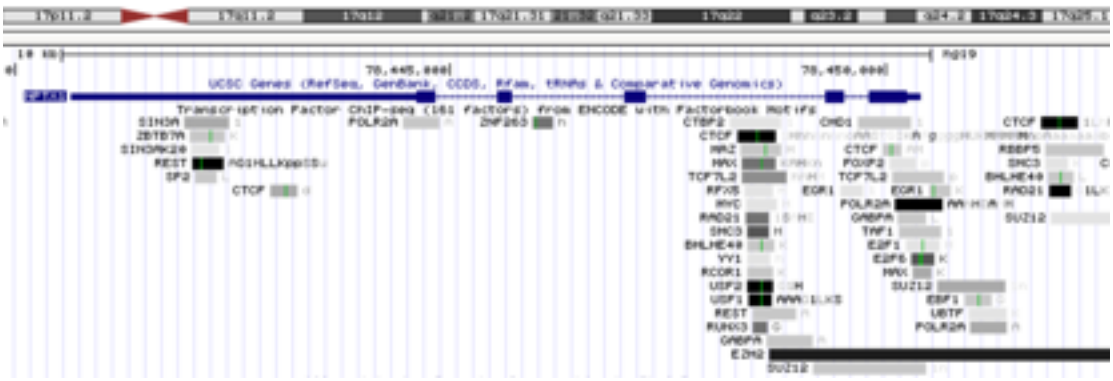

Figure 3.31. Transcription factor binding sites in NPTX1 promoter. TF binding sites from experimental chromatin immunoprecipitation sequencing data archived in the Encyclopedia of DNA Elements (ENCODE) project in UCSC genome browser.

Among those candidates, EGR1 was shown previously to affect the expression of multiple target genes including NPTX1 (Zhang et al., 2014). To test the role of EGR1 in NPTX1 expression I transiently depleted EGR1 using two independent siRNAs. EGR1 down-regulation led to reduced expression of NPTX1, suggesting that NPTX1 expression in the PANC1 cells may be at least partially regulated by the EGR1 transcription factor (Figure 3.32).

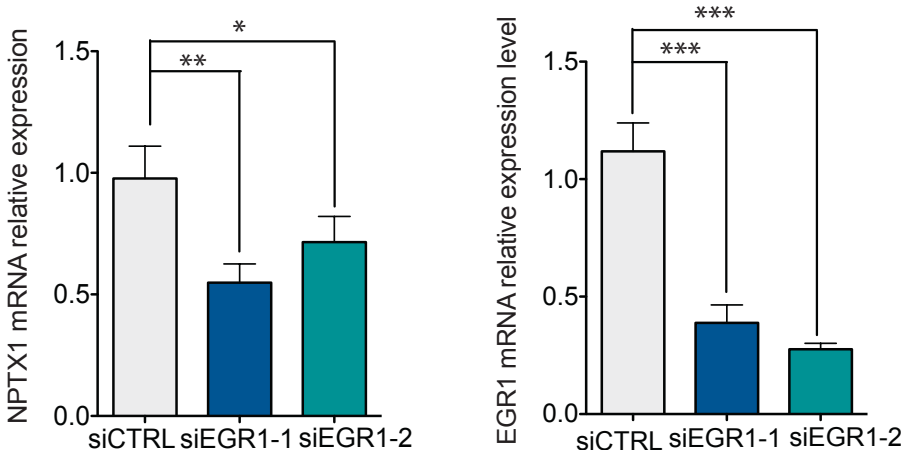

Figure 3.32 Depletion of EGR1 with siRNA lead to suppressed NPTX1 expression in PANC1 LM3 cells. PANC1 LM3 cells were directly transfected with two independent siRNA against the transcriptional factor EGR1. NPTX1 and EGR1 expression level was determined by qRT-PCR 5 days post transfection. ***p<0.001 using 1-sides student's t test. **p<0.01 using 1-sides student's t test. *p<0.05 using 1-sides student's t test.

Summary of Chapter III

In Chapter III, I sought to identify novel metastasis regulators in pancreatic cancer by first establishing both xenograft and syngeneic mouse model systems by using *in vivo* selection. The human PANC1 and murine KPC pancreatic cancer cell lines were selected for their outgrowth in the livers of mice. After two to three rounds of *in vivo* selection, PANC1 LM3 and KPC LM2 cells were isolated and their metastatic and orthotopic tumor growth capabilities were evaluated. The *in vivo* selected PANC1 LM3 and KPC LM2 cells exhibited decreased proliferation *in vitro*, but increased multi-organ metastatic and orthotopic tumor growth capabilities *in vivo,* demonstrating that *in vivo* selected tumor cells had specific growth and/or survival advantages in the tumor microenvironment.

In order to characterize the molecular programs that highly metastatic PANC1 LM3 and KPC LM2 cells utilized to promote cancer progression, I performed transcriptomic profiling comparing the *in vivo* selected, highly metastatic derivatives to their respective parental cells. RNA sequencing revealed 12 commonly de-regulated genes in both systems. Among the commonly de-regulated genes, Neuronal Pentraxin 1 (NPTX1) was ranked first by the average P-value between the two systems. NPTX1 is a secreted glycoprotein first identified in the nervous system. It is involved in the synapse formation and hypoxia induced apoptosis in the neurons, and its role in cancer has not been characterized.

To further study the role of NPTX1 in pancreatic cancer, I knocked-down NPTX1 expression in both the xenograft and syngeneic mouse pancreatic cancer models. Suppression of NPTX1 gene expression in both systems led to decreased liver metastatic colonization. In addition, knockdown of NPTX1 in both systems

suppressed orthotopic metastasis from the pancreas to multiple distal organs. Temporal suppression of NPTX1 after initial metastatic seeding in the liver also decreased metastatic growth, showing that NPTX1 was important in the progression of metastatic colonization. NPTX1 was also found to promote subcutaneous tumor growth demonstrating NPTX1's role in both distal organ metastasis and tumor growth in pancreatic cancer. However, over-expression of NPTX1 was not sufficient to promote metastasis most likely due to the non-physiological high levels of the over-expressed NPTX1 protein and its inability to form the correct oligomeric complex with other potential proteins.

After establishing the functional role of NPTX1 in promoting metastatic colonization and orthotopic tumor growth, I next sought to characterize the biochemical properties of this protein and its gene expression regulation in pancreatic cancer. Like previously described in neurons, NPTX1 was also secreted by pancreatic cancer cells and formed high molecular weight oligomers. Its expression was partially regulated by DNA methylation and the transcriptional factor EGR1. These mechanisms could be adopted by the highly metastatic, *in vivo* selected tumor cells to increase NPTX1 expression and promote tumor growth and metastatic colonization *in vivo*.

Chapter IV: Neuronal Pentraxin 1 Promotes Cancer Cell Proliferation in a Hypoxic Tumor Microenvironment

NPTX1 promotes cancer cell proliferation in the hypoxic pancreatic tumor microenvironment.

To further investigate the cellular role of NPTX1 in promoting metastatic progression and orthotopic tumor growth, I first asked if NPTX1 promotes cell proliferation or inhibits cell death *in vivo*. *In vitro*, suppression of NPTX1 expression in the PANC1 LM3 cells result in no change in cell proliferation (Figure 4.1). *In vivo*, NPTX1 knockdown in the PANC1 LM3 cells significantly reduced the percentage of proliferating cells in liver metastatic nodules, as assessed by Ki-67 staining of liver metastatic nodules and quantification (Figure 4.2). On the other hand, NPTX1 knockdown did not change the percentage of cells undergoing apoptosis as measured by using a DEVD-luciferin system *in vivo* , which assesses caspase 3/7 cleavage activity-mediated activation of luciferin substrate and consequently luminescence (Figure 4.3).

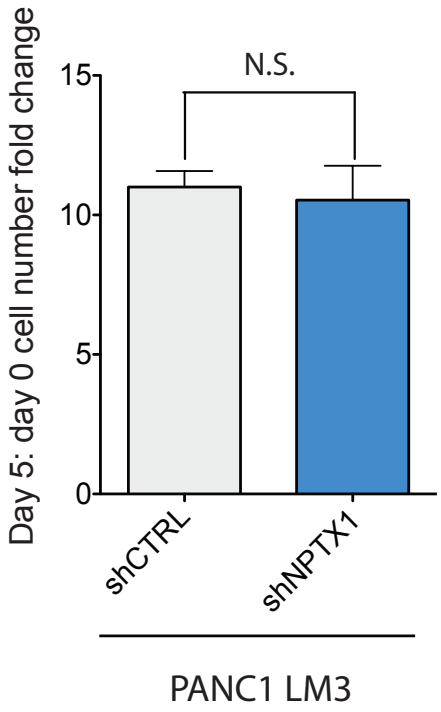

Figure 4.1 PANC1 LM3 cells with NPTX1 knockdown proliferate at the same rate as control cells under standard cell culture condition *in vitro*. $8x10^4$ PANC1 LM3 cells with NPTX1 knockdown and control cells were seeded at day 0. Cells were grown under standard cell culture condition and cell number was counted at day 5.

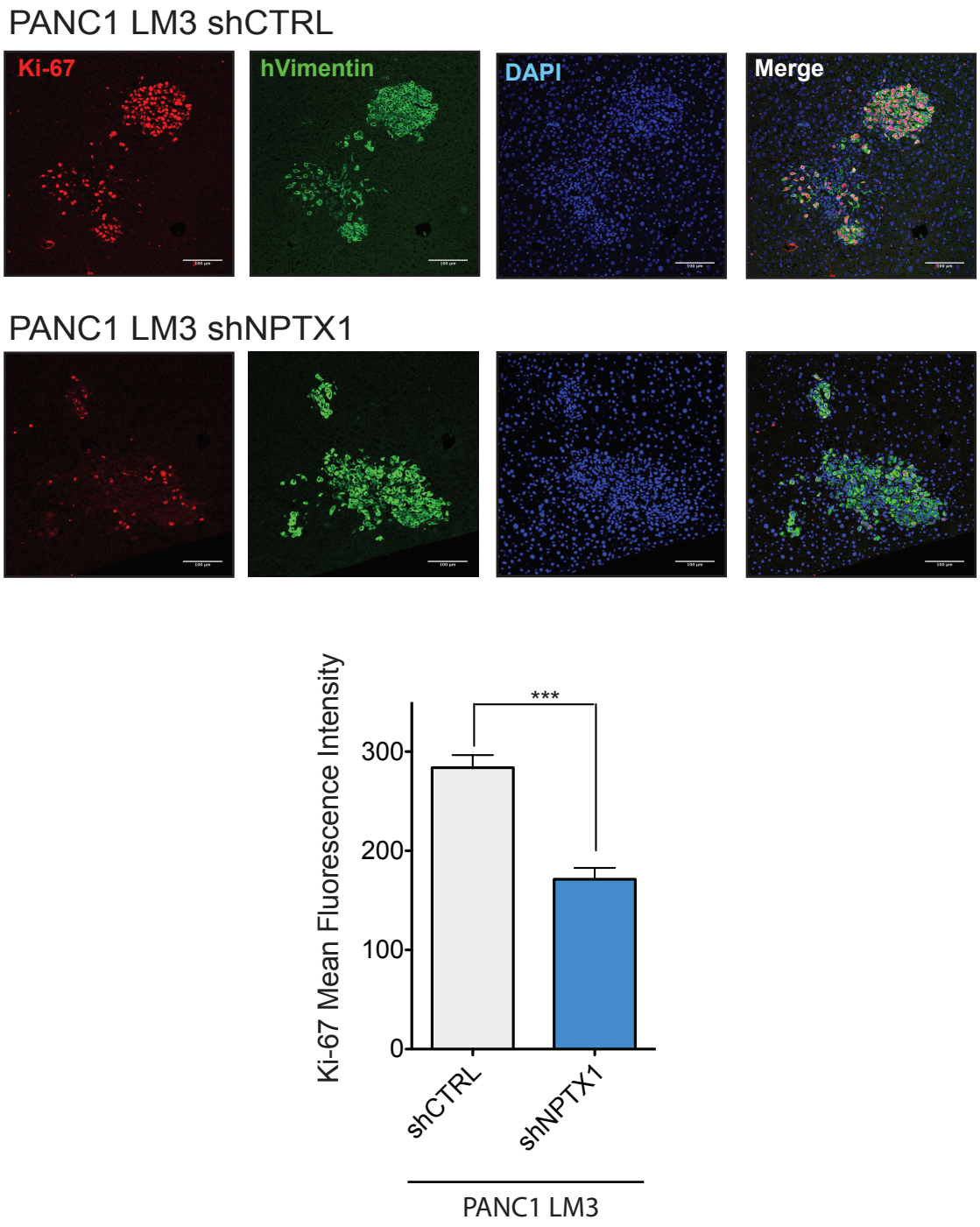

Figure 4.2 Ki-67 staining of liver metastasis sections from NSG mice xenografted with PANC1 LM3 cells shows decreased proliferation when NPTX1 expression is suppressed. Liver sections were made 14 days post splenic injection of PANC1 LM3 shCTRL and PANC1 LM3 shNPTX1 cells. ***P<0.001 by 2-tail student's t-test.

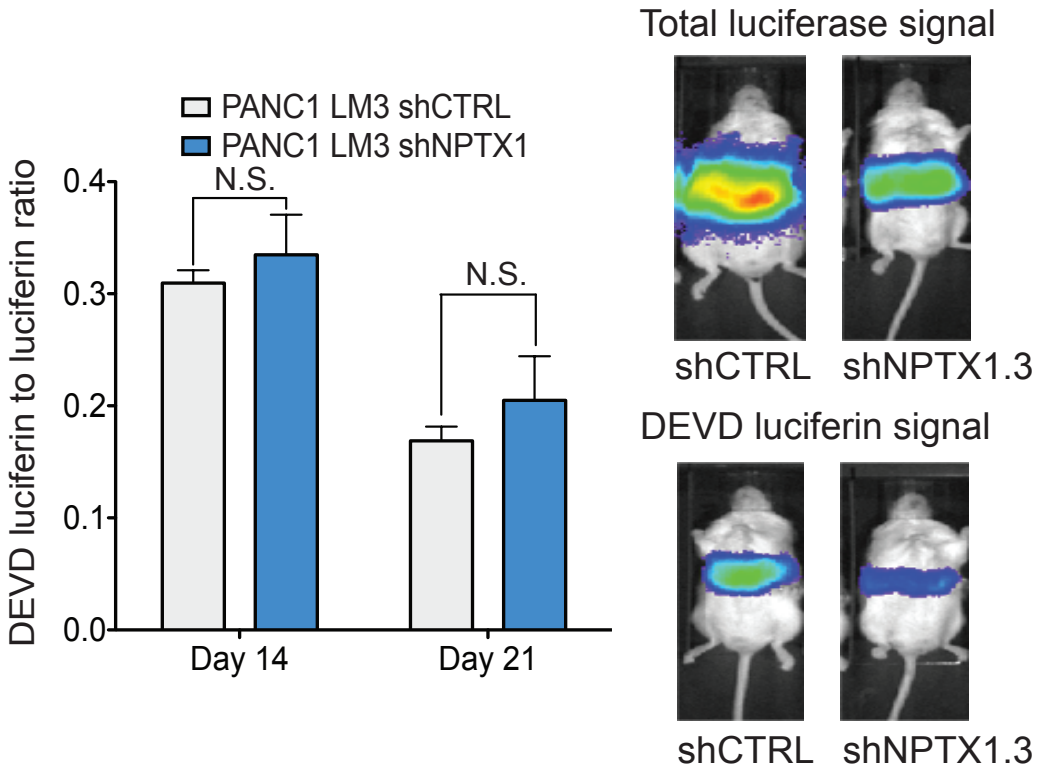

Figure 4.3 ***In vivo*** **apoptosis measured using a DEVD-luciferin system shows no significant different between PANC1 LM3 cells with and without knockdown of NPTX1.** PANC1 LM3 cells with stable knockdown of NPTX1 by a shCTRL and control cells were injected into the portal circulation. Mice were imaged at day 14 and 21 using bioluminescence imaging with both a regular luciferin (total luciferase signal) and a DEVD luciferin that must be cleaved by caspase-3 and caspase-7 to be an active substrate.

After establishing NPTX1's role in promoting cell proliferation *in vivo* but not *in vitro*, I next investigated potential tumor microenvironmental conditions that may differ from the *in vitro* cell culture condition. Pancreatic cancer is known to be severely hypovascular and fibrotic with an extremely hypoxic tumor microenvironment. Thus, I decided to investigate the extent of hypoxia in the liver metastasis microenvironment in our metastasis model. To do that, I used the chemical probe pimonidazole to detect areas with tissue oxygen tension lower than 10mmHg in metastatic nodules *in vivo*. Pimonidazole becomes chemically linked to tissues when the oxygen tension is lower than 10mmHg and can be imaged using an antibody. In the liver metastasis sections derived from poorly metastatic PANC1 parental cells, the tissue showed limited areas of hypoxia with few proliferating cancer cells. However, the highly metastatic PANC1 LM3 cells were highly proliferative in the liver even in a densely hypoxic tumor microenvironment (Figure 4.4).

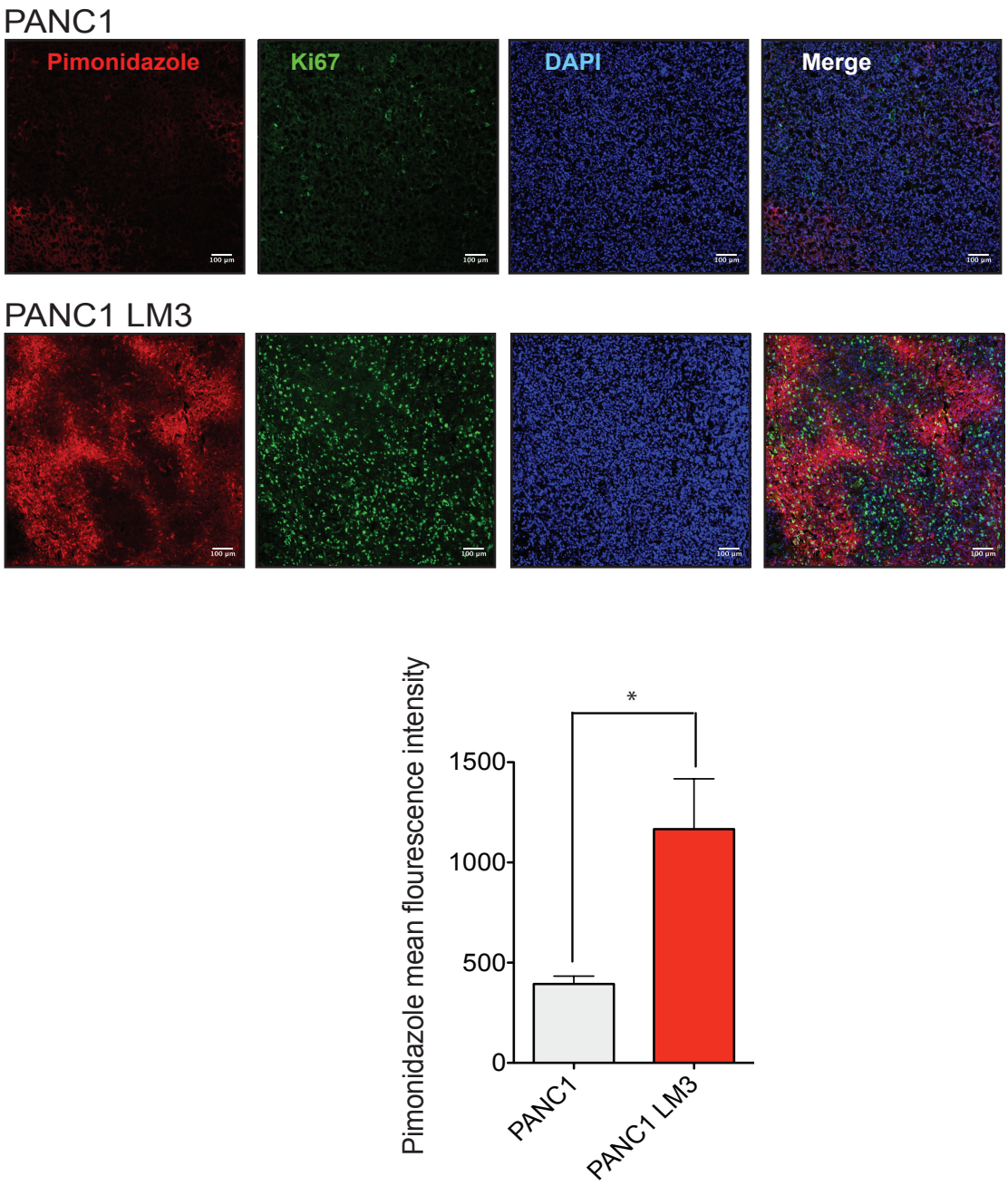

Figure 4.4 PANC1 LM3 liver metastatic nodules are extensively hypoxic compared to the parental PANC1 cells *in vivo*. The mouse livers were extracted 5 weeks post splenic injection of the 3 x 10^5 PANC1 LM3 and PANC1 cells. The highly metastatic PANC1 LM3 cells showed extensive hypoxic regions and the cancer cells were highly proliferative despite the hypoxia. *P<0.05 by 2-tail student's t-test.

To determine if the highly metastatic PANC1 LM3 cells and the poorly metastatic PANC1 cells had differential proliferative capabilities under low oxygen or no oxygen condition *in vitro*, I conducted proliferation assay comparing PANC1 LM3 cells to its parental PANC1 cells under normoxia, hypoxia (0.5% oxygen), or anoxia (0% oxygen). In normoxia, the highly metastatic PANC1 LM3 cells proliferated at a slower rate compared to the parental PANC1 cells, as previously observed. However, under hypoxia for 5 days, the highly metastatic PANC1 LM3 cells proliferated at a faster rate compared to the parental PANC1 cells. Under anoxia for 3 days, all of the lowly metastatic PANC1 cells died while the highly metastatic PANC1 LM3 cells proliferated at a slower rate (Figure 4.5). I concluded that the highly metastatic PANC1 LM3 cells gained enhanced proliferating capability under low oxygen environment.

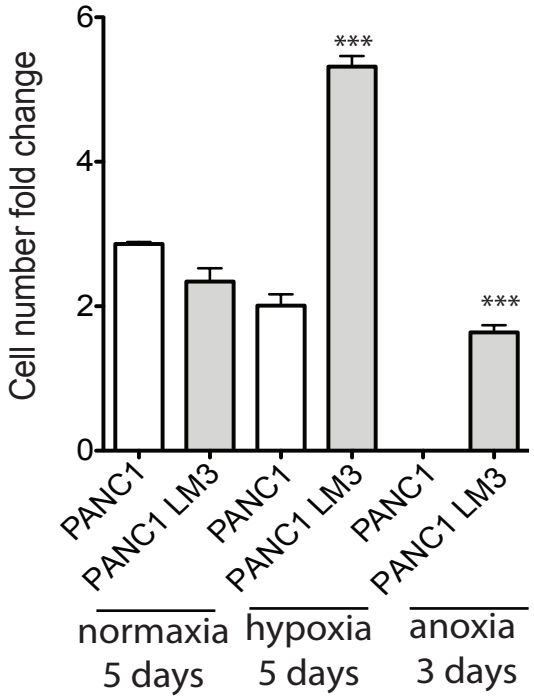

Figure 4.5 PANC1 LM3 cells proliferate faster under hypoxic and anoxic condition compared to PANC1 cells. Highly metastatic PANC1 LM3 cells proliferated at a slower rate in normoxia compared to PANC1 cells but could proliferate at significant higher rate in hypoxia compared to the lowly-metastatic PANC1 cells. In anoxia for 72 hours, the lowly metastatic PANC1 cells detach completely from the tissue culture dish while the highly-metastatic PANC1 LM3 cells survive and proliferate. ***P<0.001 by 2-tail student's t-test.

We further investigated if NPTX1 played any role in promoting cell proliferation in a hypoxic environment. Indeed, highly metastatic PANC1 LM3 cells depleted of NPTX1 by siRNA proliferated at slower rate compared to PANC1 LM3 cells transduced with a control siRNA under hypoxia for 6 days (Figure 4.6). In normoxia, depletion of NPTX1 in PANC1 LM3 cells did not significantly impact proliferation relative to control cells (Figure 4.7). I then tested the impact of modulating nutrients on the proliferative capacity of the metastatic cells, since the tumor microenvironment is known to contain regions depleted of various nutrients. NPTX1 knockdown in PANC1 LM3 cells also did not change proliferation rates under low serum (2% FBS) or low glucose (1mg/mL) conditions during normoxia (Figure 4.8 and 4.9). However, we cannot rule out that under more stringent serum and glucose deprivation an effect could be observed.

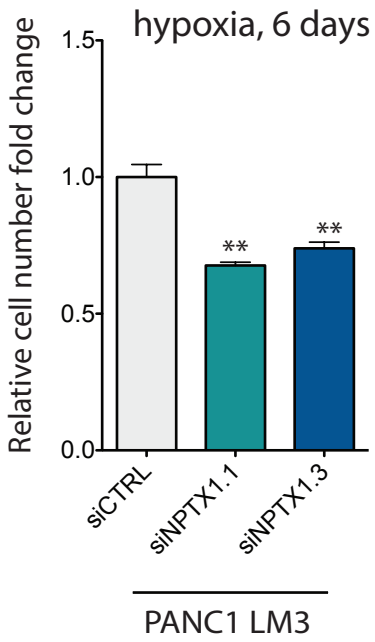

Figure 4.6 NPTX1 promotes proliferation of PANC1 LM3 cells in hypoxia. PANC1 LM3 cells with suppressed NPTX1 expression proliferate at slower rate in hypoxia (1% oxygen) compared to control cells. NPTX1 expression was transiently suppressed in PANC1 LM3 cells using two independent

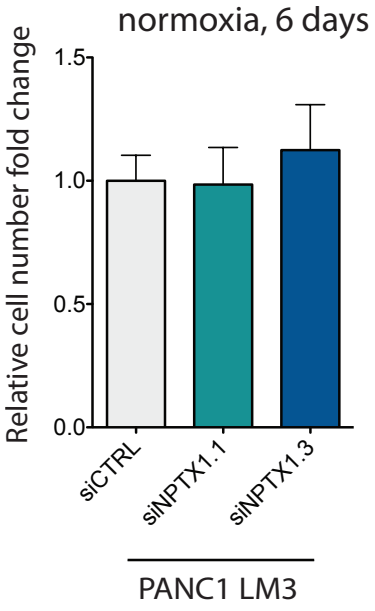

Figure 4.7 PANC1 LM3 cells with suppressed NPTX1 expression proliferate at the same rate under normoxia. NPTX1 expression was transiently suppressed in PANC1 LM3 cells using two independent siRNA.

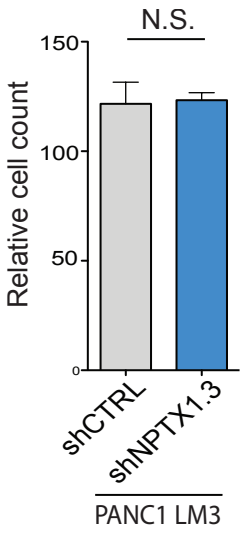

Figure 4.8 PANC1 LM3 cells with suppressed NPTX1 expression proliferate at the same rate under low serum (2% FBS) growth

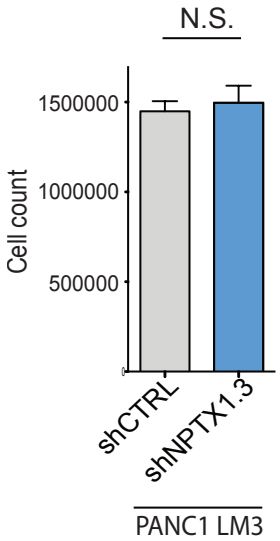

Figure 4.9 PANC1 LM3 cells with suppressed NPTX1 expression proliferate at the same rate under low glucose (1mg/mL) growth condition

Since NPTX1 is a secreted protein and can also potentially affect the infiltration of cells into tumor microenvironment, I investigated its ability to modulate the abundance of infiltrating stromal cells in the pancreatic cancer microenvironment. *In vivo*, NPTX1 depleted PANC1 LM3 cells formed liver metastatic nodules containing significantly fewer infiltrating myofibroblasts compared to control PANC1 LM3 cells (Figure 4.10). To investigate if NPTX1 was involved in recruitment of myofibroblasts, I co-injected the human hepatic stellate cell line, Lx-2, with PANC1 LM3 cells with NPTX1 knockdown. Hepatic stellate cells are the precursors of myofibroblasts in the liver. Co-injection of Lx-2 cells did not rescue the suppressed liver metastatic growth due to NPTX1 knockdown (Figure 4.11). These results suggest that either myofibroblasts are not responsible for the NPTX1-mediated enhanced liver metastatic growth of pancreatic cancer cells or that the Lx-2 cell line used for this experiment does not behave in a similar manner as endogenous hepatic stellate cells *in vivo*.

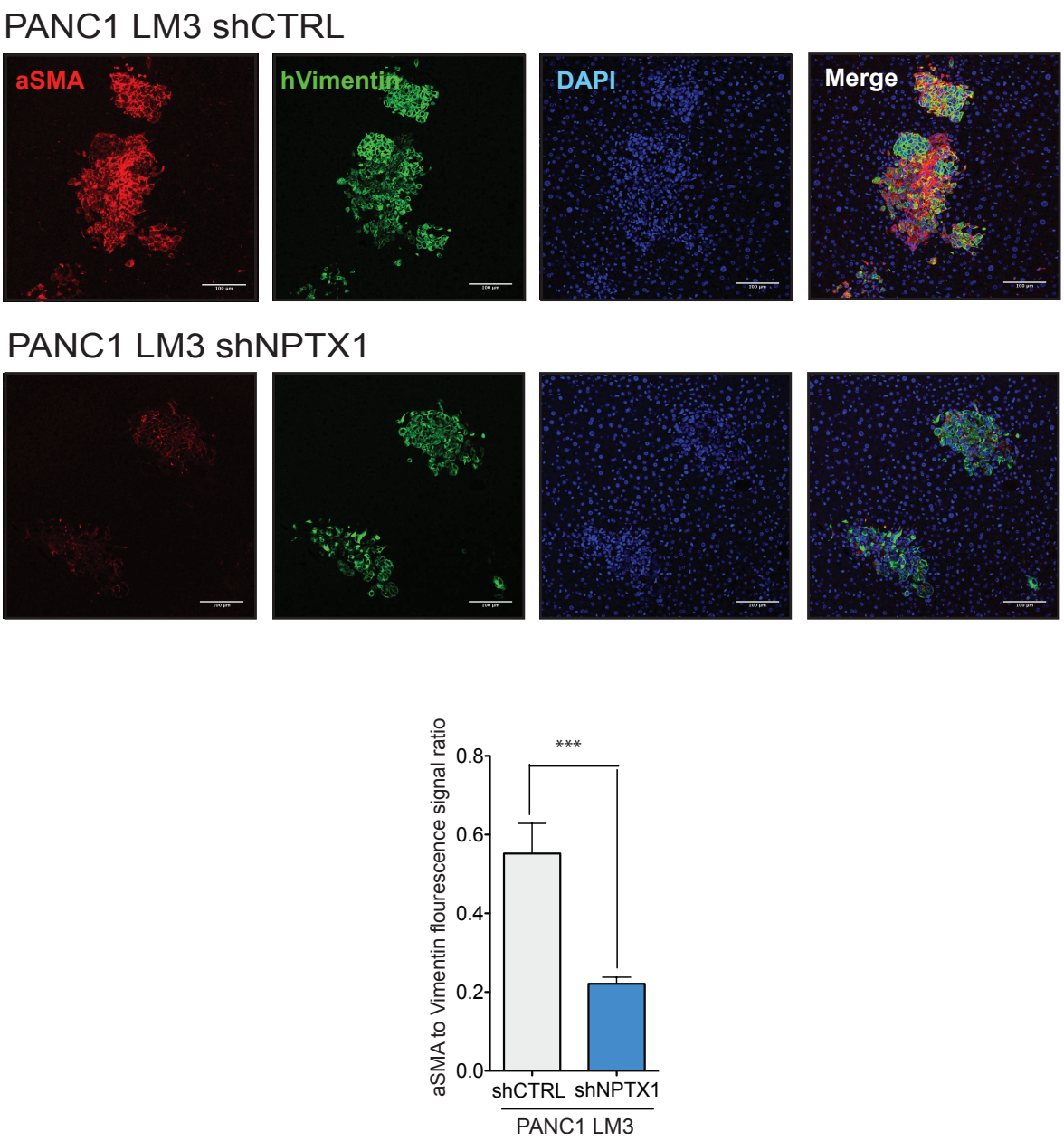

Figure 4.10 Knockdown of NPTX1 in cancer cells decreases infiltrating myofibroblasts in the liver metastatic nodules. aSMA staining of liver metastases sections from NSG mice xenografted with PANC1 LM3 cells shows decreased myofibroblasts in the metastatic nodules when NPTX1 expression was stably suppressed by shRNA. ***P<0.001 by 2-tail student's t-test.

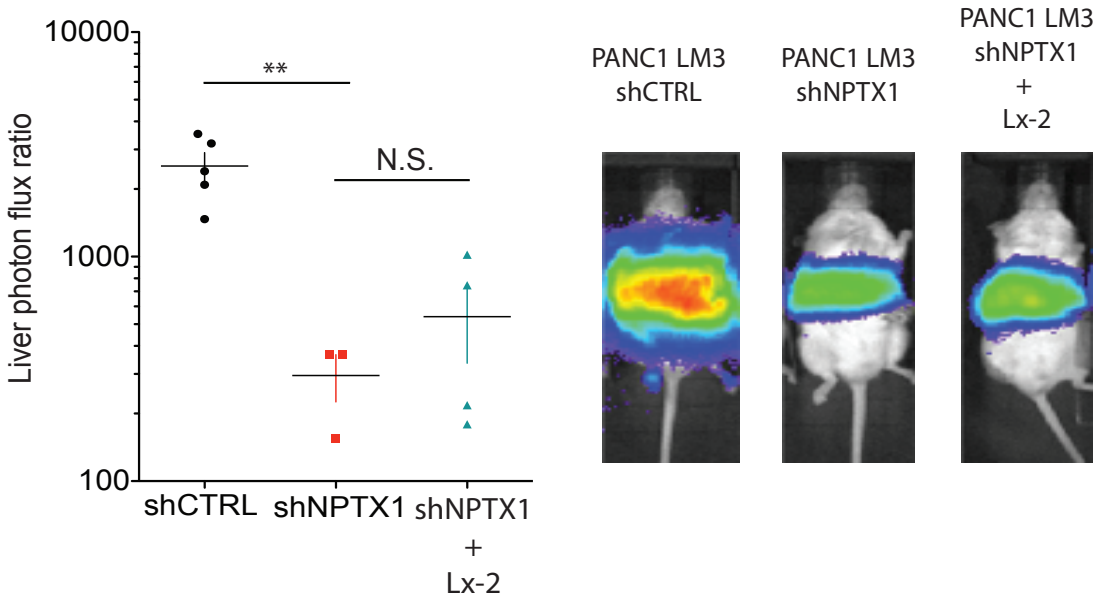

Figure 4.11 Hepatic stellate cells do not rescue suppressed metastatic growth due to NPTX1 knockdown in PANC1 LM3 cells. 1×10^5 human hepatic stellate cells, Lx-2, were co-injected with 1×10^5 PANC1 LM3 cells with NPTX1 knockdown or with control cells. Liver metastasis was monitored via bioluminescence imaging at week 5. **P<0.01 by 2-tail student's t-test.

Hepatic stellate cells are the precursors of myofibroblasts in the liver. During fibrosis, hepatic stellate cells (HSCs) are activated and transdifferentiate into myofibroblasts. During activation, HSC express increasing levels of the protein alpha-Smooth Muscle Actin (aSMA). We investigated if NPTX1 could impact the levels of myofibroblasts by activating primary murine hepatic stellate cells. *In vitro*, recombinant NPTX1 did not activate murine primary hepatic stellate cells but rather led to a slight decrease in murine aSMA expression (Figure 4.12). Conditioned media from control PANC1 LM3 cells also did not activate murine primary hepatic stellate cells greater than PANC1 LM3 cells depleted of NPTX1 (Figure 4.13). *In vivo,* knockdown of NPTX1 in PANC1 LM3 cells did not change the abundance of infiltrated endothelial cells (Figure 4.14) or macrophages (Figure 4.15) compared to the control in the xenograft mouse model. Nptx1 knockdown in KPC cells also did not alter the composition of infiltrating immune cells including macrophages, neutrophils, B and T cells (Figure 4.16). These experiments suggest that NPTX1 does not have a role on activating the differentiation of HSC into myofibroblast.

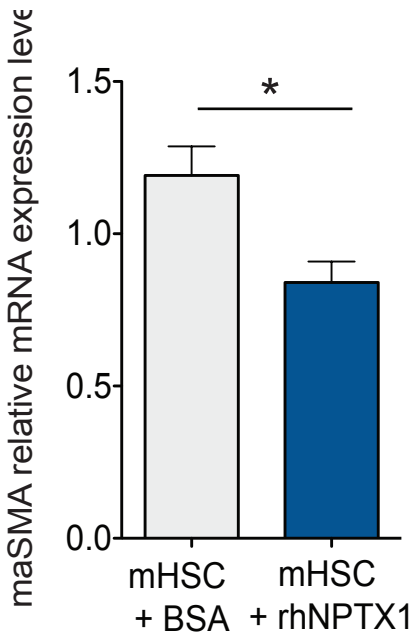

Figure 4.12 Recombinant human NPTX1 suppresses hepatic stellate cells activation *in vitro*.

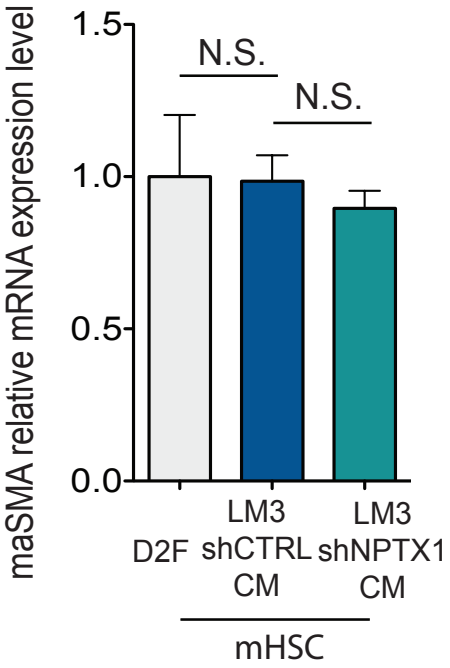

Figure 4.13 Conditioned medium from PANC1 LM3 cells with or without NPTX1 knockdown does not activate hepatic stellate cells *in vitro*.

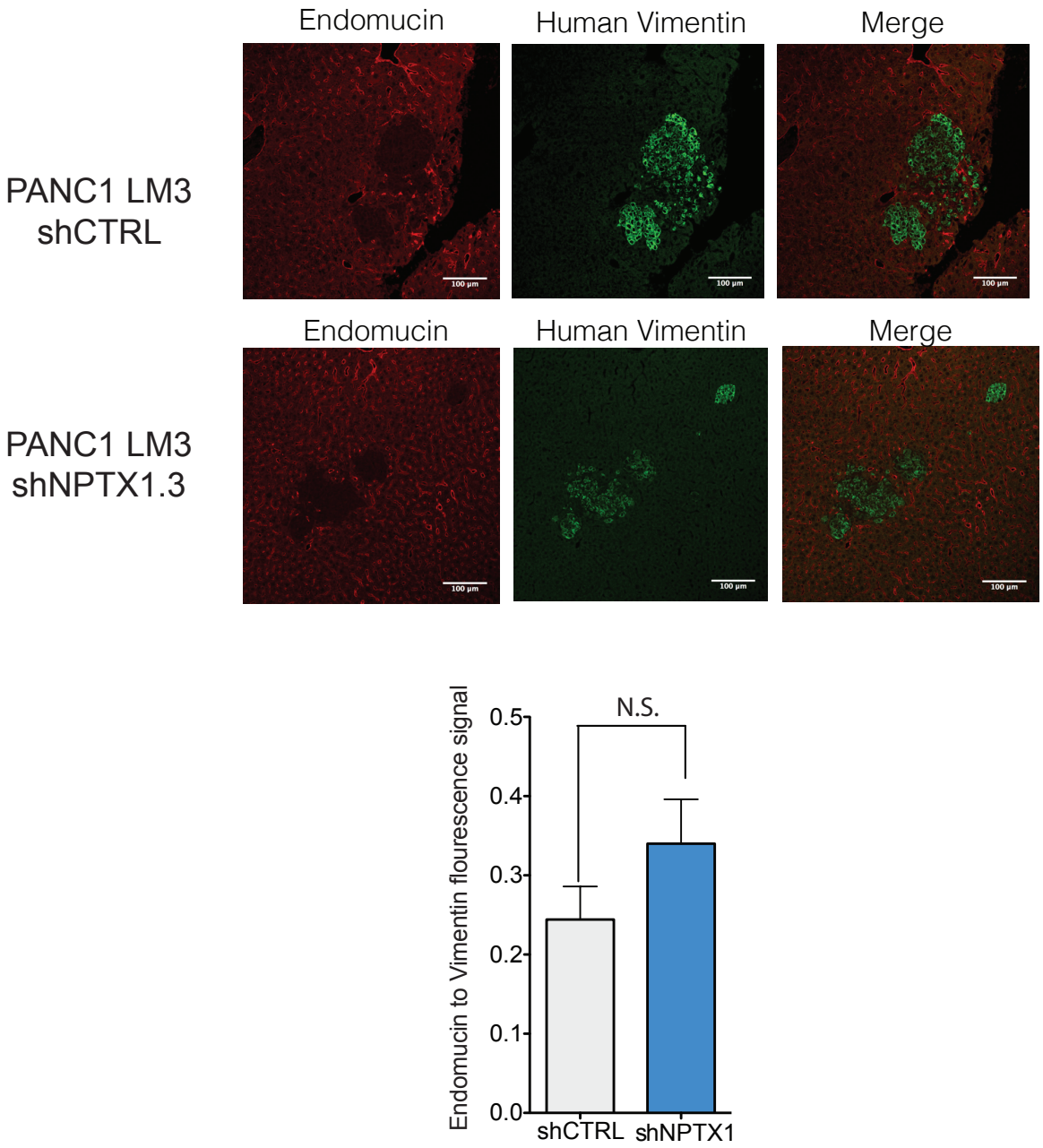

Figure 4.14 Knockdown of NPTX1 in PANC1 LM3 cells does not alter number of endothelial cells in the liver metastatic nodules. Liver sections were made 14 days post splenic injection of PANC1 LM3 shCTRL and PANC1 LM3 shNPTX1 cells.

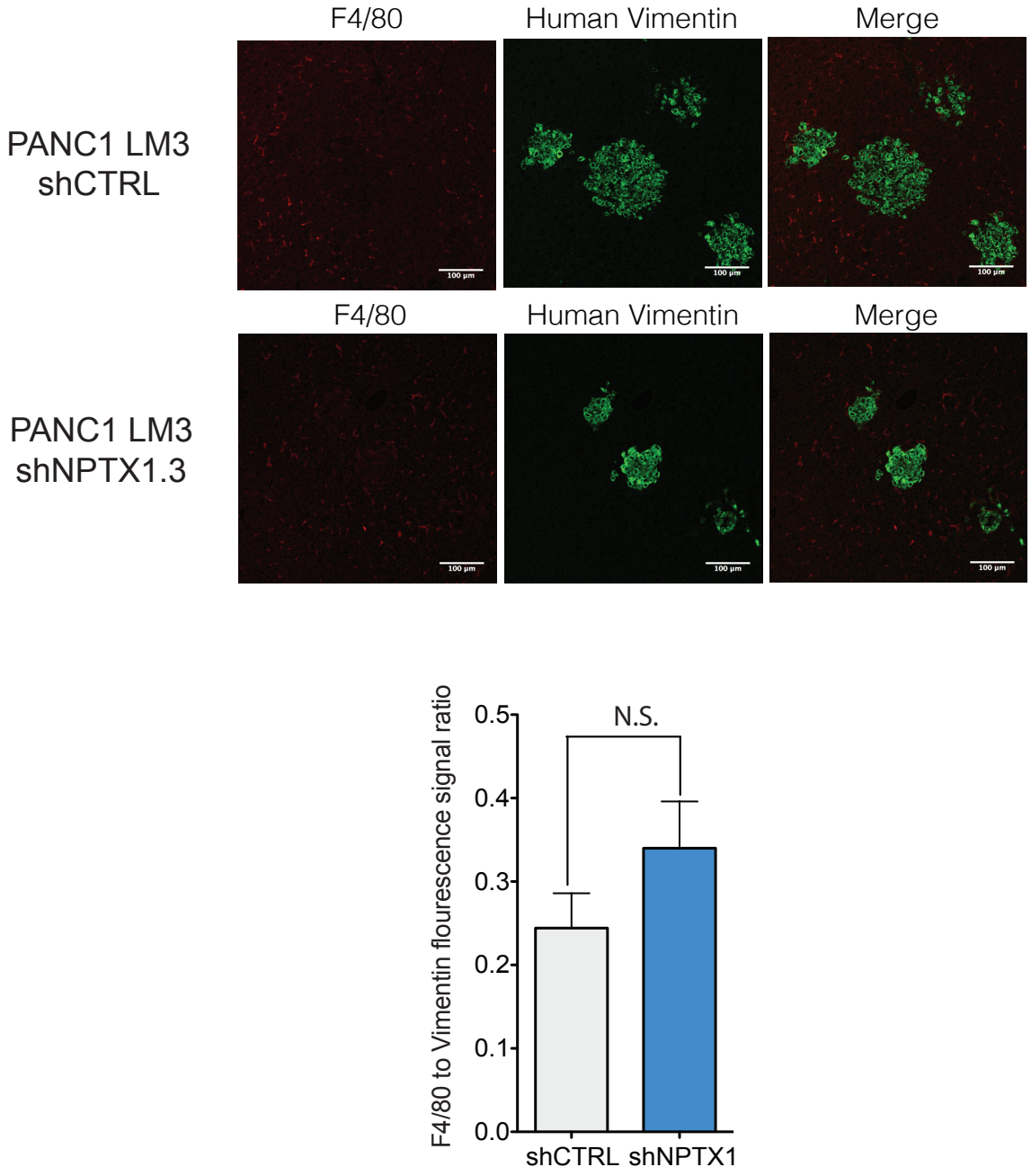

Figure 4.15 Knockdown of NPTX1 in PANC1 LM3 cells does not alter number of macrophages in the liver metastatic nodules. Liver sections were made 14 days post splenic injection of PANC1 LM3 shCTRL and PANC1 LM3 shNPTX1 cells.

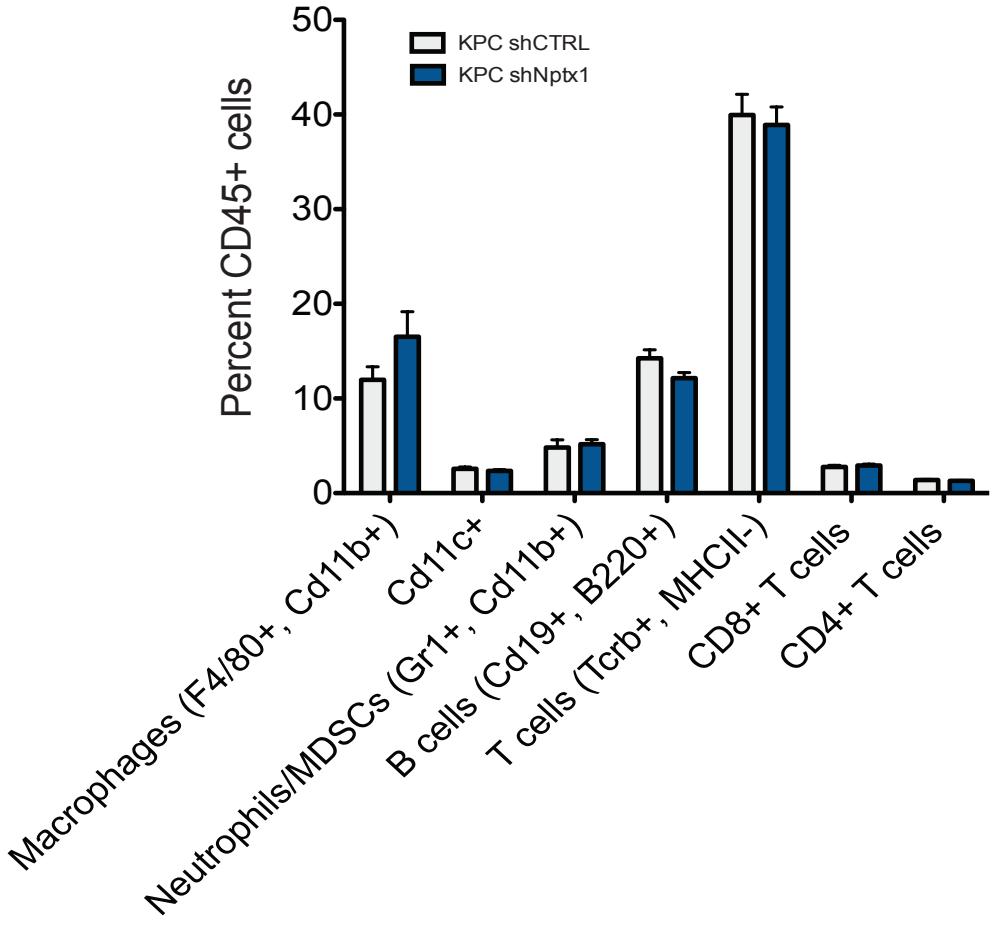

Figure 4.16 The immune cell infiltrates of KPC tumors with Nptx1 knockdown do not differ significantly from control. Liver metastases nodules were harvested 10 days post splenic injection of 5 x 10^5 control and shRNA mediated table Nptx1 knockdown KPC cells.

Pancreatic cancer cells with high expression levels of NPTX1 exhibit a growth advantage under a hypoxic microenvironment. Hypoxia-induced HIF1a response is often activated by tumor cells adapting metabolically to the hypoxic tumor micro-environment (Semenza, 2013). To investigate if this NPTX1-mediated growth advantage was mediated through a HIF1a-dependent pathway, HIF1a expression was suppressed using two independent siRNAs in the highly metastatic PANC1 LM3 cells. Hypoxic proliferation assays of the PANC1 LM3 cells with HIF1a knockdown were performed and compared to control PANC1 LM3 cells. PANC1 LM3 cells with HIF1a knockdown did not proliferate slower compared to PANC1 LM3 cells transfected with a control siRNA. These results suggest that the effect of NPTX1 on cell survival under hypoxic conditions is not mediated by HIF1a and thus potentially represent a novel mechanism the cancer cells utilize to survive under low oxygen conditions.

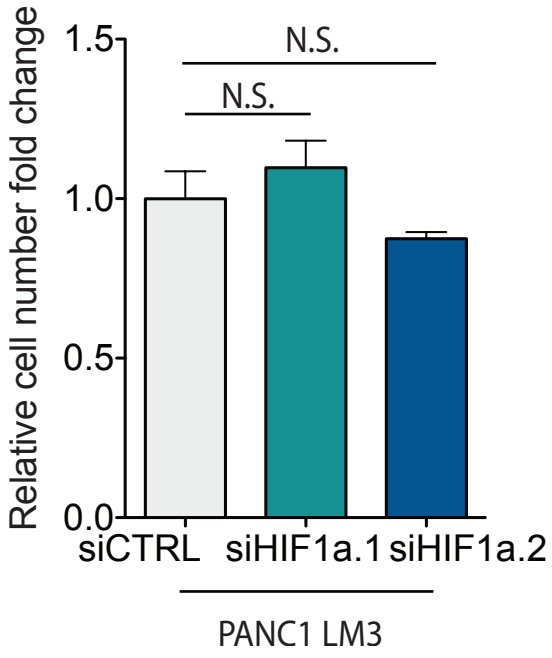

Figure 4.17 Proliferation of the highly metastatic PANC1 LM3 cells in hypoxia is not affected by suppression of HIF1a. Knockdown of HIF1a in PANC1 LM3 cells was generated using two independent siRNA. PANC1 LM3 cells with suppressed HIF1a and control cells were incubated in hypoxia for 6 days and proliferation was measured by cell counting.

Summary of Chapter IV

In Chapter IV, I investigated the cellular mechanisms of how NPTX1 promotes pancreatic cancer metastasis and tumor growth. *In vitro*, NPTX1 depletion did not alter pancreatic cancer cell proliferation. However, *in vivo*, knockdown of NPTX1 in pancreatic cancer cells suppressed cancer cell proliferation in liver metastases, demonstrating that NPTX1 promotes metastatic colonization and orthotopic tumor growth in a tumor microenvironment-dependent manner. Furthermore, NPTX1 suppression in pancreatic cancer cells did not alter cancer cell apoptosis *in vivo.*

I next sought to uncover the potential features of the tumor microenvironment that allowed pancreatic cancer cells expressing high level of NPTX1 to proliferate rapidly *in vivo*. A hallmark of pancreatic cancer is its fibrotic and hypovascular tumor environment leading to severe hypoxia. I found that the highly metastatic PANC1 LM3 liver metastases with high NPTX1 levels had extensive hypoxic regions compared to the poorly metastatic PANC1 tumors. *In vitro*, PANC1 LM3 cells grew more rapidly under hypoxia or anoxia compared to the parental PANC1 cells. Knockdown of NPTX1 in the pancreatic cancer cells suppressed proliferation under hypoxia, but not normoxia. Furthermore, this effect appears independent of the canonical master transcriptional regulator of hypoxic

response HIF1a. All of these findings suggest that NPTX1 may mediate its proliferative effects through a novel mechanism during oxygen deprivation.

In addition to NPTX1's role in promoting cancer cell proliferation under hypoxia, I wondered if as a secreted protein, NPTX1 could affect other cell types in the tumor microenvironment. In the PANC1 LM3 cells with suppressed NPTX1 expression, less myofibroblats were observed to have infiltrated into tumor nodules. However, co-injecting myofibroblasts precursor cells, the hepatic stellate cells, did not rescue the suppressed liver metastasis phenotype caused by NPTX1 depletion. Furthermore, recombinant NPTX1 or conditioned medium from PANC1 LM3 did not activate hepatic stellate cells *in vitro.* Thus, NPTX1 may not directly affect infiltrating myofibroblasts but rather may provide the cancer cells a growth advantage under the hypoxic tumor environment that in term can modulate phenotypes of stromal cells.

Chapter V: Clinical Relevances of Neuronal Pentraxin 1

NPTX1 is secreted by patient derived pancreatic cancer cells and can be detected in the plasma of tumor bearing mice.

NPTX1 is a secreted protein with a signal peptide and could be detected by western blot in the extracellular medium of the highly metastatic PANC1 LM3 cells at a higher level relative to the lowly metastatic PANC1 cells as shown previously in Figure 3.27. To determine the clinical relevance of NPTX1 in pancreatic cancer, we examined the expression levels of NPTX1 in autopsy samples of pancreatic tumors compared to normal pancreas obtained through a collaboration with Dr. Christine Iacobuzio-Donahue at Memorial Sloan Kettering Cancer Center. As previously described, under non-diseased conditions, NPTX1 was not observed to be expressed in the pancreas. In contrast to this, however, I observed that multiple pancreatic tumors expressed NPTX1 mRNA as assessed by qRT-PCR (Figure 5.1). On average, NPTX1 was expressed at more than 1000-fold higher levels in pancreatic cancer samples relative to normal pancreas samples. Moreover, NPTX1 was also expressed at relatively high level in clinical pancreatic tumor samples compared to other types of tumors (Figure 5.2). In several primary patient-derived pancreatic cancer cell lines, NPTX1 mRNA was expressed at comparable levels to the highly metastatic PANC1 LM3 cells (Figure 5.3) and was detectable in the extracellular media at the protein level by western blot (Figure 5.4).

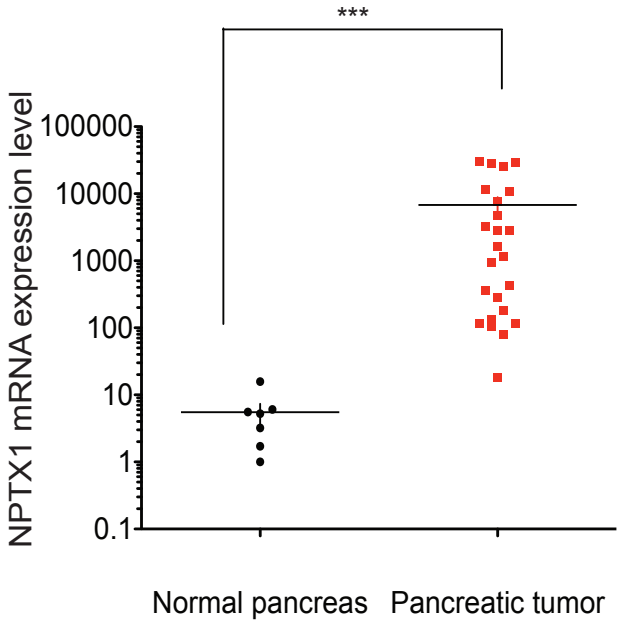

Figure 5.1 Pancreatic tumor samples express NPTX1 at significantly higher level compared to normal pancreatic tissues. NPTX1 expression by the mRNA level was detected in pancreatic tumor samples but not in the normal pancreas. RNA of pancreatic tumor was obtained from a rapid autopsy program (Memorial Sloan-Kettering, Iacobuzio-Donahue Lab) and RNA of normal pancreas was obtained from OriGene. Level of NPTX1 expression was measured by qRT-PCR. *** $p<0.001$ using 2 sided student's t-test.

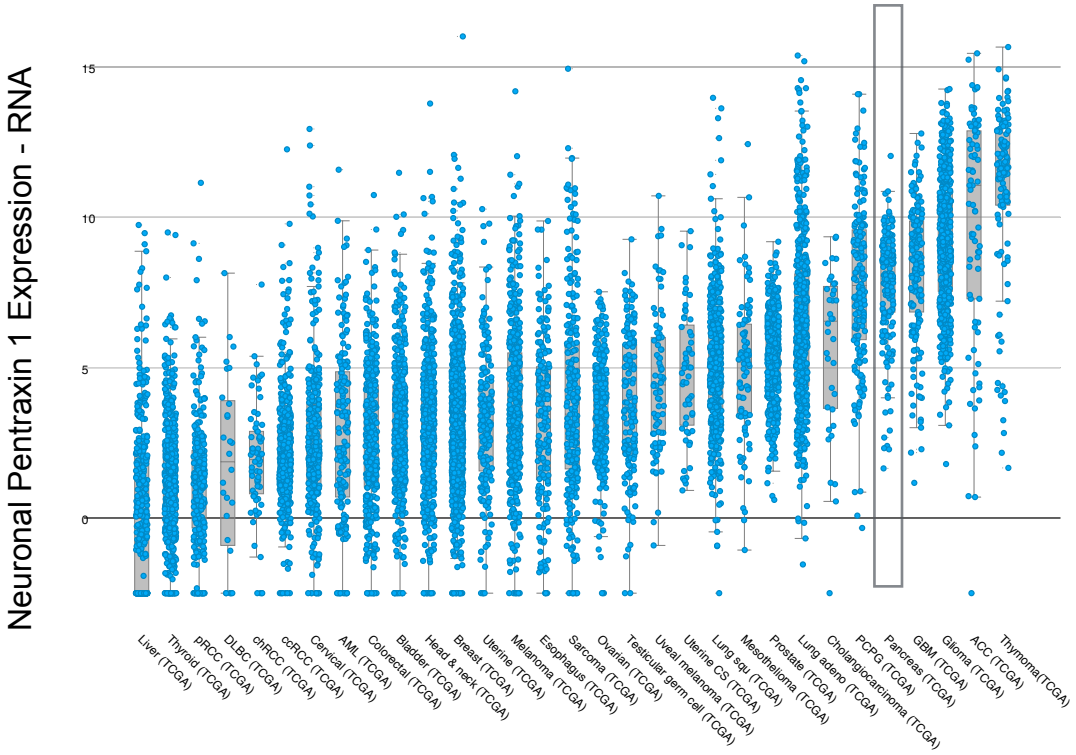

Figure 5.2 Pancreatic cancer tumors express NPTX1 at the mRNA level. RNA sequencing of primary tumors from patients reveals that NPTX1 was expressed at the mRNA level in clinical pancreatic cancer samples. Data source: cBioPortal 2017

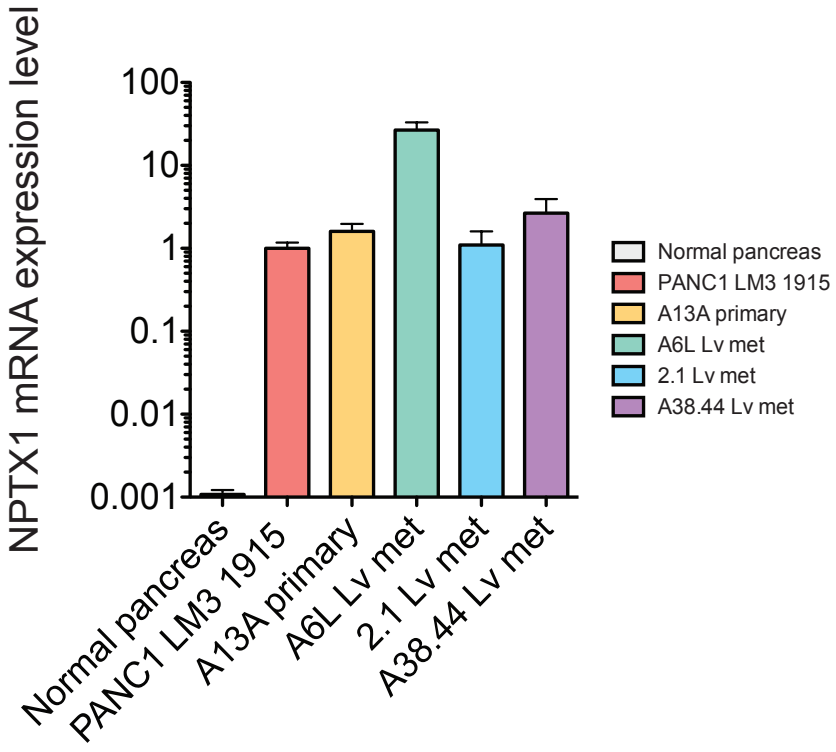

Figure 5.3 Patient derived pancreatic tumor cell lines express high level of NPTX1. Patient derived pancreatic tumor cell lines expressed high level of NPTX1 by qRT-PCR that were comparable to the expression level of the highly metastatic PANC1 LM3. Normal pancreatic tissue expressed NPTX1 at significantly lower level compared to all pancreatic cancer derived cell lines.

Since NPTX1 is a secreted protein, we examined the abundance of NPTX1 in the plasma of mice bearing PANC1 LM3 xenografted tumors versus healthy controls injected with PBS. In the tumor bearing mice, I was able to detect NPTX1 protein in the plasma of the mice at significantly higher levels (more than 17 folds) compared to healthy controls by using a commercially available ELISA kit (Figure 5.5). Pancreatic cancer remains a lethal malignancy partially due to the late diagnosis of this disease. These experiments suggest that NPTX1 can potentially serve as an early routine diagnostic marker detectable by an ELISA-based blood test.

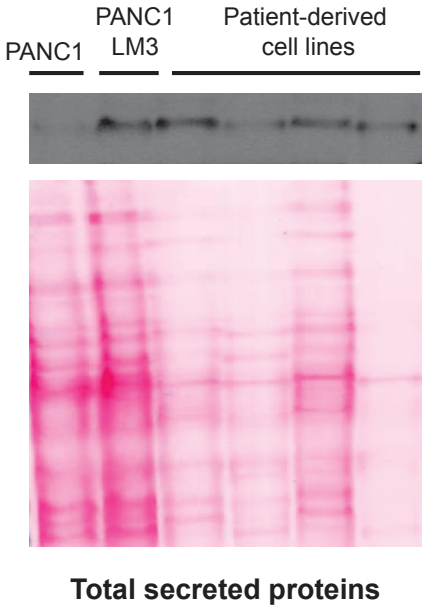

Figure 5.4 Pancreatic cancer cell lines secrete NPTX1 protein into the extracellular space. Pancreatic cancer cell lines were incubated in serum free medium for 16 hours. Extracellular medium was collected and concentrated from the cell lines PANC1, PANC1 LM3, and four patient derived cell lines (A13A primary, A6L liver met, 2.1 Lv met, A38.44 Lv met). Ponceau red stain was used to visualize total secreted protein in the extracellular medium.

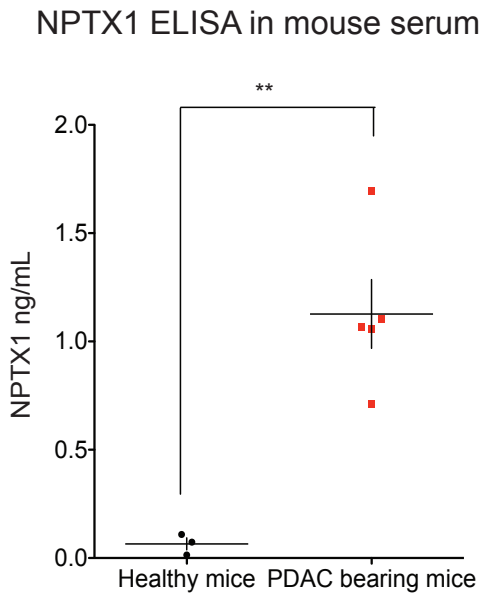

Figure 5.5 NPTX1 is detected in the plasma of the pancreatic cancer mouse xenograft model. 3 x 10^5 PANC1 LM3 cells or PBS was injected into the portal circulation through the spleen to NSG mice. Plasma of the mice were collected at week 5 and NPTX1 protein level was measured by ELISA.

Summary of Chapter V

NPTX1 was previously described to be exclusively expressed in the nervous system (Schlimgen et al., 1995). Through unbiased transcriptomic profiling, I found that the highly metastatic PANC1 LM3 cells express and secrete NPTX1 into the extracellular space at high levels compared to their less metastatic PANC1 parental cells. In Chapter V, I investigated NPTX1 expression in clinical pancreatic cancer samples. Compared to normal pancreas, NPTX1 was highly expressed by pancreatic cancers. In multiple patient-derived pancreatic cancer primary cell lines, NPTX1 protein could also be detected in the extracellular media.

NPTX1 is a secreted protein and it could be detected in the plasma of mice bearing xenografted pancreatic cancers by ELISA but not in healthy controls. Thus, these results demonstrate that NPTX1 may potentially serve as a diagnostic marker for early detection of pancreatic cancer.

Chapter 6 Summary and General Discussions

Pancreatic cancer is a deadly disease because it is usually diagnosed at an advanced stage and does not respond to current treatments. In the United States, each year about 43,000 patients die from pancreatic cancer and it is the fourth leading cause of cancer death. More than 80% of patients present with metastatic disease at the time of diagnosis (Stathis and Moore, 2010) and metastatic pancreatic adenocarcinoma has a median survival of eight to eleven months under current standard of care (Ryan et al., 2014). Efforts in using other agents to treat pancreatic cancer have mostly been fruitless and more than twenty Phase III clinical trials have failed. The dismal survival outcome of this disease and lack of success in clinical trials indicate the necessity for new models and improved approaches toward therapies. Understanding the cellular and physiological basis of metastatic pancreatic cancer is therefore of great interest to the medical and scientific community with regard to developing new targeted therapies and diagnostic biomarkers.

This thesis presents an effort to discover novel metastasis regulators in pancreatic cancer using an unbiased and systematic approach: *in vivo* selection of both xenograft and syngeneic murine models of pancreatic cancer combined with transcriptomic profiling. Using the syngeneic and xenograft mouse models allowed *in vivo* selection to be performed under both immunocompetent and

immunodeficient backgrounds and accounted for potential molecular programs that may regulate the immune component of metastasis. *In vivo* selected cells derived from both the xenograft and syngeneic models successfully established liver metastases. Unbiased and systematic transcriptomic profiling of the *in vivo* selected and highly metastatic cancer cells compared to their poorly metastatic parental cells revealed multiple commonly de-regulated genes as potential metastasis regulators in pancreatic cancer. Among all the 12 candidate genes, Neuronal Pentraxin 1 (NPTX1) was the most significantly up-regulated gene ranked by average P-value in both highly metastatic *in vivo* selected populations of the xenograft and syngeneic models compared to their respective, lowly metastatic parental populations.

NPTX1 was first described to be exclusively expressed by neurons (Schlimgen et al., 1995). Subsequent studies revealed NPTX1's role in synaptic plasticity by modulating AMPA receptor formation (Bjartmar et al., 2006; Sia et al., 2007; Xu et al., 2003). In synapses, NPTX1 forms high-molecular weight oligomers with the other members of the neuronal pentraxin family proteins, Neuronal Pentraxin-2 and Neuronal Pentraxin Receptor (NPTXR) to modulate the formation of AMPA receptors. In addition to NPTX1's role in synaptic plasticity, several reports also suggested that NPTX1 may play a role in hypoxia induced neuronal damage (Al

Rahim and Hossain, 2013; Hossain et al., 2004). NPTX1 is a 47kDa secreted glycoprotein that belongs to the pentraxin protein family (Xu et al., 2003). The pentraxin protein family includes acute phase proteins such as C-reactive protein (CRP) and Serum Amyloid P proteins (SAP). Many members of the pentraxin family are pattern recognition receptors involved in innate immunity (Du Clos, 2013) and the canonical receptors of pentraxin proteins are Fc receptors (Bodman-Smith et al., 2002). Because NPTX1 was previously thought to be exclusively expressed in the neurons, its binding affinity to Fc receptors was never characterized. While there is one report indicating altered methylation status in the NPTX1 promoter in lung cancer (Zhou et al., 2015), the functional role of NPTX1 in cancer remains elusive.

Because NPTX1 was highly expressed by both the syngeneic and xenograft *in vivo* selected, highly metastatic pancreatic cancer cells, I hypothesized that NPTX1 promotes pancreatic cancer progression. To reveal the role of NPTX1 in pancreatic cancer, I employed both syngeneic and xenograft pancreatic cancer mouse models to study functional roles of NPTX1 in pancreatic cancer progression. These functional studies established NPTX1 as both a promoter of metastatic colonization and orthotopic tumor growth in pancreatic cancer *in vivo.* Specifically, NPTX1 promoted cancer cell proliferation *in vivo*, but had no effect

on apoptosis. Importantly, NPTX1 promoted pancreatic cancer metastatic progression in the liver even after macro-metastases establishment. The mechanism of macro-metastases colonization is poorly understood compared to earlier steps of metastasis such as intravasation. However, macro-metastases colonization is clinically important because most pancreatic cancer patients present with established distal organ metastasis, and targeted therapies that suppress progression of macro-metastatic disease may serve potential therapeutic benefits.

Because NPTX1 expression outside of the nervous system was not previously described in the literature, biochemical characterization of NPTX1 in pancreatic cancer cells was performed. Similar to neurons, pancreatic cancer cells secrete NPTX1 into the extracellular space forming high-molecular weight oligomers. Investigations into the gene expression regulation of NPTX1 in pancreatic cancer revealed that NPTX1 is partially regulated by epigenetic modifications and a transcription factor, EGR1.

While loss-of-function liver metastatic colonization assays and orthotopic tumor growth studies revealed NPTX1's role in promoting pancreatic cancer progression, gain-of-function assays *in vivo* did not lead to increased metastasis nor did they rescue suppressed metastatic growth due to NPTX1 knockdown in

cancer cells. One potential explanation is the non-physiologic level of NPTX1 expressed using the over-expression construct. NPTX1 can form hetero-oligomers with the other neuronal pentraxin proteins in neurons (Xu et al., 2003), and it is possible that the stoichiometry of the over-expressed NPTX1 was non-functional. Indeed, over-expressing NPTX1 in the PANC1 LM3 cells with NPTX1 knockdown led to further suppression of liver metastasis relative to cells over-expressing GFP, demonstrating that the over-expressed NPTX1 may exert dominant negative effects.

Interestingly, while NPTX1 depletion in pancreatic cancer cells dramatically decreased liver metastatic colonization in the xenograft and syngeneic mouse models, NPTX1 depletion did not lead to obvious cellular phenotypic changes *in vitro* and did not affect cell proliferation under standard cell culture conditions. Similarly, the *in vivo* selected, highly metastatic PANC1 LM3 or KPC LM2 cells proliferated much faster compared to their respective parental cells *in vivo*, but proliferated slower compared to the parental cells *in vitro*. The difference between the *in vitro* and *in vivo* tumor cell proliferation indicated the importance of the tumor microenvironment.

One hallmark of pancreatic cancer is the hypoxic tumor microenvironment. In the *in vivo* liver metastatic colonization model, the *in-vivo* selected, highly

metastatic pancreatic cancer cells were capable of continued proliferation even after experiencing extensive hypoxia in the tumor microenvironment. Indeed, the *in vivo* selected, highly metastatic pancreatic cancer cells proliferated at significantly higher rates relative to the lowly metastatic parental cells in hypoxia *in vitro*.

Suppression of NPTX1 also specifically lowered pancreatic cancer cell proliferation under hypoxia, but not in normoxia. Hypoxia-induced HIF1a response is often activated by tumor cells for hypoxic and metabolic adaptation (Semenza, 2013). However, knockdown of HIF1a did not lead to changes in the proliferation rate of the *in vivo* selected and highly metastatic pancreatic cancer cells, indicating that these highly metastatic cancer cells utilize alternative mechanisms to promote increased proliferation in hypoxia. Further studies on the molecular mechanisms of how NPTX1 can promotes pancreatic cancer survival in hypoxia can provide important insights into the progression mechanisms of metastatic pancreatic cancer. Since NPTX1 is a secreted protein, the identification of its receptor and its extracellular roles in cancer will be an interesting topic for future investigations.

While NPTX1 can promote cell proliferation in hypoxia, since is it a secreted protein, it could potentially have non-cell autonomous roles in the tumor

microenvironment as well. Cellular components including myofibroblasts, endothelial cells, and immune cells were examined. Suppression of NPTX1 in cancer cells led to decreased infiltrating myofibroblasts, while recombinant NPTX1 and cancer conditioned medium were insufficient to activate the stellate cells (precursors of the myofibroblasts), suggesting that NPTX1 is unlikely to directly interact with the myofibroblasts. Rather, high NPTX1 expression could provide proliferative advantages to cancer cells within a hypoxic microenvironment and this environment in term may influence the survival or growth of stromal cells. For example, hepatic stellate cells have been shown to activate and transdifferentiate into myofibroblasts in hypoxia (Shi et al., 2007).

NPTX1 depletion did not change the number of endothelial cells or immune cells in the xenograft or syngeneic models. However, only relative numbers of immune cells were profiled and it is possible that NPTX1 depletion may lead to differential polarization of immune cells, such as macrophages. Given the pentraxin family protein's role in innate immunity, further investigations on NPTX1's effector cell types and potential receptors outside of the nervous system will elucidate previously unknown functions of this gene in cancer.

Analysis of NPTX1 expression revealed that NPTX1 is specifically expressed by pancreatic tumors but not in healthy pancreatic tissues. In addition, NPTX1 is

secreted by pancreatic cancer cells into the extracellular space and is detectable in the plasma of the xenografted pancreatic cancer mouse model. NPTX1 could potentially serve as a diagnostic marker in pancreatic cancer and clinical studies examining NPTX1 level in pancreatic patients' sera may provide further insights. Furthermore, NPTX1 knockout mice (Bjartmar et al., 2006) are grossly healthy. NPTX1's secreted status, role in promoting metastasis progression, and a lack of disease phenotype in the mouse knockout model suggest that NPTX1 could potentially be an attractive therapeutic target. Developing a neutralizing antibody is one possible strategy to specifically inhibit NPTX1 and may serve as potential future targeted therapy in pancreatic cancer.

References

1. Aguirre, A.J., Bardeesy, N., Sinha, M., Lopez, L., Tuveson, D.A., Horner, J., Redston, M.S., and DePinho, R.A. (2003). Activated Kras and Ink4a/Arf deficiency cooperate to produce metastatic pancreatic ductal adenocarcinoma. Genes Dev *17*, 3112-3126.
2. Al Rahim, M., and Hossain, M.A. (2013). Genetic deletion of NP1 prevents hypoxic-ischemic neuronal death via reducing AMPA receptor synaptic localization in hippocampal neurons. Journal of the American Heart Association *2*, e006098.
3. Amedei, A., Niccolai, E., and Prisco, D. (2014). Pancreatic cancer: role of the immune system in cancer progression and vaccine-based immunotherapy. Hum Vaccin Immunother *10*, 3354-3368.
4. Apte, M.V., Wilson, J.S., Lugea, A., and Pandol, S.J. (2013). A starring role for stellate cells in the pancreatic cancer microenvironment. Gastroenterology *144*, 1210-1219.
5. Atlas, H.P. (2017). NPTX1 Tissue expression by RNA.
6. Aune, D., Greenwood, D.C., Chan, D.S., Vieira, R., Vieira, A.R., Navarro Rosenblatt, D.A., Cade, J.E., Burley, V.J., and Norat, T. (2012). Body mass index, abdominal fatness and pancreatic cancer risk: a systematic review and non-linear dose-response meta-analysis of prospective studies. Ann Oncol *23*, 843-852.
7. Ballehaninna, U.K., and Chamberlain, R.S. (2012). The clinical utility of serum CA 19-9 in the diagnosis, prognosis and management of pancreatic adenocarcinoma: An evidence based appraisal. J Gastrointest Oncol *3*, 105-119.
8. Ben, Q., Xu, M., Ning, X., Liu, J., Hong, S., Huang, W., Zhang, H., and Li, Z. (2011). Diabetes mellitus and risk of pancreatic cancer: A meta-analysis of cohort studies. Eur J Cancer *47*, 1928-1937.

9. Bjartmar, L., Huberman, A.D., Ullian, E.M., Renteria, R.C., Liu, X., Xu, W., Prezioso, J., Susman, M.W., Stellwagen, D., Stokes, C.C., *et al.* (2006). Neuronal pentraxins mediate synaptic refinement in the developing visual system. The Journal of neuroscience : the official journal of the Society for Neuroscience *26*, 6269-6281.
10. Bodman-Smith, K.B., Melendez, A.J., Campbell, I., Harrison, P.T., Allen, J.M., and Raynes, J.G. (2002). C-reactive protein-mediated phagocytosis and phospholipase D signalling through the high-affinity receptor for immunoglobulin G (FcgammaRI). Immunology *107*, 252-260.
11. Bosetti, C., Lucenteforte, E., Silverman, D.T., Petersen, G., Bracci, P.M., Ji, B.T., Negri, E., Li, D., Risch, H.A., Olson, S.H., *et al.* (2012). Cigarette smoking and pancreatic cancer: an analysis from the International Pancreatic Cancer Case-Control Consortium (Panc4). Ann Oncol *23*, 1880-1888.
12. Burris, H.A., 3rd, Moore, M.J., Andersen, J., Green, M.R., Rothenberg, M.L., Modiano, M.R., Cripps, M.C., Portenoy, R.K., Storniolo, A.M., Tarassoff, P., *et al.* (1997). Improvements in survival and clinical benefit with gemcitabine as first-line therapy for patients with advanced pancreas cancer: a randomized trial. J Clin Oncol *15*, 2403-2413.
13. Caldas, C., Hahn, S.A., da Costa, L.T., Redston, M.S., Schutte, M., Seymour, A.B., Weinstein, C.L., Hruban, R.H., Yeo, C.J., and Kern, S.E. (1994). Frequent somatic mutations and homozygous deletions of the p16 (MTS1) gene in pancreatic adenocarcinoma. Nat Genet *8*, 27-32.
14. Commisso, C., Davidson, S.M., Soydaner-Azeloglu, R.G., Parker, S.J., Kamphorst, J.J., Hackett, S., Grabocka, E., Nofal, M., Drebin, J.A., Thompson, C.B., *et al.* (2013).

Macropinocytosis of protein is an amino acid supply route in Ras-transformed cells. Nature *497*, 633-637.

15. Conroy, T., Desseigne, F., Ychou, M., Bouche, O., Guimbaud, R., Becouarn, Y., Adenis, A., Raoul, J.L., Gourgou-Bourgade, S., de la Fouchardiere, C., *et al.* (2011). FOLFIRINOX versus gemcitabine for metastatic pancreatic cancer. The New England journal of medicine *364*, 1817-1825.
16. Du Clos, T.W. (2013). Pentraxins: structure, function, and role in inflammation. ISRN Inflamm *2013*, 379040.
17. Duell, E.J., Lucenteforte, E., Olson, S.H., Bracci, P.M., Li, D., Risch, H.A., Silverman, D.T., Ji, B.T., Gallinger, S., Holly, E.A., *et al.* (2012). Pancreatitis and pancreatic cancer risk: a pooled analysis in the International Pancreatic Cancer Case-Control Consortium (PanC4). Ann Oncol *23*, 2964-2970.
18. DuFort, C.C., DelGiorno, K.E., and Hingorani, S.R. (2016). Mounting Pressure in the Microenvironment: Fluids, Solids, and Cells in Pancreatic Ductal Adenocarcinoma. Gastroenterology *150*, 1545-1557 e1542.
19. Ene-Obong, A., Clear, A.J., Watt, J., Wang, J., Fatah, R., Riches, J.C., Marshall, J.F., Chin-Aleong, J., Chelala, C., Gribben, J.G., *et al.* (2013). Activated pancreatic stellate cells sequester CD8+ T cells to reduce their infiltration of the juxtatumoral compartment of pancreatic ductal adenocarcinoma. Gastroenterology *145*, 1121-1132.
20. Erkan, M., Reiser-Erkan, C., Michalski, C.W., Deucker, S., Sauliunaite, D., Streit, S., Esposito, I., Friess, H., and Kleeff, J. (2009). Cancer-stellate cell interactions perpetuate the hypoxia-fibrosis cycle in pancreatic ductal adenocarcinoma. Neoplasia *11*, 497-508.

21. Esteller, M. (2008). Epigenetics in cancer. The New England journal of medicine *358*, 1148-1159.

22. Fidler, I.J. (1973). Selection of successive tumour lines for metastasis. Nat New Biol *242*, 148-149.

23. Fong, Y., Fortner, J., Sun, R.L., Brennan, M.F., and Blumgart, L.H. (1999). Clinical score for predicting recurrence after hepatic resection for metastatic colorectal cancer: analysis of 1001 consecutive cases. Annals of surgery *230*, 309-318; discussion 318-321.

24. Guerra, C., Schuhmacher, A.J., Canamero, M., Grippo, P.J., Verdaguer, L., Perez-Gallego, L., Dubus, P., Sandgren, E.P., and Barbacid, M. (2007). Chronic pancreatitis is essential for induction of pancreatic ductal adenocarcinoma by K-Ras oncogenes in adult mice. Cancer cell *11*, 291-302.

25. Gupta, G.P., and Massague, J. (2006). Cancer metastasis: building a framework. Cell *127*, 679-695.

26. Haeno, H., Gonen, M., Davis, M.B., Herman, J.M., Iacobuzio-Donahue, C.A., and Michor, F. (2012). Computational modeling of pancreatic cancer reveals kinetics of metastasis suggesting optimum treatment strategies. Cell *148*, 362-375.

27. Hanahan, D., and Weinberg, R.A. (2011). Hallmarks of cancer: the next generation. Cell *144*, 646-674.

28. He, J., Ahuja, N., Makary, M.A., Cameron, J.L., Eckhauser, F.E., Choti, M.A., Hruban, R.H., Pawlik, T.M., and Wolfgang, C.L. (2014). 2564 resected periampullary adenocarcinomas at a single institution: trends over three decades. HPB (Oxford) *16*, 83-90.

29. Hingorani, S.R., Petricoin, E.F., Maitra, A., Rajapakse, V., King, C., Jacobetz, M.A., Ross, S., Conrads, T.P., Veenstra, T.D., Hitt, B.A., *et al.* (2003). Preinvasive and invasive ductal pancreatic cancer and its early detection in the mouse. Cancer cell *4*, 437-450.

30. Hingorani, S.R., Wang, L., Multani, A.S., Combs, C., Deramaudt, T.B., Hruban, R.H., Rustgi, A.K., Chang, S., and Tuveson, D.A. (2005). Trp53R172H and KrasG12D cooperate to promote chromosomal instability and widely metastatic pancreatic ductal adenocarcinoma in mice. Cancer cell *7*, 469-483.

31. Hossain, M.A., Russell, J.C., O'Brien, R., and Laterra, J. (2004). Neuronal pentraxin 1: a novel mediator of hypoxic-ischemic injury in neonatal brain. The Journal of neuroscience : the official journal of the Society for Neuroscience *24*, 4187-4196.

32. Hustinx, S.R., Leoni, L.M., Yeo, C.J., Brown, P.N., Goggins, M., Kern, S.E., Hruban, R.H., and Maitra, A. (2005). Concordant loss of MTAP and p16/CDKN2A expression in pancreatic intraepithelial neoplasia: evidence of homozygous deletion in a noninvasive precursor lesion. Mod Pathol *18*, 959-963.

33. Inman, K.S., Francis, A.A., and Murray, N.R. (2014). Complex role for the immune system in initiation and progression of pancreatic cancer. World journal of gastroenterology : WJG *20*, 11160-11181.

34. Iqbal, J., Ragone, A., Lubinski, J., Lynch, H.T., Moller, P., Ghadirian, P., Foulkes, W.D., Armel, S., Eisen, A., Neuhausen, S.L., *et al.* (2012). The incidence of pancreatic cancer in BRCA1 and BRCA2 mutation carriers. Br J Cancer *107*, 2005-2009.

35. Jones, S., Hruban, R.H., Kamiyama, M., Borges, M., Zhang, X., Parsons, D.W., Lin, J.C., Palmisano, E., Brune, K., Jaffee, E.M., *et al.* (2009). Exomic sequencing identifies PALB2 as a pancreatic cancer susceptibility gene. Science *324*, 217.

36. Kanda, M., Matthaei, H., Wu, J., Hong, S.M., Yu, J., Borges, M., Hruban, R.H., Maitra, A., Kinzler, K., Vogelstein, B., *et al.* (2012). Presence of somatic mutations in most early-stage pancreatic intraepithelial neoplasia. Gastroenterology *142*, 730-733 e739.

37. Kang, Y., Siegel, P.M., Shu, W., Drobnjak, M., Kakonen, S.M., Cordon-Cardo, C., Guise, T.A., and Massague, J. (2003). A multigenic program mediating breast cancer metastasis to bone. Cancer cell *3*, 537-549.

38. Kim, M.P., Evans, D.B., Wang, H., Abbruzzese, J.L., Fleming, J.B., and Gallick, G.E. (2009). Generation of orthotopic and heterotopic human pancreatic cancer xenografts in immunodeficient mice. Nature protocols *4*, 1670-1680.

39. Klein, A.P., Brune, K.A., Petersen, G.M., Goggins, M., Tersmette, A.C., Offerhaus, G.J., Griffin, C., Cameron, J.L., Yeo, C.J., Kern, S., *et al.* (2004). Prospective risk of pancreatic cancer in familial pancreatic cancer kindreds. Cancer research *64*, 2634-2638.

40. Koong, A.C., Mehta, V.K., Le, Q.T., Fisher, G.A., Terris, D.J., Brown, J.M., Bastidas, A.J., and Vierra, M. (2000). Pancreatic tumors show high levels of hypoxia. Int J Radiat Oncol Biol Phys *48*, 919-922.

41. Lee, J.J., Perera, R.M., Wang, H., Wu, D.C., Liu, X.S., Han, S., Fitamant, J., Jones, P.D., Ghanta, K.S., Kawano, S., *et al.* (2014). Stromal response to Hedgehog signaling restrains pancreatic cancer progression. Proc Natl Acad Sci U S A *111*, E3091-3100.

42. Lesina, M., Kurkowski, M.U., Ludes, K., Rose-John, S., Treiber, M., Kloppel, G., Yoshimura, A., Reindl, W., Sipos, B., Akira, S., *et al.* (2011). Stat3/Socs3 activation by IL-6 transsignaling promotes progression of pancreatic intraepithelial neoplasia and development of pancreatic cancer. Cancer Cell *19*, 456-469.

43. Loo, J.M., Scherl, A., Nguyen, A., Man, F.Y., Weinberg, E., Zeng, Z., Saltz, L., Paty, P.B., and Tavazoie, S.F. (2015). Extracellular metabolic energetics can promote cancer progression. Cell *160*, 393-406.

44. Mace, T.A., Ameen, Z., Collins, A., Wojcik, S., Mair, M., Young, G.S., Fuchs, J.R., Eubank, T.D., Frankel, W.L., Bekaii-Saab, T., *et al.* (2013). Pancreatic cancer-associated stellate cells promote differentiation of myeloid-derived suppressor cells in a STAT3-dependent manner. Cancer research *73*, 3007-3018.

45. McDonald, O.G., Li, X., Saunders, T., Tryggvadottir, R., Mentch, S.J., Warmoes, M.O., Word, A.E., Carrer, A., Salz, T.H., Natsume, S., *et al.* (2017). Epigenomic reprogramming during pancreatic cancer progression links anabolic glucose metabolism to distant metastasis. Nat Genet *49*, 367-376.

46. Mederacke, I., Dapito, D.H., Affo, S., Uchinami, H., and Schwabe, R.F. (2015). High-yield and high-purity isolation of hepatic stellate cells from normal and fibrotic mouse livers. Nature protocols *10*, 305-315.

47. Minn, A.J., Gupta, G.P., Siegel, P.M., Bos, P.D., Shu, W., Giri, D.D., Viale, A., Olshen, A.B., Gerald, W.L., and Massague, J. (2005). Genes that mediate breast cancer metastasis to lung. Nature *436*, 518-524.

48. Neesse, A., Frese, K.K., Bapiro, T.E., Nakagawa, T., Sternlicht, M.D., Seeley, T.W., Pilarsky, C., Jodrell, D.I., Spong, S.M., and Tuveson, D.A. (2013). CTGF antagonism

with mAb FG-3019 enhances chemotherapy response without increasing drug delivery in murine ductal pancreas cancer. Proc Natl Acad Sci U S A *110*, 12325-12330.

49. Oberstein, P.E., and Olive, K.P. (2013). Pancreatic cancer: why is it so hard to treat? Therapeutic advances in gastroenterology *6*, 321-337.
50. Ohlund, D., Handly-Santana, A., Biffi, G., Elyada, E., Almeida, A.S., Ponz-Sarvise, M., Corbo, V., Oni, T.E., Hearn, S.A., Lee, E.J., *et al.* (2017). Distinct populations of inflammatory fibroblasts and myofibroblasts in pancreatic cancer. The Journal of experimental medicine *214*, 579-596.
51. Ozdemir, B.C., Pentcheva-Hoang, T., Carstens, J.L., Zheng, X., Wu, C.C., Simpson, T.R., Laklai, H., Sugimoto, H., Kahlert, C., Novitskiy, S.V., *et al.* (2014). Depletion of carcinoma-associated fibroblasts and fibrosis induces immunosuppression and accelerates pancreas cancer with reduced survival. Cancer cell *25*, 719-734.
52. Pencheva, N., Tran, H., Buss, C., Huh, D., Drobnjak, M., Busam, K., and Tavazoie, S.F. (2012). Convergent multi-miRNA targeting of ApoE drives LRP1/LRP8-dependent melanoma metastasis and angiogenesis. Cell *151*, 1068-1082.
53. Png, K.J., Halberg, N., Yoshida, M., and Tavazoie, S.F. (2011). A microRNA regulon that mediates endothelial recruitment and metastasis by cancer cells. Nature *481*, 190-194.
54. Preis, M., and Korc, M. (2011). Signaling pathways in pancreatic cancer. Crit Rev Eukaryot Gene Expr *21*, 115-129.

55. Provenzano, P.P., Cuevas, C., Chang, A.E., Goel, V.K., Von Hoff, D.D., and Hingorani, S.R. (2012). Enzymatic targeting of the stroma ablates physical barriers to treatment of pancreatic ductal adenocarcinoma. Cancer cell *21*, 418-429.

56. Rahib, L., Smith, B.D., Aizenberg, R., Rosenzweig, A.B., Fleshman, J.M., and Matrisian, L.M. (2014). Projecting cancer incidence and deaths to 2030: the unexpected burden of thyroid, liver, and pancreas cancers in the United States. Cancer research *74*, 2913-2921.

57. Rebours, V., Boutron-Ruault, M.C., Schnee, M., Ferec, C., Maire, F., Hammel, P., Ruszniewski, P., and Levy, P. (2008). Risk of pancreatic adenocarcinoma in patients with hereditary pancreatitis: a national exhaustive series. Am J Gastroenterol *103*, 111-119.

58. Rhim, A.D., Mirek, E.T., Aiello, N.M., Maitra, A., Bailey, J.M., McAllister, F., Reichert, M., Beatty, G.L., Rustgi, A.K., Vonderheide, R.H., *et al.* (2012). EMT and dissemination precede pancreatic tumor formation. Cell *148*, 349-361.

59. Rhim, A.D., Oberstein, P.E., Thomas, D.H., Mirek, E.T., Palermo, C.F., Sastra, S.A., Dekleva, E.N., Saunders, T., Becerra, C.P., Tattersall, I.W., *et al.* (2014). Stromal elements act to restrain, rather than support, pancreatic ductal adenocarcinoma. Cancer cell *25*, 735-747.

60. Roberts, N.J., Norris, A.L., Petersen, G.M., Bondy, M.L., Brand, R., Gallinger, S., Kurtz, R.C., Olson, S.H., Rustgi, A.K., Schwartz, A.G., *et al.* (2016). Whole Genome Sequencing Defines the Genetic Heterogeneity of Familial Pancreatic Cancer. Cancer Discov *6*, 166-175.

61. Ryan, D.P., Hong, T.S., and Bardeesy, N. (2014). Pancreatic adenocarcinoma. The New England journal of medicine *371*, 1039-1049.

62. Schlimgen, A.K., Helms, J.A., Vogel, H., and Perin, M.S. (1995). Neuronal pentraxin, a secreted protein with homology to acute phase proteins of the immune system. Neuron *14*, 519-526.

63. Semenza, G.L. (2013). HIF-1 mediates metabolic responses to intratumoral hypoxia and oncogenic mutations. J Clin Invest *123*, 3664-3671.

64. Seymour, A.B., Hruban, R.H., Redston, M., Caldas, C., Powell, S.M., Kinzler, K.W., Yeo, C.J., and Kern, S.E. (1994). Allelotype of pancreatic adenocarcinoma. Cancer research *54*, 2761-2764.

65. Shi, Y.F., Fong, C.C., Zhang, Q., Cheung, P.Y., Tzang, C.H., Wu, R.S., and Yang, M. (2007). Hypoxia induces the activation of human hepatic stellate cells LX-2 through TGF-beta signaling pathway. FEBS Lett *581*, 203-210.

66. Sia, G.M., Beique, J.C., Rumbaugh, G., Cho, R., Worley, P.F., and Huganir, R.L. (2007). Interaction of the N-terminal domain of the AMPA receptor GluR4 subunit with the neuronal pentraxin NP1 mediates GluR4 synaptic recruitment. Neuron *55*, 87-102.

67. Slamon, D.J., Leyland-Jones, B., Shak, S., Fuchs, H., Paton, V., Bajamonde, A., Fleming, T., Eiermann, W., Wolter, J., Pegram, M., *et al.* (2001). Use of chemotherapy plus a monoclonal antibody against HER2 for metastatic breast cancer that overexpresses HER2. The New England journal of medicine *344*, 783-792.

68. Stathis, A., and Moore, M.J. (2010). Advanced pancreatic carcinoma: current treatment and future challenges. Nature reviews Clinical oncology *7*, 163-172.

69. Tanaka, M. (2014). Thirty years of experience with intraductal papillary mucinous neoplasm of the pancreas: from discovery to international consensus. Digestion *90*, 265-272.

70. Tavazoie, S.F., Alarcon, C., Oskarsson, T., Padua, D., Wang, Q., Bos, P.D., Gerald, W.L., and Massague, J. (2008). Endogenous human microRNAs that suppress breast cancer metastasis. Nature *451*, 147-152.

71. Taylor, I. (1996). Liver metastases from colorectal cancer: lessons from past and present clinical studies. The British journal of surgery *83*, 456-460.

72. Thatipamula, S., and Hossain, M.A. (2014). Critical role of extracellularly secreted neuronal pentraxin 1 in ischemic neuronal death. BMC Neurosci *15*, 133.

73. Torre, L.A., Bray, F., Siegel, R.L., Ferlay, J., Lortet-Tieulent, J., and Jemal, A. (2015). Global cancer statistics, 2012. CA Cancer J Clin *65*, 87-108.

74. Torres, M.P., Rachagani, S., Souchek, J.J., Mallya, K., Johansson, S.L., and Batra, S.K. (2013). Novel pancreatic cancer cell lines derived from genetically engineered mouse models of spontaneous pancreatic adenocarcinoma: applications in diagnosis and therapy. PloS one *8*, e80580.

75. Tuveson, D.A., and Neoptolemos, J.P. (2012). Understanding metastasis in pancreatic cancer: a call for new clinical approaches. Cell *148*, 21-23.

76. Vasen, H.F., Gruis, N.A., Frants, R.R., van Der Velden, P.A., Hille, E.T., and Bergman, W. (2000). Risk of developing pancreatic cancer in families with familial atypical multiple mole melanoma associated with a specific 19 deletion of p16 (p16-Leiden). International journal of cancer Journal international du cancer *87*, 809-811.

77. Von Hoff, D.D., Ervin, T., Arena, F.P., Chiorean, E.G., Infante, J., Moore, M., Seay, T., Tjulandin, S.A., Ma, W.W., Saleh, M.N., *et al.* (2013). Increased survival in pancreatic cancer with nab-paclitaxel plus gemcitabine. The New England journal of medicine *369*, 1691-1703.

78. Xu, D., Hopf, C., Reddy, R., Cho, R.W., Guo, L., Lanahan, A., Petralia, R.S., Wenthold, R.J., O'Brien, R.J., and Worley, P. (2003). Narp and NP1 form heterocomplexes that function in developmental and activity-dependent synaptic plasticity. Neuron *39*, 513-528.

79. Yachida, S., and Iacobuzio-Donahue, C.A. (2009). The pathology and genetics of metastatic pancreatic cancer. Arch Pathol Lab Med *133*, 413-422.

80. Yang, S., Wang, X., Contino, G., Liesa, M., Sahin, E., Ying, H., Bause, A., Li, Y., Stommel, J.M., Dell'antonio, G., *et al.* (2011). Pancreatic cancers require autophagy for tumor growth. Genes Dev *25*, 717-729.

81. Ying, H., Dey, P., Yao, W., Kimmelman, A.C., Draetta, G.F., Maitra, A., and DePinho, R.A. (2016). Genetics and biology of pancreatic ductal adenocarcinoma. Genes Dev *30*, 355-385.

82. Zhang, H., Chen, X., Wang, J., Guang, W., Han, W., Zhang, H., Tan, X., and Gu, Y. (2014). EGR1 decreases the malignancy of human non-small cell lung carcinoma by regulating KRT18 expression. Sci Rep *4*, 5416.

83. Zhou, C., Qin, Y., Xie, Z., Zhang, J., Yang, M., Li, S., and Chen, R. (2015). NPTX1 is a novel epigenetic regulation gene and associated with prognosis in lung cancer. Biochem Biophys Res Commun *458*, 381-386.